

1 **Responses to Referee #1:**

2 We thank Referee #1 for their comments and suggestions: all of which were helpful in improving the manuscript.  
3 We detail our response to each item below.

4 **The fuels themselves appear very representative; whether the emissions from the FLAME burns are**  
5 **representative of real-world emissions is a difficult question to answer and probably beyond the scope of this**  
6 **work. However, since the authors are experts in this area of research – some discussion on the validity of lab-**  
7 **to-field representativeness is warranted for the emissions factors reported here.**

8 This is an important point that we were greatly concerned with in a companion paper, but did not address clearly  
9 enough in this paper. We now address this in three additional ways.

10 (1) We mention early on in the introduction that the representativeness of the FLAME-4 fire emissions was explored  
11 in great detail by examining agreement with field measurements in an already published companion paper  
12 (Stockwell et al. 2014). In that paper we show that much of the FLAME-4 data is representative as is and - for fuel  
13 types warranted - we suggest simple, specific adjustment procedures to make the laboratory data more representative  
14 of field data.

15 Changes in the text are as follows:

16 P22167, L15-20: Old text: “In this work, we perform, to our knowledge, the first application of PTR-TOF-MS  
17 technology to laboratory biomass burning smoke to characterize emissions from a variety of authentic globally  
18 significant fuels. We report on several new or rarely measured gases and present a large set of useful emission ratios  
19 (ERs) and emission factors (EFs) for major fuel types that can inform/update current atmospheric models.”

20 New text: “In a companion paper the FLAME-4 emissions were compared extensively to field measurements of fire  
21 emissions and they were shown to be representative of “real-world” biomass burning either as is or after  
22 straightforward adjustment procedures detailed therein (Stockwell et al., 2014). In this work, we describe, to our  
23 knowledge, the first application of PTR-TOF-MS technology to laboratory biomass burning smoke to characterize  
24 emissions from a variety of authentic globally significant fuels. We report on several new or rarely measured gases  
25 and present a large set of useful emission ratios (ERs) and emission factors (EFs) that can represent major fuel types  
26 and inform/update current atmospheric models.”

27 (2) We now better clarify that the main compilation of new recommended EF is in Table S3. This important table  
28 appears in the supplement simply because of its large size. We also better clarify that any adjustment procedures  
29 required based on the comparisons in the companion paper have been applied to the data in Table S3. One exception  
30 is for cooking fires. We did not have enough TOF data from analyzing just three fires to get a useful EF vs MCE  
31 relationship so we instead computed adjusted EF for any NMOC “X” as the average X/CH<sub>4</sub> ratio from FLAME-4  
32 times the literature average EF(CH<sub>4</sub>) for cooking fires from Akagi et al., (2011).

33 Changes in text are as follows:

34 P22173 L5-7, Old text: “Finally, the EFs reported in Supplement Table S3 were adjusted according to procedures  
35 established in Stockwell et al. (2014) to improve laboratory representation of real-world biomass burning  
36 emissions.”

37 New text: “Finally, the EFs reported in Supplement Table S3 were adjusted (when needed) according to procedures  
38 established in Stockwell et al. (2014) to improve laboratory representation of real-world biomass burning emissions.  
39 This table contains the EF we recommend other workers use and it appears in the Supplement only because of its  
40 large size.”

41 P22173, L17: changed “S1 and S2” to “S1-S3”

42 To further clarify the relative importance of Tables S3 and Table 2 we made the following change:

43 P22176, L14-20: Existing text: “To facilitate discussion we grouped many of the assigned (or tentatively assigned)  
44 mass peak features into categories including: aromatic hydrocarbons; phenolic compounds; furan and its derivatives;  
45 nitrogen-containing compounds; sulfur-containing compounds; and miscellaneous compounds at increasing  $m/z$ .”

46 New text: “To facilitate discussion we grouped many of the assigned (or tentatively assigned) mass peak features  
47 into categories including: aromatic hydrocarbons; phenolic compounds; furans; nitrogen-containing compounds; and  
48 sulfur-containing compounds. These categories do not account for the majority of the emitted NMOC mass, but  
49 account for most of the rarely-measured species reported in this work. We then also discuss miscellaneous  
50 compounds at increasing  $m/z$ .”

51 P22190, L1, changed “and should aid” to “and (especially the recommended values in Table S3) should aid”

52 (3) We found two recent additional field studies of biomass burning to compare to (Geron and Hays, 2013; Kudo et  
53 al., 2014). They both support the “realism” of our FLAME-4 EF in Table S3.

54 Changes in text are as follows:

55 We include the following sentence in the text immediately following the above mentioned sentence at P22173 L7:  
56 “In addition to the comparisons considered in Stockwell et al. (2014), we find that our EFs in Table S3 are  
57 consistent (for the limited number of overlap species) with additional, recent field studies including Kudo et al.  
58 (2014) for Chinese crop residue fires and Geron and Hays (2013) for NC peat fires.”

59 These additional references were added to the paper:

60 “Kudo, S., Tanimoto, H., Inomata, S., Saito, S., Pan, X., Kanaya, Y., Taketani, F., Wang, Z., Chen, H., Dong, H.,  
61 Zhang, M., and Yamaji, K.: Emissions of nonmethane volatile organic compounds from open crop residue burning

62 in the Yangtze River Delta region, China, J. Geophys. Res. Atmos., 119, 7684-7698, doi: 10.1002/2013JD021044,  
63 2014.”

64 “Geron, C., and Hays, M.: Air emissions from organic soil burning on the coastal plain of North Carolina, Atmos.  
65 Environ., 64, 192-199, doi: 10.1016/j.atmosenv.2012.09.065, 2013.”

66 **The authors report a conservative bound of +/- 50% measurement uncertainty about emissions by compound.**  
67 **This uncertainty is not surprising given the inherent limitations of PTR-MS and the fact that their calibration**  
68 **standards were mostly hydrocarbon based (with only a few heteroatom molecules beyond C-H-O). Perhaps**  
69 **the biggest weakness of this work is the choice of calibration gasses. The authors report emissions factors for**  
70 **many previously unstudied compounds (especially oxygenates and a few S- and N- containing compounds),**  
71 **yet, they did not generate calibration curves for these compounds. Standards for S- and N- compounds are**  
72 **likely difficult to obtain (especially those that are semi-volatile), however, the development of a phenol- and**  
73 **furan-containing calibration mixture would have strengthened this work considerably.**

74 **P22170 lines 16-19. This sentence is awkward. “In cases where a compound contains a non-oxygen**  
75 **heteroatom (such as methanethiol), the mass dependent calibration factor was determined using the**  
76 **relationship established using the oxygenated species.” More importantly, it is unclear whether this approach**  
77 **is valid. What is the uncertainty associated with assuming that such heteroatomic compounds will follow the**  
78 **oxygenated calibration curve? The deviation of dimethylsulphide from the ‘oxygenates’ calibration line**  
79 **(Figure 3) indicates that this assumption may not be valid.**

80 We agree that additional calibration gases would be useful. This would be especially true for stand-alone use of the  
81 PTR-TOF-MS and we do note that we used the OP-FTIR furan data in this work. In our case, the instrument was  
82 rented for only three months and calibration gases were ordered ahead of time to meet the needs of several different  
83 experiments. We chose a variety of gases that were already known to be emitted by fires (including hydrocarbons  
84 and C-H-O heteroatoms), but operationally could not add calibration gases during the experiment. It is no longer  
85 possible to run more calibration gases, but for any group that owns or rents a TOF for smoke characterization in the  
86 future we recommend including more calibration species and measuring more fragmentation patterns. We now  
87 mention these issues in the conclusions where we summarized the lessons learned from our first attempt.

88 P22189 L2 before sentence beginning with: “Despite these practical...” add: “We were limited to our pre-chosen  
89 calibration mixture based primarily on gases previously observed in smoke. For future experiments we suggest  
90 adding more standards to generate more accurate calibration factors, specifically including major species such as  
91 furan and phenol and more compounds with S and N heteroatoms. In addition, measuring the fragmentation, if any,  
92 of more of the species identified in this work would be of great value.”

93 On the subject of our treatment of heteroatoms, such as in the case of DMS and Acetonitrile, we agree with the  
94 reviewers that perhaps this is not the best treatment of these species. One would expect that approximation of  
95 sensitivities would most accurately be calculated *via* grouping families of compounds (e.g. alcohols, carbonyls,

96 alkenes) rather than general subgroups of oxygenates and hydrocarbons. Unfortunately due to the limitations in this  
97 study and the lack of additional calibration standards as mentioned above we are forced to make some assumptions  
98 as in the case of compounds containing heteroatoms. Here we only have two calibrated examples both of which  
99 show a wide range in sensitivities. While sulfur and nitrogen containing compounds should be treated separately in a  
100 more complete analysis, we have chosen to consider these species collectively in order to increase sample size.  
101 When considered as a group these compounds more closely follow the trend for the oxygenated family. This does  
102 result in an increased error on the calculated calibration factors which has been approximated using the scatter on  
103 the fits derived from the oxygenated + heteroatom relationship. Unfortunately without any additional information  
104 we cannot more accurately approximate the error though we do admit the cited error is likely a lower limit on the  
105 actual errors associated with this method of determination. This is a valid criticism of this work and the  
106 approximation of calibrations factors is a problem that is and will continue to be an issue with the analysis of TOF  
107 data moving forward, however, a detailed treatment is beyond the scope of this paper.

108 P22170, L16: Existing text: "In cases where a compound contains a non-oxygen heteroatom (such as methanethiol),  
109 the mass dependent calibration factor was determined using the relationship established using the oxygenated  
110 species."

111 New text: "Sulfur and nitrogen-containing compounds were considered collectively and together they more closely  
112 followed the trend of the oxygenated species. Thus, in cases where a compound contains a non-oxygen heteroatom  
113 (such as methanethiol), the mass dependent calibration factor was determined using the relationship established  
114 using the oxygenated species."

115 Then in addition to recognize the higher uncertainty for these species we added this change:

116 P22171, L6: We append after "prescribed" " , but with larger errors possible for compounds with N and S  
117 heteroatoms."

118 **Table 2 (body text). Are the numbers in parentheses standard deviations or some other measure of**  
119 **variability? This comment applies to nearly every Table in the manuscript; footnotes should be added to each**  
120 **table to explain accordingly.**

121 Thank you for bringing this to our attention. Table 2 should include the following footnote "Note: "nm" indicates  
122 not measured; blank indicates species remained below the detection limits; values in parenthesis indicate one  
123 standard deviation"

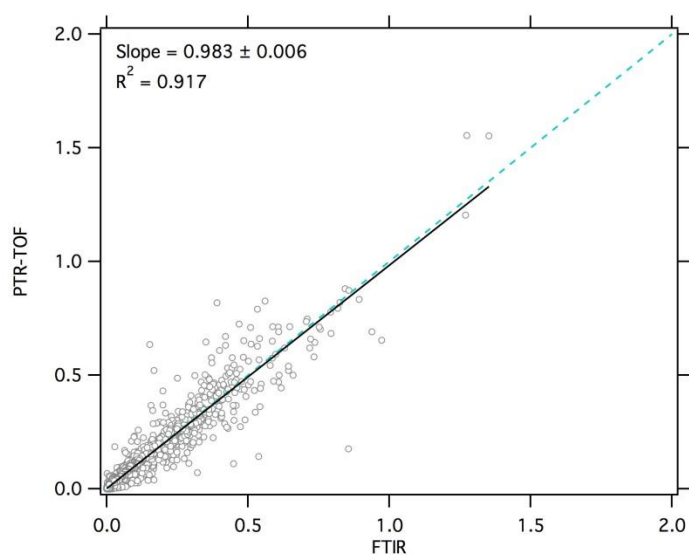
124 **The authors use methanol concentrations, as measured by OP FTIR, as an internal standard to account for**  
125 **variations associated with PTR-MS instrument. This is an innovative approach and one that will likely reduce**  
126 **measurement variability. Inclusion of more intercomparison data between the PTR and FTIR instruments**  
127 **for other shared compounds (perhaps as supplementary material) would strengthen this manuscript as these**

128 **data would shed light on PTR measurement reliability. Showing the methanol comparison plot (1:1) would be**  
129 **helpful, too.**

130 Developing detailed inter-comparisons for more species for numerous fires is a large body of work that is the focus  
131 of an in-progress companion paper describing both contributions and inter-comparisons for the PTR-TOF-MS, OP-  
132 FTIR, WAS, and 2D-GC data from FLAME-4. The in-progress study comparing and identifying the strengths of  
133 four techniques promises to be more valuable than comparing two techniques. Thus, we prefer not to lengthen the  
134 current already-long paper, which is focused on expanding the amount of data concerning NMOCs emitted by BB.

135 The point of using methanol as the internal standard for calculating fire-integrated ERs is that it actually cancels  
136 errors even if the PTR-MS and OP-FTIR disagree on occasion for methanol due to reagent ion depletion, timing, etc.  
137 We have already included the slope and  $R^2$  value for this comparison in the manuscript. The lack of overall bias  
138 between the two instruments for methanol that we observed is nice, but already a departure from the main point. As  
139 noted above, adding more comparisons or the 1:1 methanol comparison plot would lengthen the manuscript and shift  
140 focus when a separate, comprehensive paper detailing measurement issues is already in progress. Thus, while the  
141 Referees concerns are warranted we address them elsewhere and did not add figures or comparisons at this time.

142 It is also important to note that depending on how we define the intercomparison (e.g. fire-integrated or real-time,  
143 etc.) the results vary a bit - and this takes time/space to describe, thus further supporting our decision to devote a  
144 separate paper to the topic of the intercomparison. As an example we show (in this response only) an FTIR/PTR  
145 methanol comparison with a slightly different filter applied than in the example quoted in the text. The slope and  $R^2$   
146 are then different, but still good. We trust the forthcoming companion paper comparing four techniques will provide  
147 the best way to gain insights into the bulk of the FLAME-4 NMOC fuel-specific emission factor results.



149 The good agreement for several species measured by both proton-transfer-reaction mass spectrometry and OP-FTIR  
150 spectroscopy has been demonstrated in numerous past manuscripts focused on laboratory biomass burning emissions

151 (Christian et al., 2004; Karl et al., 2007; Veres et al. 2010; Warneke et al., 2011). To reflect this discussion in the  
152 paper we modified the sentence on P22172, L1-2 as follows:

153 Old sentence: “The agreement between these two measurements is within the uncertainties of both instruments.”

154 New sentence: “This result is consistent with the good agreement for several species measured by both PTR-MS and  
155 OP-FTIR observed in numerous past studies of laboratory biomass burning emissions (Christian et al., 2004; Karl et  
156 al., 2007; Veres et al. 2010; Warneke et al., 2011).”

157 **The compound-specific emissions factors that are included as supplemental tables is a great contribution of**  
158 **this work; these data will likely be used by many researchers. Is the use of 3+ significant figures justified,**  
159 **given the uncertainty in these EF data?**

160 We simply chose to mass-produce the data with enough places after the decimal point to account for the large range  
161 in EF/ER. The co-tabulated standard deviations should make the actual number of significant figures clear. The  
162 important table (S3) uses 3 significant figures and researchers can use less if they prefer. It seems unnecessary to go  
163 through such large tables and manually edit them because there is so much variation on how many 0s are in front of  
164 the numbers. In addition, the rounding off the CO<sub>2</sub> emission factors to less than four digits could be warranted, but is  
165 never done in the literature. Reporting significant figures only introduces “round-off error” into any subsequent  
166 calculations with the data.

167 **Figure 3 is difficult to comprehend based on the information presented in the title and legend. Only a single**  
168 **reference to this figure appears in the text body, but that reference is not explanatory. Many questions follow.**  
169 **There are three categories for ‘oxygenates’, ‘phenolics’, and ‘furans’ for each fuel type. Why? What do the**  
170 **parentheses mean, number of independent tests? I ‘think’ this plot is meant to compare FTIR to PTR**  
171 **measurements, but if so, I don’t know which instrument is which since there are four bars per fuel.**

172 Thank you for pointing out that this figure needs a more detailed explanation. The data in these figures are based on  
173 the synthesis of the FTIR and PTR measurements and do not compare the two. Instead we lumped the emissions into  
174 the following categories: non-methane hydrocarbons, oxygenates containing only 1 oxygen, oxygenates containing 2  
175 oxygen atoms, and oxygenates containing 3 oxygen atoms. To give an even greater level of detail we then indicated  
176 within each category what emissions were directly from phenolic compounds or furan and substituted furans.

177 To clarify these changes in the text are as follows:

178 Added sentence before “As shown in Fig. 3...” P 22176 L8: “Figure 3 includes both FTIR and PTR emissions  
179 grouped into the following categories: non-methane hydrocarbons, oxygenates containing only one oxygen,  
180 oxygenates containing two oxygen atoms, and oxygenates containing three oxygen atoms. Within these categories,  
181 the contribution from aromatics, phenolic compounds, and furans are further indicated.”

182 Also change the figure description to add further clarity, P22210:

183 “Figure 3. The emission factors ( $\text{g kg}^{-1}$ ) of total observed hydrocarbons and total observed species oxygenated to  
184 different degrees averaged for each fire type based on a synthesis of PTR-TOF-MS and OP-FTIR data. The  
185 patterned sections indicate the contribution to each of the above categories by selected functionalities discussed in  
186 the text (aromatic hydrocarbons, phenolics, furans). The parenthetical expressions indicate how many oxygen atoms  
187 are present.”

188 **For the emissions factors tables, can the authors indicate which tests were true replicates? I suspect such**  
189 **information exists elsewhere but it would be very helpful to know how repeatable the measurements were for**  
190 **repeat tests (i.e., EF’s determined from the same set of experimental conditions).**

191 If by true replicates the author means burning “the exact same fire again and seeing how the emissions changed”  
192 then we have no true replicates. This is partly because on the scale of the fires we burned (several cubic meters of  
193 fuel) no exact duplicates could be constructed, but also because we instead aimed to vary the fires (moisture,  
194 geometry, etc.) in hope of capturing the natural EF dependence on MCE. We did perform replications of the smog  
195 chamber perturbations that will be described elsewhere.

196 **The authors might try breaking Figure 4a and 5a into two panels each. One panel would contain EF’s for**  
197 **those fuels whose sum exceeds > 1 g/kg and one for those fuels whose sum is less than 1 g/kg (the latter scaled**  
198 **appropriately). The bars for fuels with low EF’s (i.e., less than 1 g/kg) are practically unreadable in these**  
199 **figures.**

200 We thank the reviewer for bringing this to our attention and we have scaled Figures 4a, 5a, and 6a accordingly.

#### 201 **Responses to Referee # 2:**

202 We thank the Anonymous Referee #2 for their comments and suggestions. All of the comments have been  
203 considered and were helpful in improving the manuscript. We address the specific comments below.

204 **Abstract Page 22165, Line 3 – There should be no hyphen between crop and residue**

205 P22165 L3 We have changed “crop-residue” to “crop residue”

206 **Page 22165, Line 5 – Suggest changing standards to standard**

207 P22165 L5 We have changed to “a combination of gas standard calibrations”

208 **Page 22615, Line 10 – The abbreviation FTIR has not been defined**

209 P22165 L5 We have defined FTIR, subsequently changing “FTIR” to “Fourier transform infrared (FTIR)  
210 spectroscopy”

211 **Page 22166, Lines 23-24 – There should be hyphens in proton transfer reactions**

212 P22166 L 23-24 We have added hyphens, changing “proton transfer reactions” to “proton-transfer-reactions”

213 **2.3.Proton-transfer-reaction time-of-flight mass spectrometer Page 22171, Line 8 – The abbreviation VOC**  
214 **has not been defined**

215 P22171 L8 We have now defined VOC in the sentence: “volatile organic compound (VOC)”

216 **2.4.OP-FTIR Page 22171, Line 10 – The chemical formula used has not been defined**

217 P22171 L10 We have now defined CO “ratios to carbon monoxide (CO)”

218 **Page 22185, Line 17 – There should be no hyphen between crop and residue**

219 P22185 L17 We have changed “Crop-residue” to “Crop residue”

220 **4.7.Cookstoves Page 22187, Line 18 – Envirofit is misspelled**

221 P22187 L18 We have respelled “Envriofit” to “Envirofit”

222 **References Page 22912, Line 6 – Believe it should be St. Clair, J.M.**

223 P22912 L6 We have fixed our mistake concerning the location of the St. in the following reference

224 “Alvarado, M. J., Logan, J. A., Mao, J., Apel, E., Riemer, D., Blake, D., Cohen, R. C., Min, K.-E., Perring, A. E.,  
225 Browne, E. C., Wooldridge, P. J., Diskin, G. S., Sachse, G. W., Fuelberg, H., Sessions, W. R., Harrigan, D. L., Huey,  
226 G., Liao, J., Case-Hanks, A., Jimenez, J. L., Cubison, M. J., Vay, S. A., Weinheimer, A. J., Knapp, D. J., Montzka,  
227 D. D., Flocke, F. M., Pollack, I. B., Wennberg, P. O., Kurten, A., Crounse, J., St. Clair, J. M., Wisthaler, A.,  
228 Mikoviny, T., Yantosca, R. M., Carouge, C. C., and Le Sager, P.: Nitrogen oxides and PAN in plumes from boreal  
229 fires during ARCTAS-B and their impact on ozone: an integrated analysis of aircraft and satellite observations,  
230 *Atmos. Chem. Phys.*, 10, 9739–9760, doi:10.5194/acp-10-9739-2010, 2010.”

231 **Page 22912, line 27 – There is an extra d at the end of European**

232 P22912 L27 We have corrected misspelling by changing “Europeand” to “European”

233 **Page 22195, Line 8 – There should be an and before Hjorth**

234 P22195 L8 We have added an “and” changing the reference to “Gomez Alvarez, E. G., Borrás, E., Viidanoja, J., and  
235 Hjorth, J.: Unsaturated dicarbonyl products from the OH-initiated photo-oxidation of furan, 2-methylfuran and 3-  
236 methylfuran, *Atmos. Environ.*, 43, 1603-1612, doi:10.1016/j.atmosenv.2008.12.019, 2009.”

237 **Page 22199, Line 29 – There should be an and before Fanelli**

238 P22199 L29 We have added an “and” changing the reference to “Natangelo, M., Mangiapan, S., Bagnati, R.,  
239 Benfenati, E., and Fanelli, R.: Increased concentrations of nitrophenols in leaves from a damaged forestal site,  
240 *Chemosphere*, 38, 1495–1503, doi: 10.1016/S0045-6535(98)00370-1, 1999.”

241 **General Comment: -The order of the references in the citations seems to vary through the paper of being in**  
242 **alphabetical or chronological order. Either way is actually fine, but it should be consistent throughout. I have**  
243 **tried to point out the ones I noticed below in my specific comments.**

244 We thank the referee for noticing the alphabetical and chronological variations in our reference citations. We have  
245 addressed all discrepancies as indicated below.

246 P22166 L7-9 Re-ordered to read “(Reid et al., 1998; Trentmann et al., 2005; Alvarado and Prinn, 2009; Yokelson et  
247 al., 2009; Vakkari et al., 2014)”

248 P22174 L10 Re-ordered to read “(Akagi et al., 2011; Yokelson et al., 2013, etc.)”

249 P22174 L19 Re-ordered to read “(Liu et al., 2012; Pittman Jr. et al., 2012; Li et al., 2013; more citations in Table  
250 S4)”

251 P22174 L25 Re-ordered to read “(Lobert, 1991; Ge et al., 2011; etc.)”

252 P22177 L11-12 Re-ordered to read “(Phoussongphouang and Arey, 2002; Ziemann and Atkinson, 2012).”

253 P22177 L21 Re-ordered to read “(Andreae and Merlet, 2001; Henze et al., 2008)”



254 P22180 L5-6 Re-ordered to read “(Atkinson et al., 1992; Olariu et al., 2002; Harrison et al., 2005; Lauraguais et al.,  
255 2014)”

256 P22180 L12-13 Re-ordered to read “(Kitanovski et al., 2012; Desyaterik et al., 2013; Mohr et al., 2013; Zhang et al.,  
257 2013)”

258 P22180 L15-16 Re-ordered to read “(Inuma et al., 2010; Kitanovski et al., 2012; Lauraguais et al., 2014)”

259 P22181 L5-6 Re-ordered to read “(Cabañas et al., 2005; Villanueva et al., 2007)

260 P22182 L21-22 Re-ordered to read “(Lobert et al., 1991; Schade and Crutzen, 1995; Ma and Hays et al., 2008;  
261 Barnes et al., 2010; Ge et al., 2011).”

262 P22184 L7 Re-ordered to read “(Friedli et al., 2001; Meinardi et al., 2003; Akagi et al., 2011; Simpson et al., 2011)”

263 P22185 L11 Re-ordered to read “(Holzinger et al., 1999; Christian et al., 2004)”

264 P22186 L11-12 Re-ordered to read “(Christian et al., 2003; Akagi et al., 2011; Yokelson et al., 2013; St. Clair et al.,  
265 2014)”

266 P22187 L10 Re-ordered to read “(Simpson et al., 2011; Akagi et al., 2013)

267 **Tables Table 2 -Line 2 of the caption - Suggest adding the word type after fuel**

268 The table caption now reads “Table 2a. Emission ratios to benzene, phenol, and furan for aromatic hydrocarbons,  
269 phenolic compounds, and substituted furans in lumped fuel-type categories.

270 **Figures Figure 1 -Suggest labeling each plot as a, b, or c since they are referred to this way in the text**

271 Thanks for the suggestion and we have labeled the three sections of the figure a, b, and c.

272 **Figure 3 -Suggest indicating in the caption that the number of oxygen atoms for the three various oxygenated  
273 classes are indicated in parenthesis in the legend**

274 This has been addressed both in the text and in the figure caption as initially prompted by Anonymous Referee 1.

275 **Figure 5 -Line 3 of the caption - Suggest changing considered the fuel average to considered in the fuel  
276 average**

277 We have changed the caption to read “Figure 5. (a) The distribution in average fuel EF for several phenolic  
278 compounds, where compound specific contributions are indicated by color. The EFs for compounds additionally  
279 analyzed a single time for select fires are included but are not a true average. (b) The linear correlation of select  
280 phenolic compounds with phenol during an organic hay burn (Fire 119).”

281 **Voluntary changes:**

282 P22190, L11: “was” changed to “were” – L12: changed “regions biofuel” to “regions where biofuel” - L18:  
283 changed “chlorine organic gases were not readily detectable” to “chlorine containing organic gases were not readily  
284 observed”

285 We changed “Ringed Aromatics” to “Aromatics” on the y axis label of Figure 4.

286 We eliminated m/z 81 from the Supplementary Tables because it is a fragment considered in the calculation of total  
287 carbon, but not a primary emission.

288 We added the EFs for the tire fire to the supplementary tables based on using HCOOH as an internal standard

289 We've also added several rows of additional species to Table S3. We have also extended the column averages in the  
290 supplemental tables for fuel types to include extended species even if there was no standard deviation.

291 We added an extra row for MCE in Tables 2a and 2b.

292 At the end of the acknowledgements we added: "We thank C. Geron for providing a sample of NC peat."

293 In the reference section the following reference we should eliminate misplaced "5": "Müller, M., Mikoviny, T., Jud,  
294 W., D'Anna, B., and Wisthaler, A.: A new software tool for the 5analysis of high resolution PTR-TOF mass spectra,  
295 *Chemometr. Intell. Lab.*, 127, 158–165, doi:10.1016/j.chemolab.2013.06.011, 2013."

296 It was changed to: "Müller, M., Mikoviny, T., Jud, W., D'Anna, B., and Wisthaler, A.: A new software tool for the  
297 analysis of high resolution PTR-TOF mass spectra, *Chemometr. Intell. Lab.*, 127, 158–165,  
298 doi:10.1016/j.chemolab.2013.06.011, 2013."

299 In Figure 6's caption we've changed "furan derivatives" to "substituted furans". We've also clarified which  
300 compounds are not averaged: The caption now reads "Figure 6. (a) The distribution in average fuel EF for furan and  
301 substituted furans, where individual contributions are indicated by color. The EFs for substituted furans additionally  
302 analyzed a single time are not true averages. (b) The linear correlation of furan with select substituted furans for an  
303 African grass fire (Fire 49)."

304 In Figure 4's caption we've changed "The EF for p-Cymene is only calculated for select burns and should not be  
305 considered an average for each particular fuel type." To: "The EFs for p-Cymene are only calculated for select fires  
306 and should not be considered a true average."

307 Please update the following reference: "Yu, F. and Luo, G.: Modelling of gaseous dimethylamine in the global  
308 atmosphere: impacts of oxidation and aerosol uptake, *Atmos. Chem. Phys. Discuss.*, 14, 17727–17748,  
309 doi:10.5194/acpd-14-17727-2014, 2014." To "Yu, F. and Luo, G.: Modeling of gaseous methylamines in the global  
310 atmosphere: impacts of oxidation and aerosol uptake, *Atmos. Chem. Phys.*, 14, 12455–12464, doi:10.5194/acp-14-  
311 12455-2014, 2014."

312 Please update the following reference: "Stockwell, C. E., Yokelson, R. J., Kreidenweis, S. M., Robinson, A. L.,  
313 DeMott, P. J., Sullivan, R. C., Reardon, J., Ryan, K. C., Griffith, D. W. T., and Stevens, L.: Trace gas emissions  
314 from combustion of peat, crop residue, biofuels, grasses, and other fuels: configuration ad FTIR component of the  
315 fourth Fire Lab at Missoula Experiment (FLAME-4), *Atmos. Chem. Phys. Discuss.*, 14, 10061-10134,  
316 doi:10.5194/acpd-14-10061-2014, 2014. " To: "Stockwell, C. E., Yokelson, R. J., Kreidenweis, S. M., Robinson, A.  
317 L., DeMott, P. J., Sullivan, R. C., Reardon, J., Ryan, K. C., Griffith, D. W. T., and Stevens, L.: Trace gas emissions  
318 from combustion of peat, crop residue, biofuels, grasses, and other fuels: configuration and Fourier transform  
319 infrared (FTIR) component of the fourth Fire Lab at Missoula Experiment (FLAME-4), *Atmos. Chem. Phys.*, 14,  
320 9727-9754, doi:10.5194/acp-14-9727-2014, 2014."

321 **Characterization of biomass burning smoke from cooking fires, peat,**  
322 **crop residue and other fuels with high resolution proton-transfer-**  
323 **reaction time-of-flight mass spectrometry**

324

325 **C. E. Stockwell<sup>1</sup>, P. R. Veres<sup>2,3</sup>, J. Williams<sup>4</sup>, R. J. Yokelson<sup>1</sup>**

326 [1] University of Montana, Department of Chemistry, Missoula, MT, USA

327 [2] Cooperative Institute for Research in Environmental Sciences, University of Colorado, Boulder, CO, USA

328 [3] Chemical Sciences Division, Earth System Research Laboratory, National Oceanic and Atmospheric  
329 Administration, Boulder, CO, USA

330 [4] Max Planck Institute for Chemistry, Atmospheric Chemistry Department, 55128 Mainz, Germany

331 **Abstract**

332 We deployed a high-resolution proton-transfer-reaction time-of-flight mass spectrometer (PTR-TOF-MS) to  
333 measure biomass burning emissions from peat, crop-residue, cooking fires, and many other fire types during the  
334 fourth Fire Lab at Missoula Experiment (FLAME-4) laboratory campaign. A combination of gas standards  
335 calibrations and composition sensitive, mass dependent calibration curves were applied to quantify gas-phase non-  
336 methane organic compounds (NMOCs) observed in the complex mixture of fire emissions. We used several  
337 approaches to assign best identities to most major “exact masses” including many high molecular mass species.  
338 Using these methods approximately 80-96% of the total NMOC mass detected by PTR-TOF-MS and [Fourier](#)  
339 [transform infrared \(FTIR\) spectroscopy](#) was positively or tentatively identified for major fuel types. We report data  
340 for many rarely measured or previously unmeasured emissions in several compound classes including aromatic  
341 hydrocarbons, phenolic compounds, and furans; many of which are suspected secondary organic aerosol precursors.  
342 A large set of new emission factors (EFs) for a range of globally significant biomass fuels is presented.  
343 Measurements show that oxygenated NMOCs accounted for the largest fraction of emissions of all compound  
344 classes. In a brief study of various traditional and advanced cooking methods, the EFs for these emissions groups  
345 were greatest for open 3-stone cooking in comparison to their more advanced counterparts. Several little-studied  
346 nitrogen-containing organic compounds were detected from many fuel types that together accounted for 0.1-8.7% of  
347 the fuel nitrogen and some may play a role in new particle formation.

348 **1 Introduction**

349 Biomass burning (BB) injects large amounts of primary, fine carbonaceous particles and trace gases into the global  
350 atmosphere and significantly impacts its physical and chemical properties (Crutzen and Andreae, 1990; Bond et al.,  
351 2004, 2013). While BB emissions are recognized as the second largest global atmospheric source of gas-phase non-  
352 methane organic compounds (NMOCs) after biogenic emissions, a significant portion of the higher molecular  
353 weight species remain unidentified (Christian et al., 2003; Warneke et al., 2011; Yokelson et al., 2013). It is widely

354 accepted that the addition of large amounts of these highly reactive species into the atmosphere alters chemistry on  
355 local to global scales (Andreae and Merlet, 2001; Andreae et al., 2001; Karl et al., 2007). NMOCs particularly  
356 impact smoke evolution by rapid formation of secondary organic aerosols (SOA) and secondary gases including  
357 photochemical ozone (O<sub>3</sub>) (Reid et al., 1998; Trentmann et al., 2005; Alvarado and Prinn, 2009; Reid et al., 1998;  
358 ~~Trentmann et al., 2005~~; Yokelson et al., 2009; Vakkari et al., 2014).

359 The many unknowns and initial gas-phase variability of BB emissions limit our ability to accurately model the  
360 atmospheric impacts of fire at all scales (Trentmann et al., 2005; Mason et al., 2006; Alvarado and Prinn, 2009;  
361 Alvarado et al., 2009; Wiedinmyer et al., 2011). Estimating or modeling the potential of smoke photochemistry to  
362 generate secondary aerosols or O<sub>3</sub> requires realistic estimates of NMOC emissions in fresh smoke and knowledge of  
363 the chemical processing environment. Measurements capable of identifying and quantifying rarely measured and  
364 presently unidentified emissions of NMOCs, in particular the chemically complex low volatility fraction, are vital to  
365 advance current understanding of the BB impact on air quality and climate.

366 Proton-transfer-reaction time-of-flight mass spectrometry (PTR-TOF-MS) is an emerging technique that  
367 simultaneously detects most NMOCs present in air samples including: oxygenated organics, aromatics, alkenes, and  
368 nitrogen-containing species at parts per trillion detection limits (pptv) (Jordan et al., 2009; Graus et al., 2010). The  
369 instrument uses H<sub>3</sub>O<sup>+</sup> reagent ions to ionize NMOCs via proton-transfer-reactions to obtain high resolution mass  
370 spectra of protonated NMOCs with a low degree of molecular fragmentation at a mass accuracy sufficient enough to  
371 determine molecular formulas (C<sub>w</sub>H<sub>x</sub>N<sub>y</sub>O<sub>z</sub>).

372 Although there are many advantages to PTR-TOF-MS over conventional PTR quadrupole mass spectrometers  
373 (increased mass range, high measurement frequency, and high mass resolution) there remain several difficulties  
374 involving PTR technology including (1) detection is limited to molecules with a proton affinity greater than water,  
375 (2) complicated spectra due to parent ion fragmentation or cluster ion formation, and (3) the inability of the method  
376 to isolate isomers. Despite the limitations of this technology, PTR-TOF-MS is ideal for studying complex gaseous  
377 mixtures such as those present in BB smoke.

378 This study was carried out as part of a large scale experiment to characterize the initial properties and aging of gas-  
379 and particle-phase emissions in smoke from globally significant fuels. Experiments were conducted from October to  
380 November of 2012 during the fourth Fire Lab at Missoula Experiment (FLAME-4) as detailed by Stockwell et al.  
381 (2014). A major goal of the study focused on the identification and quantification of highly reactive NMOCs in  
382 order to: (1) better characterize the overall chemical and physical properties of fresh BB emissions, (2) better  
383 understand the distribution of emitted carbon across a range of volatilities in fresh and aged smoke, and (3) improve  
384 the capability of current photochemical models to simulate the climatic, radiative, chemical, and ecological impacts  
385 of smoke on local to global scales. In a companion paper the FLAME-4 emissions were compared extensively to  
386 field measurements of fire emissions and they were shown to be representative of “real-world” biomass burning  
387 either as is or after straightforward adjustment procedures detailed therein (Stockwell et al., 2014). In this work, we  
388 describe, to our knowledge, the first application of PTR-TOF-MS technology to laboratory biomass burning smoke

389 | ~~to characterize emissions from a variety of authentic globally significant fuels. In this work, we perform, to our~~  
390 | ~~knowledge, the first application of PTR-TOF-MS technology to laboratory biomass burning smoke to characterize~~  
391 | ~~emissions from a variety of authentic globally significant fuels.~~ We report on several new or rarely measured gases  
392 | and present a large set of useful emission ratios (ERs) and emission factors (EFs) for major fuel types that can  
393 | inform/update current atmospheric models.

## 394 | **2 Experimental details**

### 395 | **2.1 Missoula fire sciences laboratory**

396 | The US Forest Service Fire Sciences Laboratory (FSL) in Missoula, MT houses a large indoor combustion room  
397 | described in detail elsewhere (Christian et al., 2003; Burling et al., 2010; Stockwell et al., 2014). Briefly, fuels are  
398 | burned on a bed located directly below a 1.6 m diameter exhaust stack. The room is slightly pressurized by outdoor  
399 | air that generates a large flow that entrains the fire emissions up through the stack. Emissions are drawn into  
400 | sampling lines fixed in the stack at a platform height 17 m above the fuel bed. Past studies demonstrated that  
401 | temperature and mixing ratios are constant across the width of the stack at the platform height, confirming well-  
402 | mixed emissions (Christian et al., 2004).

403 | Burns were conducted using two separate configurations as described in Stockwell et al. (2014). In this paper we  
404 | will focus on 125 of the 157 burns. During these fires, well mixed fresh smoke was sampled directly from the  
405 | combustion stack by PTR-TOF-MS, roughly 5 s after emission. Results obtained during the remaining burns  
406 | investigating photochemically processed smoke composition in dual smog chambers with a suite of state-of-the-art  
407 | instrumentation are presented elsewhere (Tkacik et al., 2014).

### 408 | **2.2 Biomass fuels**

409 | Descriptions and ignition methods of each fuel type burned during FLAME-4 are detailed in Stockwell et al. (2014).  
410 | Authentic globally significant fuels were collected including: African savanna grasses; US grasses; US and Asian  
411 | crop-residue; Indonesian, temperate, and boreal peat; temperate and boreal coniferous canopy fuels; woods in  
412 | traditional and advanced cooking stoves; shredded tires; and trash. The range of fuel loading was chosen to simulate  
413 | real-world conditions for the investigated fuel types with global examples of biomass consumption shown in Akagi  
414 | et al. (2011).

### 415 | **2.3 Proton-transfer-reaction time-of-flight mass spectrometer**

416 | Real-time analysis of NMOCs was performed using a commercial PTR-TOF-MS 8000 instrument from Ionicon  
417 | Analytik GmbH (Innsbruck, Austria) that is described in detail by Jordan et al. (2009). The PTR-TOF-MS sampled  
418 | continuously at a frequency of 0.2 Hz through heated PEEK tubing (0.0003 m o.d., 80°C) positioned facing upward  
419 | to limit particulate uptake. The instrument was configured with a mass resolution ( $m/\Delta m$ ) in the range of 4000 to  
420 | 5000 at  $m/z$  21 and a typical mass range from  $m/z$  10-600. The drift tube was operated at 600 V with a pressure of  
421 | 2.30 mbar at 80 °C ( $E/N \sim 136$ Td, with E as the electric field strength and N as the concentration of neutral gas; 1

422  $T_d=10^{-17}$  V cm<sup>2</sup>). A dynamic dilution system was set up to reduce the concentration of sampled smoke and minimize  
423 reagent ion depletion. Mass calibration was performed by permeating 1,3-diiodobenzene (protonated parent mass at  
424  $m/z$  330.85; fragments at  $m/z$  203.94 and 204.94) into a 1 mm section of Teflon tubing used in the inlet flow system.  
425 The high mass accuracy of the data allowed for the determination of the atomic composition of protonated NMOC  
426 signals where peaks were clearly resolved. The post-acquisition data analysis to retrieve counts per second based on  
427 peak analysis was performed according to procedures described in detail elsewhere (Müller et al., 2013, 2011,  
428 2010). An initial selection of ions (~68 masses up to  $m/z$  ~143) was chosen based upon incidence and abundance for  
429 post-acquisition analysis. In select cases (nominally one fire of each fuel type), additional compounds (~50 masses)  
430 were analyzed and are reported separately within this paper. A reasonable estimation procedure showed that the  
431 peaks selected for analysis accounted for >99% of the NMOC mass up to  $m/z$  165 in our PTR-TOF-MS spectra. An  
432 earlier BB study (Yokelson et al., 2013) using mass scans to  $m/z$  214 found that ~1.5% of NMOC mass was present  
433 at  $m/z > 165$ .

434 Calibration of the PTR-TOF-MS was performed every few days at the FSL using a bottle gas standard (Apel-Riemer  
435 Environmental). Calibrations were performed by adding a known quantity of calibration gas directly to the end of  
436 the PTR-TOF-MS sample inlet. The calibration mixture included: formaldehyde (HCHO); methanol (CH<sub>3</sub>OH);  
437 acetonitrile (CH<sub>3</sub>CN); acetaldehyde (CH<sub>3</sub>CHO); acetone (C<sub>3</sub>H<sub>6</sub>O); dimethyl sulfide (C<sub>2</sub>H<sub>6</sub>S); isoprene (C<sub>5</sub>H<sub>8</sub>);  
438 methyl vinyl ketone (C<sub>4</sub>H<sub>6</sub>O); methyl ethyl ketone (C<sub>4</sub>H<sub>8</sub>O); benzene (C<sub>6</sub>H<sub>6</sub>); toluene (C<sub>6</sub>H<sub>5</sub>CH<sub>3</sub>); p-xylene (C<sub>8</sub>H<sub>10</sub>);  
439 1,3,5-trimethylbenzene (C<sub>9</sub>H<sub>12</sub>); and  $\alpha$ -pinene (C<sub>10</sub>H<sub>16</sub>).

440 The normalized sensitivity of the instrument (ncps/ppbv) was determined for calibrated compounds based on the  
441 slope of the linear fit of signal intensities (normalized to the H<sub>3</sub>O<sup>+</sup> signal, ~10<sup>6</sup> cps) versus a range of volumetric  
442 mixing ratios (VMR). Multi-point calibration curves varied due to instrumental drift and dilution adjustments,  
443 accordingly, and average calibration factors (CFs, ncps/ppbv) were determined throughout the field campaign as  
444 described by Warneke et al. (2011) and were used to calculate concentrations.

445 Quantification of the remaining species was performed using calculated mass-dependent calibration factors based on  
446 the measured calibration factors. Figure 1a shows the spread in the normalized response of compounds versus mass  
447 (labeled by compound name) overlaid with the linearly fitted mass-dependent, transmission curve (black markers  
448 and dotted line). It is clear from Fig. 1a that the oxygenated species (blue labels) and the hydrocarbon species (green  
449 labels) exhibit a slightly different mass dependent behavior, however, both groups show a linear increase with mass  
450 that is similar to that observed for the transmission efficiency (Fig. 1b and 1c). To reduce bias, mass dependent  
451 calibration factors were determined using a linear approximation for oxygenated and hydrocarbon species separately  
452 (Fig. 1b and 1c).  $\alpha$ -Pinene was not included in the linear approximation for hydrocarbons as this compound is well-  
453 known to be susceptible to substantial fragmentation in the drift tube. Sulfur and nitrogen-containing compounds  
454 were considered collectively and together they more closely follow the trend of the oxygenated species. Thus, in  
455 cases where a compound contains a non-oxygen heteroatom (such as methanethiol), the mass dependent calibration  
456 factor was determined using the relationship established using the oxygenated species. Calibration factors were then  
457 determined according to the exact mass for all peaks where the chemical formula has been determined. Our

458 approach does not yet account for the potential for ions to fragment and/or cluster, however, we expect this impacts  
459 less than 30% of NMOC and usually to a small degree for any individual species. These latter issues change the  
460 mass distribution of observed carbon, but should not have a large effect on the total observed carbon.

461 It is difficult to assess the overall error introduced using this method of calibration factor approximation, as only a  
462 limited number of comparable measurements of calibration factors are available. The deviation of measured  
463 calibration factors for species contained in the gas standard from the linear approximation yields a range of errors  
464 ( $21 \pm 19\%$ ) with a maximum of 50% observed in all cases (excluding  $\alpha$ -pinene, for reasons detailed above). While  
465 PTR-TOF-MS is typically known as a soft ionization method, fragmentation is common among higher molecular  
466 weight species and therefore needs to be considered as a limitation of this technique. For the individual species  
467 identified it would be misleading to give a set error based on this limited analysis, however, in the absence of any  
468 known molecular fragmentation a maximum error of 50% is prescribed, but with larger errors possible for  
469 compounds with N and S heteroatoms. Better methods for the calculation of mass dependent calibration factors by  
470 compound class should be developed in the near future to improve the accuracy of volatile organic compound  
471 (VOC) measurements using PTR-TOF-MS.

## 472 2.4 OP-FTIR

473 To enhance application of the MS data, emission ratios to carbon monoxide (CO) were calculated where possible  
474 using measurements from an open-path Fourier transform infrared (OP-FTIR) spectrometer described elsewhere  
475 (Stockwell et al., 2014). The system includes a Bruker Matrix-M IR Cube spectrometer with an open White cell that  
476 was positioned to span the width of the stack to sample the continuously rising emissions. The spectral resolution  
477 was set to  $0.67 \text{ cm}^{-1}$  and spectra were collected every 1.5 s with a duty cycle greater than 95%. Other gas-phase  
478 species quantified by this method included carbon dioxide ( $\text{CO}_2$ ), methane ( $\text{CH}_4$ ), ethyne ( $\text{C}_2\text{H}_2$ ), ethene ( $\text{C}_2\text{H}_4$ ),  
479 propylene ( $\text{C}_3\text{H}_6$ ), formaldehyde (HCHO), formic acid (HCOOH), methanol ( $\text{CH}_3\text{OH}$ ), acetic acid ( $\text{CH}_3\text{COOH}$ ),  
480 glycolaldehyde ( $\text{C}_2\text{H}_4\text{O}_2$ ), furan ( $\text{C}_4\text{H}_4\text{O}$ ), water ( $\text{H}_2\text{O}$ ), nitric oxide (NO), nitrogen dioxide ( $\text{NO}_2$ ), nitrous acid  
481 (HONO), ammonia ( $\text{NH}_3$ ), hydrogen cyanide (HCN), hydrogen chloride (HCl), and sulfur dioxide ( $\text{SO}_2$ ) and were  
482 obtained by multi-component fits to selected regions of the mid-IR transmission spectra with a synthetic calibration  
483 non-linear least-squares method (Griffith, 1996; Yokelson et al., 2007).

484 The OP-FTIR system had the highest time resolution with no sampling line, storage, fragmentation, or clustering  
485 artifacts; thus, for species in common with PTR-TOF-MS, the OP-FTIR data was used as the primary data. The  
486 results from the inter-comparison (for methanol) of OP-FTIR and PTR-TOF-MS show excellent agreement using an  
487 orthogonal distance regression to determine slope ( $0.995 \pm 0.008$ ) and the  $R^2$  coefficient (0.789). The agreement  
488 between these two measurements is within the uncertainties of both instruments. This result is consistent with the  
489 good agreement for several species measured by both PTR-MS and OP-FTIR observed in numerous past studies of  
490 laboratory biomass burning emissions (Christian et al., 2004; Karl et al., 2007; Veres et al. 2010; Warneke et al.,  
491 2011).

## 492 2.5 Emission ratio and emission factor determination

493 Excess mixing ratios (denoted  $\Delta X$  for each species “X”) were calculated by applying an interpolated background  
 494 correction (determined from the pre and post fire concentrations). The molar emission ratio (ER) for each species  
 495 “X” relative to  $\text{CH}_3\text{OH}$  ( $\Delta X/\Delta\text{CH}_3\text{OH}$ ) is the ratio between the integral of  $\Delta X$  over the entire fire relative to the  
 496 integral of  $\Delta\text{CH}_3\text{OH}$  over the entire fire. We selected  $\text{CH}_3\text{OH}$  as the species in common with the OP-FTIR to serve  
 497 as an internal standard for the calculation of the fire-integrated ERs of each species X to CO (Supplement Table S1).  
 498 We do this by multiplying the MS-derived ER ( $\Delta X/\Delta\text{CH}_3\text{OH}$ ) by the FTIR-derived ER ( $\Delta\text{CH}_3\text{OH}/\Delta\text{CO}$ ), which  
 499 minimizes error due to occasional reagent ion depletion or the different sampling frequencies between instruments  
 500 that would impact calculating  $\Delta X$  to  $\Delta\text{CO}$  directly. Several fires have been excluded from this calculation as data  
 501 was either not collected by OP-FTIR and/or PTR-TOF-MS or alternatively, methanol data could not be applied for  
 502 the conversion because (1) the mixing ratios remained below the detection limit or (2) methanol was used to assist  
 503 ignition purposes during a few fires. As discussed in Sect. 2.3.1, ~50 additional masses were analyzed for selected  
 504 fires and the ERs (to CO) for these fires are included in the bottom panels of Table S1. The combined ERs to CO  
 505 from the FTIR and PTR-TOF were then used to calculate emission factors (EFs,  $\text{g kg}^{-1}$  dry biomass burned) by the  
 506 carbon mass-balance method (CMB), based on the assumption that all of the burned carbon is volatilized and that all  
 507 of the major carbon-containing species have been measured (Ward and Radke, 1993; Yokelson et al., 1996, 1999;  
 508 Burling et al., 2010). EFs were previously calculated solely from FLAME-4 OP-FTIR data as described in Stockwell  
 509 et al. (2014) and a new larger set of EFs, which include more carbon-containing species quantified by PTR-TOF-  
 510 MS, are now shown in Supplement Table S2. With the additional carbon compounds quantified by PTR-TOF-MS,  
 511 the EFs calculated by CMB decreased ~1-2% for most major fuels with respect to the previous EFs reported in  
 512 Stockwell et al. (2014). In the case of peat and sugar cane fires, the OP-FTIR derived EFs are now reduced by a  
 513 range of ~2-5% and 3.5-7.5%, respectively. Along with these small reductions, this work now provides EFs for  
 514 many additional species that were unavailable in Stockwell et al. (2014). Finally, the EFs reported in Supplement  
 515 Table S3 were adjusted (when needed) according to procedures established in Stockwell et al. (2014) to improve  
 516 laboratory representation of real-world biomass burning emissions. This table contains the EF we recommend other  
 517 workers use and it appears in the Supplement only because of its large size. In addition to the comparisons  
 518 considered in Stockwell et al. (2014), we find that our EFs in Table S3 are consistent (for the limited number of  
 519 overlap species) with additional, recent field studies including Kudo et al. (2014) for Chinese crop residue fires and  
 520 Geron and Hays (2013) for NC peat fires.

521 Fire emissions are partially dependent on naturally changing combustion processes. To estimate the relative amount  
 522 of smoldering and flaming combustion that occurred over the course of each fire, the modified combustion  
 523 efficiency (MCE) is calculated by (Yokelson et al., 1996):

$$524 \quad MCE = \frac{\Delta\text{CO}_2}{\Delta\text{CO}_2 + \Delta\text{CO}} = \frac{1}{\left(1 + \left(\frac{\Delta\text{CO}}{\Delta\text{CO}_2}\right)\right)} \quad (1)$$



525 Though flaming and smoldering combustion often occur simultaneously, a higher MCE value (approaching 0.99)  
526 designates relatively pure flaming combustion (more complete oxidation), a lower MCE (0.75-0.84) designates pure  
527 smoldering combustion and, thus, an MCE of ~0.90 represents roughly equal amounts of flaming and smoldering.  
528 Each fire-integrated MCE is reported in Tables S1-S2S3.

### 529 3 Results

#### 530 3.1 Peak assignment

531 As exemplified by a typical PTR-TOF-MS spectrum of diluted smoke (Fig. 2a), the complexity of BB smoke  
532 emissions presents challenges to mass spectral interpretation and ultimately emissions characterization. Figure 2b  
533 shows a smaller mass range of the smoke sample shown in Fig. 2a on a linear scale to illustrate the typical relative  
534 importance of the masses (note the intensity of acetaldehyde ( $m/z$  45) and acetic acid plus glycolaldehyde ( $m/z$  61),  
535 which together account for almost 25% of the total signal). Although the spectra are very complex, systematic  
536 treatment of the burn data, assisted at some  $m/z$  by extensive published “off-line” analyses can generate reasonable  
537 assignments for many major peaks and result in useful emissions quantification.

538 As described earlier, the PTR-TOF-MS scans have sufficiently high resolution to assign molecular formulas  
539 ( $C_wH_xN_yO_z$ ) to specific ion peaks by matching the measured exact mass with possible formula candidates for the  
540 protonated compound. Specific compound identification for formula candidates can be unambiguous if only one  
541 species is structurally plausible or explicit identification of the compound had previously been confirmed by BB  
542 smoke analysis ([Akagi et al., 2011](#); Yokelson et al., 2013; ~~[Akagi et al., 2014](#)~~, etc.). Supplement Table S4 lists every  
543 mass and formula assignment for observable peaks up to  $m/z$  165 and categorizes each mass as a confirmed identity,  
544 a tentative (most likely) species assignment, or an unknown compound. For several confirmed identities, the most  
545 abundant species at that exact mass is listed with likely contributions to the total signal from the secondary species  
546 listed in column 5. Most of the tentatively identified species have, to our knowledge, typically not been directly  
547 observed in BB smoke, but have been frequently verified with off-line techniques as major products in the extensive  
548 literature describing biomass pyrolysis experiments of various fuel types (Liu et al., 2012; [Li et al., 2013](#); Pittman Jr.  
549 et al., 2012; [Li et al., 2013](#); more citations in Table S4). Several tentative assignments are supported by off-line  
550 analyses being published elsewhere (Hatch et al., 2014), for example, simultaneous grab samples analyzed by two  
551 dimensional gas chromatography (2D-GC) support tentative assignments for furan methanol, salicylaldehyde, and  
552 benzofuran. In the case of nitrogen-containing formulas, the suggested compounds have been observed in the  
553 atmosphere, tobacco smoke, or lab fire smoke at moderate levels ([Lobert, 1991](#); Ge et al., 2011; ~~[Lobert, 1991](#)~~; etc.).  
554 Select studies supporting these assignments are referenced in the mass table with alternative possibilities also listed.  
555 An exhaustive list of all the many papers supporting the assignments is beyond the scope of this work. Several  
556 remaining compounds are also classified as tentative assignments as the identities designated are thought to be the  
557 most structurally likely. We anticipate that some or even many of the tentative assignments (and a few of the  
558 confirmed assignments) will be refined in future years as the results of more studies become available. We offer the

559 tentative assignments here as a realistic starting point that improves model input compared to an approach in which  
560 these species are simply ignored.

### 561 **3.2 Unidentified compounds**

562 The identities of several compounds remain unknown, especially at increasing mass where numerous structural and  
563 functional combinations are feasible. However, compared to earlier work at unit mass resolution (Warneke et al.,  
564 2011; Yokelson et al., 2013), the high-resolution capability of the PTR-TOF-MS has enhanced our ability to assign  
565 mass peaks while always identifying atomic composition. With unit mass resolution spectrometers, FTIR, and GC-  
566 MS grab samples, Yokelson et al. (2013) estimated that ~31% to ~72% of the gas-phase NMOC mass remained  
567 unidentified for several fuel types. For similar, commonly burned biomass fuels (chaparral, grasses, crop residue,  
568 etc.), considering a PTR-TOF range up to  $m/z$  165, we estimate that ~7% of the detected NMOC mass remains  
569 unidentified, while ~12% is tentatively assigned using selection criteria described in Sect. 3.1. The compounds  
570 considered in this study cover a smaller mass range (up to  $m/z$  165 rather than  $m/z$  214) than in the earlier study, but  
571 in that earlier study, the compounds in the range  $m/z$  165-214 accounted for only ~1.5% of the NMOC mass  
572 (Yokelson et al., 2013). Thus, the molecular formula assignments from the PTR-TOF aided in positive and tentative  
573 identification and quantification resulting in a reduction of the estimate of unidentified NMOCs from ~31% down to  
574 ~7%.

575 Calculations of unidentified and tentatively assigned emissions relative to overall NMOC emissions (including FTIR  
576 species) for several lumped fuel groups are summarized in Table 1. Estimates of total intermediate and semivolatile  
577 gas-phase organic compounds (IVOC + SVOC, estimated as the sum of species at or above the mass of toluene) are  
578 also included as these less volatile compounds are likely to generate SOA via oxidation and/or cooling. Similar to  
579 previous organic soil fire data, the percentages of unidentified and tentatively identified NMOCs for peat burns are  
580 significantly larger than for other fuel types (sum ~37%) and they could be a major source of impacts and  
581 uncertainty during El-Niño years when peat combustion is a major global emission source (Page et al., 2002; Akagi  
582 et al., 2011).

### 583 **4 Discussion**

584 For all fuel types, there is noticeable variability concerning which compounds have the most significant emissions.  
585 Figure 3 includes both FTIR and PTR emissions grouped into the following categories: non-methane hydrocarbons,  
586 oxygenates containing only one oxygen, oxygenates containing two oxygen atoms, and oxygenates containing three  
587 oxygen atoms. Within these categories, the contribution from aromatics, phenolic compounds, and furans are further  
588 indicated. As shown in Fig. 3, oxygenated compounds account for the majority of the emissions for all fuels where  
589 EF calculations were possible (several fuels are excluded including tires and plastic bags due to insufficient FTIR  
590 methanol data). Oxygenated compounds containing only a single oxygen atom accounted for ~ 50% of the total raw  
591 mass signal ( $> m/z$  28, excluding  $m/z$  37) on average and normally had greater emissions than oxygenated  
592 compounds containing two oxygen atoms or hydrocarbons. Sugar cane has the highest emissions of oxygenated  
593 compounds as was noted earlier in the FTIR data (Stockwell et al., 2014) and is one of the few fuels where the

594 emissions of compounds containing two oxygens are the largest. To facilitate discussion we grouped many of the  
595 assigned (or tentatively assigned) mass peak features into categories including: aromatic hydrocarbons; phenolic  
596 compounds; furans and its derivatives; nitrogen-containing compounds; and sulfur-containing compounds; These  
597 categories do not account for the majority of the emitted NMOC mass, but account for most of the rarely-measured  
598 species reported in this work. We then also discuss and miscellaneous compounds at increasing  $m/z$ .

#### 599 **4.1 Aromatic hydrocarbons**

600 Aromatic hydrocarbons contributed most significantly to the emissions for several major fuel types including  
601 ponderosa pine, peat, and black spruce. The identities of these ringed structures are more confidently assigned due to  
602 the small H to C ratio at high masses. The aromatics confidently identified in this study include benzene ( $m/z$  79),  
603 toluene ( $m/z$  93), phenylacetylene ( $m/z$  103), styrene ( $m/z$  105), xylenes/ethylbenzene ( $m/z$  107), 1,3,5-  
604 trimethylbenzene ( $m/z$  121), and naphthalene ( $m/z$  129), while masses more tentatively assigned include  
605 dihydronaphthalene ( $m/z$  131), p-cymene ( $m/z$  135), and methylnaphthalenes ( $m/z$  143). All masses are likely to have  
606 minor contributions from other hydrocarbon species. The EFs for aromatic species quantified during all fires are  
607 averaged by fuel type and shown in Fig. 4a. The EF for p-cymene was only calculated for select burns and has been  
608 included in Fig. 4a for comprehensiveness.

609 Aromatic structures are susceptible to multiple oxidation pathways and readily drive complex chemical reactions in  
610 the atmosphere that are highly dependent on hydroxyl radical (OH) reactivity ([Phoungphouang and Arey, 2002](#);  
611 [Ziemann and Atkinson, 2012](#); [Phoungphouang and Arey, 2002](#)). Ultimately these gas-phase aromatic species have  
612 high yields for SOA as their physical and chemical evolution lead to lower volatility species that condense into the  
613 particle phase. SOA yields from these parent aromatic HCs have been shown to strongly vary depending on  
614 environmental parameters including relative humidity, temperature, aerosol mass concentration, and particularly the  
615 level of nitrogen oxides ( $\text{NO}_x$ ) and availability of  $\text{RO}_2$  radicals, further adding to the complexity in modeling the  
616 behavior and fate of these compounds (Ng et al., 2007; Song et al., 2007; Henze et al., 2008; Chhabra et al., 2010,  
617 2011; Im et al., 2014).

618 Biofuel and biomass burning together comprise the largest global atmospheric source of benzene ([Andreae and](#)  
619 [Merlet, 2001](#); Henze et al., 2008; [Andreae and Merlet, 2001](#)), thus not surprisingly benzene is a significant aromatic  
620 in our dataset. The ERs relative to benzene for the aromatics listed above are shown in Table 2 and are positively  
621 correlated with benzene as demonstrated by Fig. 4b. Henze et al. (2008) outlines how ERs to CO of major aromatics  
622 (benzene, xylene, and toluene) can be implemented as a part of a model to predict SOA formation. An identical or  
623 similar approach that incorporates the additional aromatics detected by PTR-TOF-MS in this work may be useful to  
624 predict the contribution of aromatics from BB to global SOA by various reaction pathways.

625 Toluene, another major emission, often serves as a model compound to study the formation of SOA from other  
626 small ringed volatile organic compounds (Hildebrandt et al., 2009). Black spruce yielded the greatest toluene ER (to  
627 benzene) during FLAME-4 ( $3.24 \pm 0.42$ ) and has been linked to significant OA enhancement during chamber photo-

628 oxidation aging experiments investigating open biomass burning emissions during FLAME-III, though not  
629 significant enough to account for all of the observed SOA (Hennigan et al., 2011).

630 Naphthalene is the simplest species in a class of carcinogenic and neurotoxic compounds known as polycyclic  
631 aromatic hydrocarbons (PAH) and was detected from all fuels. The rapid rate of photo-oxidation of these smaller-  
632 ringed gas-phase PAHs (including naphthalene and methylnaphthalenes) can have important impacts on the amount  
633 and properties of SOA formed and yields significantly more SOA over shorter timespans in comparison to lighter  
634 aromatics (Chan et al., 2009). Under low-NO<sub>x</sub> conditions (BB events generate NO<sub>x</sub> though at lower ratios to NMOC  
635 and/or CO than those present in urban environments) the SOA yield for benzene, toluene, and *m*-xylene was ~ 30%  
636 (Ng et al., 2007), while naphthalene yielded enhancements as great as 73% (Chan et al., 2009).

637 In summary, many of the species identified and detected during FLAME-4 are associated with aerosol formation  
638 under diverse ambient conditions (Fisseha et al., 2004; Na et al., 2006; Ng et al., 2007; Chan et al., 2009). We  
639 present here initial emissions for a variety of aromatics from major global fuels. A more focused study to probe the  
640 extent and significance of SOA formation in BB plumes by these aromatic precursors was performed by chamber  
641 oxidation during the FLAME-4 campaign and will be presented in Tkacik et al. (2014).

#### 642 **4.2 Phenolic compounds**

643 Phenol is detected at *m/z* 95. Earlier studies burning a variety of biomass fuels found that OP-FTIR measurements of  
644 phenol accounted for the observed PTR-MS signal at this mass even at unit mass resolution, though small  
645 contributions from other species such as vinyl furan were possible, but not detected (Christian et al., 2004). 2D-GC  
646 grab samples in FLAME-4 find that other species with the same formula (only vinyl furan) are present at levels less  
647 than ~2% of phenol (Hatch et al., 2014). Thus, we assume that within experimental uncertainty *m/z* 95 is a phenol  
648 measurement in this study and find that phenol is one of the most abundant oxygenated aromatic compounds  
649 detected. Several phenol derivatives were speciated for every fire and included catechol (*m/z* 111), vinylphenol (*m/z*  
650 121), salicylaldehyde (*m/z* 123), xylenol (*m/z* 123), and guaiacol (*m/z* 125) (Fig. 5a). Several additional species were  
651 quantified for selected fires and included cresol (*m/z* 109), creosol (*m/z* 139), 3-methoxycatechol (*m/z* 141), 4-  
652 vinylguaiacol (*m/z* 151), and syringol (*m/z* 155). The EFs for these additional phenolic compounds were calculated  
653 for select burns and are included in Fig. 5a with the regularly analyzed compounds. Significant emissions of these  
654 compounds are reported in Table 2 relative to phenol and the selected compounds shown in Fig. 5b demonstrate the  
655 tight correlation between these derivatives and phenol.

656 Phenol, methoxyphenols (guaiacols), dimethoxyphenols (syringol), and their derivatives are formed during the  
657 pyrolysis of lignin (Simoneit et al., 1993) and can readily react with OH radicals leading to SOA formation (Coeur-  
658 Tourneur et al, 2010; Lauraguais et al., 2014). Hawthorne et al. (1989,1992) found that phenols and guaiacols  
659 accounted for 21% and 45% of aerosol mass from wood smoke, while Yee et al. (2013) noted large SOA yields for  
660 phenol (24-44%), guaiacol (44-50%), and syringol (25-37%) by photo-oxidation chamber experiments under low-  
661 NO<sub>x</sub> conditions (<10 ppb).

662 Softwoods are considered lignin-rich and are associated predominately with guaiacyl units (Shafizadeh, 1982). Thus  
663 not surprisingly, guaiacol emissions were significant for ponderosa pine. Peat, an accumulation of decomposing  
664 vegetation (moss, herbaceous, woody materials), has varying degrees of lignin-content depending on the extent of  
665 decomposition, sampling depth, water table levels, etc. (Williams et al., 2003). The peat burns all emitted significant  
666 amounts of phenolic compounds, with noticeable compound specific variability between regions (Indonesia,  
667 Canada, and North Carolina). It is also noteworthy that sugar cane, which also produced highly oxygenated  
668 emissions based on FTIR and PTR-TOF-MS results, had the greatest total emissions of phenolic compounds.

669 The photochemical formation of nitrophenols and nitroguaiacols by atmospheric oxidation of phenols and  
670 substituted phenols via OH radicals in the presence of NO<sub>x</sub> is a potential reaction pathway for these compounds  
671 | ([Atkinson et al., 1992](#); [Olariu et al., 2002](#); Harrison et al., 2005; [Atkinson et al., 1992](#); [Olariu et al., 2002](#);  
672 | [Lauraguais et al., 2014](#)). Nitration of phenol in either the gas or aerosol phase is anticipated to account for a large  
673 portion of nitrophenols in the environment. Higher nitrophenol levels are correlated with increased plant damage  
674 (Hinkel et al., 1989; Natangelo et al., 1999) and consequently are linked to forest decline in central Europe and  
675 North America (Rippen et al., 1987). Nitrophenols are also important components of brown carbon and can  
676 | contribute to SOA formation in biomass burning plumes ([Kitanovski et al., 2012](#); [Desyaterik et al., 2013](#); [Mohr et](#)  
677 | [al., 2013](#); [Zhang et al., 2013](#); [Kitanovski et al., 2012](#)). Nitrated phenols including nitroguaiacols and methyl-  
678 nitrocatechols are suggested as suitable BB molecular tracers for secondary BB aerosol considering their reactivity  
679 | with atmospheric oxidants is limited ([Iinuma et al., 2010](#); [Kitanovski et al., 2012](#); [Lauraguais et al., 2014](#); [Iinuma et](#)  
680 | [al., 2010](#)). The oxidation products from the phenolic compounds detected in fresh smoke here have not been directly  
681 examined and would require a more focused study beyond the scope of this paper.

682 As with the aromatic compounds, the ERs provided in Table 2 can be used to estimate initial BB emissions of  
683 phenolic species, both rarely measured or previously unmeasured, from a variety of fuels in order to improve  
684 atmospheric modeling of SOA and nitrophenol formation.

### 685 **4.3 Furans**

686 Other significant oxygenated compounds include furan and substituted furans which arise from the pyrolysis of  
687 cellulose and hemicellulose. The substituted furans regularly quantified included 2-methylfuran (*m/z* 83), 2-furanone  
688 (*m/z* 85), furfural (*m/z* 97), furfuryl alcohol (*m/z* 99), methylfurfural (*m/z* 111), benzofuran (*m/z* 119), and  
689 hydroxymethylfurfural (*m/z* 127), while 2,5-dimethylfuran (*m/z* 97) and methylbenzofurans (*m/z* 133) were  
690 occasionally quantified. The ERs to furan for these compounds are summarized in Table 2 and Fig. 6a shows the  
691 average EF for the regularly quantified masses and the individual fire EFs for the occasionally quantified  
692 compounds.

693 Furan and substituted furans are oxidized in the atmosphere primarily by OH (Bierbach et al., 1995), but also by  
694 | NO<sub>3</sub> (Berndt et al., 1997) or Cl atoms ([Cabañas et al., 2005](#); Villanueva et al., 2007; [Cabañas et al., 2005](#)). Photo-  
695 | oxidation of furan, 2-methylfuran, and 3- methylfuran produce butenedial, 4-oxo-2-pentenal, and 2-  
696 methylbutenedial (Bierbach et al 1994, 1995). These products are highly reactive and can lead to free radical

697 (Wagner et al., 2003), SOA, or O<sub>3</sub> formation. In fact, aerosol formation from photo-oxidation chamber experiments  
698 has been observed for furans and their reactive intermediates listed above (Gomez Alvarez et al., 2009; Strollo and  
699 Ziemann, 2013). Even less is known concerning SOA yields from furans with oxygenated functional groups, which  
700 comprise the majority of the furan emissions in this study. Alvarado and Prinn (2009) added reaction rates for furans  
701 based on 2-methylfuran and butenedial values (Bierbach et al., 1994, 1995) to model O<sub>3</sub> formation in an aging  
702 savanna smoke plume. Although a slight increase in O<sub>3</sub> was observed after 60 min, it was not large enough to  
703 account for the observed O<sub>3</sub> concentrations in the plume. The furan and substituted furan ERs compiled here may  
704 help explain a portion of the SOA and O<sub>3</sub> produced from fires that cannot be accounted for based upon previously  
705 implemented precursors (Grieshop et al., 2009).

706 Furfural was generally the dominant emission in this grouping consistent with concurrent 2D-GC measurements  
707 (Hatch et al., 2014) while emissions from 2-furanone and furan also contributed significantly. Friedli et al. (2001)  
708 observed that ERs of alkyl furans linearly correlated with furan and concluded that these alkylated compounds likely  
709 break down to furan. Our expanded substituted furan list includes a variety of functionality ranging from oxygenated  
710 substituents to those fused with benzene rings for diverse fuel types. Similar to the behavior observed for alkylated  
711 furans, the emissions of our substituted furans linearly correlate with furan as shown in Fig. 6b. As noted for  
712 phenolic compounds, sugar cane produced the largest emissions of furans excluding Canadian peat, supporting sugar  
713 cane as an important emitter of oxygenated compounds. The emissions from furan, phenol, and their derivatives  
714 reflect variability in cellulose and lignin composition of different fuel types. Cellulose and hemicellulose compose  
715 ~75% of wood while lignin only accounts for ~25% on average (Sjöström, 1993). Accordingly the  $\Sigma$ furans/ $\Sigma$ phenols  
716 for initially analyzed compounds indicate that furans are dominant in nearly every fuel type.

#### 717 **4.4 Nitrogen-containing compounds**

718 Many nitrogen (N)-containing peaks were not originally selected for post-acquisition analysis in every fire.  
719 However, the additional analysis of selected fires included a suite of N-containing organic compounds to investigate  
720 their potential contribution to the N-budget and new particle formation (NPF). Even at our mass resolution of ~5000,  
721 the mass peak from N-compounds can sometimes be overlapped by broadened <sup>13</sup>C “isotope” peaks of major carbon  
722 containing emissions. This interference was not significant for the following species that we were able to quantify in  
723 the standard or added analysis: C<sub>2</sub>H<sub>3</sub>N (acetonitrile, calibrated), C<sub>2</sub>H<sub>7</sub>N (dimethylamine; ethylamine), C<sub>2</sub>H<sub>5</sub>NO  
724 (acetamide), C<sub>3</sub>H<sub>9</sub>N (trimethylamine), C<sub>4</sub>H<sub>9</sub>NO (assorted amides), C<sub>4</sub>H<sub>11</sub>NO (assorted amines), C<sub>7</sub>H<sub>5</sub>N  
725 (benzonitrile). As illustrated by the multiple possibilities for some formulas, several quantified nitrogen-containing  
726 species were observed but explicit single identities or relative contributions could not be confirmed. The logical  
727 candidates we propose are based upon atmospheric observations and include classes of amines and amides shown in  
728 Table S4 (~~Ge et al., 2011~~; Lobert et al., 1991; Schade and Crutzen, 1995; [Ma and Hays et al., 2008](#); Barnes et al.,  
729 [2010](#); [Ge et al., 2011](#) ~~Ma and Hays et al., 2008~~). Additional N-containing compounds were clearly observed in the  
730 mass spectra such as acrylonitrile, propanenitrile, pyrrole, and pyridine, but they were often overlapped with isotopic  
731 peaks of major carbon compounds, thus a time-intensive analysis would be necessary to provide quantitative data.

732 For the species in this category, quantification was possible for select fires by 2D-GC-MS and they are reported by  
733 Hatch et al. (2014) for the FLAME-4 campaign.

734 We present in Supplement Table S5 the abundance of each N-containing gas quantified by PTR-TOF-MS and FTIR  
735 relative to NH<sub>3</sub> for selected fires. The additional nitrogen-containing organic gases detected by PTR-TOF-MS for  
736 these 29 fires summed to roughly 22 ± 23% of NH<sub>3</sub> on average and accounted for a range of 0.1-8.7% of the fuel  
737 nitrogen. These compounds contributed most significantly to fuel N for peat and this varied by sampling location.  
738 This is not surprising since environmental conditions and field sampling depths varied considerably. Stockwell et al.  
739 (2014) reported large differences for N-containing compounds quantified by FTIR between FLAME-4 and earlier  
740 laboratory studies of emissions from peat burns. In any case, the additional NMOCs (including N-containing  
741 compounds) speciated by PTR-TOF-MS substantially increases the amount of information currently available on  
742 peat emissions.

743 The relevance of the N-containing organics to climate and the N-cycle is briefly summarized next. Aerosol particles  
744 acting as cloud condensation nuclei (CCN) critically impact climate by production and modification of clouds and  
745 precipitation (Novakov and Penner, 1993). NPF, the formation of new stable nuclei, is suspected to be a major  
746 contributor to the amount of CCN in the atmosphere (Kerminen et al., 2005; Laaksonen et al., 2005; Sotiropoulou et  
747 al., 2006). Numerous studies have suggested that organic compounds containing nitrogen can play an important role  
748 in the formation and growth of new particles (Smith et al., 2008; Kirkby et al., 2011; Yu and Luo, 2014). The  
749 primary pathways to new particle formation include (1) reaction of organic compounds with each other or  
750 atmospheric oxidants to form higher molecular weight, lower volatility compounds that subsequently partition into  
751 the aerosol phase or (2) rapid acid/base reactions forming organic salts. The observation of significant emissions of  
752 N-containing organic gases in FLAME-4 could improve understanding of the compounds, properties, and source  
753 strengths contributing to new particle formation and enhance model predictions on local to global scales. The  
754 identities and amounts of these additional nitrogen containing emissions produced by peat and other BB fuels are  
755 also important in rigorous analysis of the atmospheric nitrogen budget.

#### 756 **4.5 Sulfur, phosphorous, and chlorine-containing compounds**

757 Sulfur emissions are important for their contribution to acid deposition and climate effects due to aerosol formation.  
758 Several S-containing gases have been detected in BB emissions including SO<sub>2</sub>, carbonyl sulfide (OCS),  
759 dimethylsulphide (DMS), and dimethyl disulphide (DMDS), where DMS is one of the most significant organosulfur  
760 compounds emitted by BB and is quantified by PTR-TOF-MS in our primary dataset ([Friedli et al., 2001](#); [Meinardi  
761 et al., 2003](#); Akagi et al., 2011; [Meinardi et al., 2003](#); [Friedli et al., 2001](#); Simpson et al., 2011). The signal at *m/z* 49  
762 had a significant mass defect and is attributed to methanethiol (methyl mercaptan, CH<sub>3</sub>SH), which to our knowledge  
763 has not been previously reported in real-world BB smoke though it has been observed in cigarette smoke (Dong et  
764 al., 2010) and in emissions from pulp and paper plants (Toda et al., 2010). Like DMS, the photochemical oxidation  
765 of CH<sub>3</sub>SH leads to SO<sub>2</sub> formation (Shon and Kim, 2006), which can be further oxidized to sulfate or sulfuric acid  
766 and contribute to the aerosol phase. The emissions of CH<sub>3</sub>SH are dependent on the fuel S-content and are

767 negatively-correlated with MCE. The greatest EF(CH<sub>3</sub>SH) in our additional analyses arose from organic alfalfa,  
768 which had the highest S-content of the selected fuels and also produced significant emissions of SO<sub>2</sub> detected by  
769 FTIR.

770 Other organic gases containing chlorine and phosphorous were expected to be readily detectable because of their  
771 large, unique mass defects and possible enhancement by pesticides and fertilizers in crop residue fuels. However,  
772 they were not detected in significant amounts by our full mass scans. Fuel P and Cl may have been emitted primarily  
773 as aerosol, ash, low proton affinity gases, or as a suite of gases that were evidently below our detection limit.

#### 774 **4.6 Miscellaneous (order of increasing m/z)**

775 *m/z 41*: The assignment of propyne is reinforced by previous observations in BB fires, and it is of some interest as a  
776 BB marker even though it has a relatively short lifetime of ~2 days (Simpson et al., 2011; Akagi et al., 2013;  
777 Yokelson et al., 2013). Considering that propyne was not detected in every fuel type, a level of uncertainty is added  
778 to any use of this compound as a BB tracer and in general, the use of multiple tracers is preferred when possible.

779 *m/z 43*: The high-resolution capabilities of the PTR-TOF-MS allowed propylene to be distinguished from ketene  
780 fragments at *m/z* 43. The propylene concentrations are superseded in our present dataset by FTIR measurements,  
781 however, the two techniques agree well.

782 *m/z 45*: PTR technology has already been reported as a reliable way to measure acetaldehyde in BB smoke  
783 | ([Holzinger et al., 1999](#); Christian et al., 2004; [Holzinger et al., 1999](#)). Photolysis of acetaldehyde can play an  
784 important role in radical formation and is the main precursor of peroxy acetyl nitrate (PAN) (Trentmann et al.,  
785 2003). A wide range in EF(acetaldehyde) (0.13-4.3 g kg<sup>-1</sup>) is observed during FLAME-4 and reflects variability in  
786 fuel type. The detailed emissions from a range of fuels in this dataset can aid in modeling and interpretation of PAN  
787 formation in aging BB plumes of various regions (Alvarado et al., 2010, 2013). Crop-residue fuels regularly had the  
788 greatest emissions of acetaldehyde, which is important considering many crop-residue fires evade detection and are  
789 considered both regionally and globally underestimated. Sugar cane burning had the largest acetaldehyde EF (4.3 ±  
790 1.4 g kg<sup>-1</sup>) and had significant emissions of oxygenated and N-containing compounds, consequently it is likely to  
791 form a significant amount of PAN.

792 *m/z 57*: The signal at *m/z* 57 using unit-mass resolution GC-PTR-MS was observed to be primarily acrolein with  
793 minor contributions from alkenes (Karl et al., 2007). In the PTR-TOF-MS, the two peaks at *m/z* 57 (C<sub>3</sub>H<sub>5</sub>O<sup>+</sup> and  
794 C<sub>4</sub>H<sub>9</sub><sup>+</sup>) are clearly distinguished and acrolein is often the dominant peak during the fire with the highest emissions  
795 from ponderosa pine and sugar cane.

796 *m/z 69*: The high resolution of the PTR-TOF-MS allowed three peaks to be distinguished at *m/z* 69, identities  
797 attributed to carbon suboxide (C<sub>3</sub>O<sub>2</sub>), furan (C<sub>4</sub>H<sub>4</sub>O), and mostly isoprene (C<sub>5</sub>H<sub>8</sub>) (Fig. 7). Distinguishing between  
798 isoprene and furan is an important capability of the PTR-TOF-MS. The atmospheric abundance and relevance of  
799 carbon suboxide is fairly uncertain and with an atmospheric lifetime of ~10 days (Kessel et al., 2013) the reactivity



800 and transport of C<sub>3</sub>O<sub>2</sub> emitted by fires could have critical regional impacts. The emissions of C<sub>3</sub>O<sub>2</sub> by BB will be  
801 interpreted in detail at a later date (S. Kessel, personal communication, 2014).

802  
803 *m/z* 75: Hydroxyacetone emissions have been reported from both field and laboratory fires ([Christian et al., 2003](#);  
804 [Akagi et al., 2011](#); [Yokelson et al., 2013](#); St. Clair et al., 2014; [Yokelson et al., 2013](#); [Akagi et al., 2011](#); [Christian et al., 2003](#)). Christian et al. (2003) first reported BB emissions of hydroxyacetone, and noted very large quantities  
805 from burning rice straw. The EF(C<sub>3</sub>H<sub>6</sub>O<sub>2</sub>) for rice straw was noticeably high (1.10 g kg<sup>-1</sup>) in the FLAME-4 dataset  
806 and only sugar cane had greater emissions.  
807

808  
809 *m/z* 85, 87: The largest peak at *m/z* 85 was assigned as pentenone as it was monitored/confirmed by PIT-MS/ GC-  
810 MS in an earlier BB study (Yokelson et al., 2013). Pentenone was a substantial emission from several fuels with  
811 ponderosa pine having the greatest EF. By similar evidence the minor peak at *m/z* 87 was assigned to pentanone but  
812 was only detected in a few of the fires in the second set of analyses with the most significant emissions arising from  
813 Indonesian peat.

814  
815 *m/z* 107: Benzaldehyde has the same unit mass as xylenes, but is clearly separated by the TOF-MS. Greenberg et al.  
816 (2006) observed benzaldehyde during low temperature pyrolysis experiments with the greatest emissions from  
817 ponderosa needles (ponderosa pine produced the greatest EF in our dataset, range 0.10-0.28 g kg<sup>-1</sup>). Benzaldehyde  
818 emissions were additionally quantified by GC-MS during a laboratory BB campaign and produced comparable EF to  
819 that of xylenes (Yokelson et al., 2013). During FLAME-4 the EF(benzaldehyde) was comparable to EF(xylenes  
820 calibrated as p-xylene) as seen earlier except for peat burns where p-xylene was significantly higher.

821  
822 *m/z* 137: At unit mass resolution the peak at *m/z* 137 is commonly recognized as monoterpenes which can further be  
823 speciated by GC-MS. However, as shown in Fig. 8 there can be up to three additional peaks at this mass that  
824 presently remain unidentified oxygenated compounds. As anticipated, the hydrocarbon monoterpene peak is  
825 significant for coniferous fuels such as ponderosa pine but much smaller for grasses. In this work we calibrated for  
826  $\alpha$ -pinene, which has been reported as a major monoterpene emission from fresh smoke ([Akagi et al., 2013](#); Simpson  
827 et al., 2011; [Akagi et al., 2013](#)).

#### 828 **4.7 Cookstoves**

829 Trace gas emissions were measured for four cookstoves including: a traditional 3-stone cooking fire, the most  
830 widely used stove design worldwide; two “rocket” type designs (Envirofit G3300 and Ezy stove); and a “gasifier”  
831 stove (Philips HD4012). Several studies focus on fuel efficiency of cookstove technology (Jetter et al., 2012), while  
832 the detailed emissions of many rarely measured and previously unmeasured gases are reported here and in Stockwell  
833 et al. (2014) for FLAME-4 burns. For cooking fires, ~3-6% of the NMOC mass remained unidentified, with the  
834 Envirofit rocket stove design generating the smallest percentage in the study. To improve the representativeness of  
835 our laboratory open cooking emissions, the EFs of smoldering compounds reported for 3-stone cooking fires were  
836 adjusted by multiplying the mass ratio of each species “X” to CH<sub>4</sub> by the literature-average field EF(CH<sub>4</sub>) for open

837 cooking in Akagi et al. (2011). Flaming compounds were adjusted by a similar procedure based on their ratios to  
838 CO<sub>2</sub>. The preferred values are reported in Table S3. With these adjustments, the emissions of aromatic hydrocarbons  
839 (Fig. 9a), phenolic compounds (Fig. 9b), and furans (Fig. 9c) distinctively increased with the primitiveness of  
840 design, thus, 3-stone cooking fires produced the greatest emissions. The advancement in emissions characterization  
841 for these sources will be used to upgrade models of exposure to household air pollution and the ERs/EFs should be  
842 factored in to chemical-transport models to assess atmospheric impacts.

843 BB is an important source of reactive nitrogen in the atmosphere producing significant emissions of NO<sub>x</sub> and NH<sub>3</sub>  
844 while non-reactive HCN and CH<sub>3</sub>CN are commonly used as BB marker compounds (Yokelson et al., 1996, 2007;  
845 Goode et al., 1999; de Gouw et al., 2003). The FTIR used in FLAME-4 provided the first detection of HCN  
846 emissions from cooking fires and the HCN/CO ER was about a factor of 5 lower than most other BB fuels burned  
847 (Stockwell et al., 2014). Similarly, acetonitrile emissions were measured for the first time for cooking fires by PTR-  
848 TOF-MS in this study and the CH<sub>3</sub>CN/CO ERs from cooking fires are much lower (on average a factor of ~15) than  
849 those from other fuels. This should be considered when using CH<sub>3</sub>CN/CO ERs to drive source apportionment in  
850 areas with substantial emissions from biofuel cooking sources.

## 851 5 Conclusions

852 We investigated the primary BB NMOC emissions from laboratory simulated burns of globally significant fuels  
853 using a PTR-TOF-MS instrument. In this first PTR-TOF-MS deployment dedicated to fires we encountered some  
854 specific challenges. The fast change in concentration necessitated a fast acquisition rate, which decreases the signal  
855 to noise for the emissions above background. The large dynamic concentration range necessitated dilution to  
856 minimize reagent ion depletion at peak emissions and the dilution further reduced the signal to noise ratio. Positive  
857 identification of some species by co-deployed grab sampling techniques will be explored further in a separate paper,  
858 but is challenged by the difficulty of transmitting some important fire emissions through GC columns (Hatch et al.,  
859 2014). We attempted to enhance compound identification by switching reagent ions (O<sub>2</sub><sup>+</sup> and NO<sup>+</sup>), however, this  
860 approach with two broadly sensitive ions in a complex mixture resulted in spectra with complexity whose  
861 comparative analysis is beyond the scope of the present effort. Future experiments might consider instead using a  
862 less broadly sensitive reagent ion such as NH<sub>3</sub><sup>+</sup> as the alternate reagent ion. We were limited to our pre-chosen  
863 calibration mixture based primarily on gases previously observed in smoke. For future experiments we suggest  
864 adding more standards to generate more accurate calibration factors, specifically including major species such as  
865 furan and phenol and more compounds with S and N heteroatoms. In addition, measuring the fragmentation, if any,  
866 of more of the species identified in this work would be of great value. Despite these practical limitations, the  
867 experiment produced a great deal of useful new information.

868 The PTR-TOF-MS obtains full mass scans of NMOCs with high enough resolution to distinguish multiple peaks at  
869 the same nominal mass and high enough accuracy to assign chemical formulas from the “exact” masses. This aided  
870 in compound identification and more than 100 species were categorized as a confirmed identity, a tentative (most  
871 likely) assignment, or unidentified but with a chemical formula. Chemical identification was aided by observations

872 of compounds reported in smoke emissions, pyrolysis experiments, and those species at relevant concentrations in  
873 the atmosphere. This allowed the identification of more masses up to  $m/z$  165 than in earlier work at unit mass  
874 resolution though an estimated range of 12-37% of the total mass still remains unidentified and tentatively  
875 identified. The analysis provides a new set of emission factors for ~68 compounds in all fires plus ~50 more in  
876 select fires, in addition to species previously quantified by FTIR (Stockwell et al., 2014) and other techniques during  
877 FLAME-4 (Hatch et al., 2014). While significant variability was observed between fuels, oxygenated compounds  
878 collectively accounted for the majority of emissions in all fuels with sugar cane producing the highest EF of  
879 oxygenated species on average possibly due to its high sugar content.

880 We also report emission ratios to benzene, phenol, or furan for the aromatic hydrocarbons, phenolic compounds, and  
881 substituted furans, respectively. Reporting emissions of previously unmeasured or rarely measured compounds  
882 relative to these more regularly measured compounds facilitates adding several new compounds to fire emissions  
883 models. To our knowledge this is the first on-line, real-time characterization of several compounds within these  
884 “families” for biomass burning. Emissions were observed to vary considerably between fuel types. Several example  
885 compounds within each class (i.e. toluene, guaiacol, methylfuran, etc.) have been shown, by chamber experiments,  
886 to be highly reactive with atmospheric oxidants and contribute significantly to SOA formation. The ERs and EFs  
887 characterized by PTR-TOF-MS of fresh BB smoke are presented in Tables S1-S3 and [\(especially the recommended](#)  
888 [values in Table S3\)](#) should aid model predictions of  $O_3$  and SOA formation in BB smoke and the subsequent effects  
889 on air quality and climate on local-global scales.

890 A large number of organic nitrogen-containing species were detected with several identities speculated as amines or  
891 amides. These N-containing organic gases may play an important role in new particle formation by physical,  
892 chemical, and photochemical processes, though a more focused study is necessary to measure NPF yields from these  
893 compounds and processes. The additional N-containing gases detected here account for a range of 1-87% of  $NH_3$   
894 dependent on fuel type with the most significant contribution of additional N-species to fuel N arising from peat  
895 burns. The ERs of acetonitrile to CO for cooking fires ~~was~~ were significantly lower than other fuels and should be  
896 factored into source apportionment models in regions where biofuel use is prevalent if  $CH_3CN$  is used as a tracer.

897 The S-containing compounds detected by PTR-TOF-MS included dimethyl sulfide and methanethiol, where  
898 methanethiol was detected for the first time in BB smoke to our knowledge. These compounds may play a role in  
899 acid deposition and aerosol formation though to what extent has yet to be extensively studied. Phosphorous and  
900 chlorine organic gases were not readily ~~detectable~~ observed in our dataset, which may reflect that these species were  
901 below our detection limit.

902 Using full mass scans from a high resolution PTR-TOF-MS to characterize fresh smoke has aided in identification  
903 of several compounds and provided the chemical formula of other organic trace gases. The additional NMOCs  
904 identified in this work are important in understanding fresh BB emissions and will improve our understanding of BB  
905 atmospheric impacts. The subsequent oxidation products of these gases are the focus of a companion paper probing

906 BB aging. Taken together, this work should improve BB representation in atmospheric models, particularly the  
907 formation of ozone and secondary organic aerosol at multiple scales.

## 908 **Acknowledgements**

909 FLAME-4, rental of PTR-TOF-MS, C. S. and R. Y. were supported primarily by NSF grant ATM-0936321. FSL  
910 operational costs were supported by NASA Earth Science Division Award NNX12AH17G to S. Kreidenweis, P.  
911 DeMott, and G. McMeeking whose collaboration in organizing and executing FLAME-4 is gratefully  
912 acknowledged. The collaboration of A. Robinson in organizing FLAME-4, and the cooking fires is also gratefully  
913 acknowledged. [We thank C. Geron for providing a sample of NC peat.](#)

## 914 **References**

915 Akagi, S. K., Yokelson, R. J., Wiedinmyer, C., Alvarado, M. J., Reid, J. S., Karl, T., Crounse, J. D., and Wennberg,  
916 P. O.: Emission factors for open and domestic biomass burning for use in atmospheric models, *Atmos. Chem. Phys.*,  
917 11, 4039–4072, doi:10.5194/acp-11-4039-2011, 2011.

918 Akagi, S. K., Craven, J. S., Taylor, J.W., McMeeking, G. R., Yokelson, R. J., Burling, I. R., Urbanski, S. P., Wold,  
919 C. E., Seinfeld, J. H., Coe, H., Alvarado, M. J., and Weise, D. R.: Evolution of trace gases and particles emitted by a  
920 chaparral fire in California, *Atmos. Chem. Phys.*, 12, 1397–1421, doi:10.5194/acp-12-1397- 2012, 2012.

921 Akagi, S. K., Yokelson, R. J., Burling, I. R., Meinardi, S., Simpson, I., Blake, D. R., McMeeking, G. R., Sullivan,  
922 A., Lee, T., Kreidenweis, S., Urbanski, S., Reardon, J., Griffith, D. W. T., and Weise, D. R.: Measurements of  
923 reactive trace gases and variable O<sub>3</sub> formation rates in some South Carolina biomass burning plumes, *Atmos. Chem.*  
924 *Phys.*, 13, 1141–1165, doi:10.5194/acp-13-1141-2013, 2013.

925 Alvarado, M. J. and Prinn, R. G.: Formation of ozone and growth of aerosols in young smoke plumes from biomass  
926 burning: 1. Lagrangian parcel studies, *J. Geophys. Res.*, 114, D09306, doi:10.1029/2008JD011144, 2009.

927 Alvarado, M. J., Wang, C., and Prinn, R. G.: Formation of ozone and growth of aerosols in young smoke plumes  
928 from biomass burning: 2. Three-dimensional Eulerian studies, *J. Geophys. Res.*, 114, D09307,  
929 doi:10.1029/2008JD011186, 2009.

930 Alvarado, M. J., Logan, J. A., Mao, J., Apel, E., Riemer, D., Blake, D., Cohen, R. C., Min, K.-E., Perring, A. E.,  
931 Browne, E. C., Wooldridge, P. J., Diskin, G. S., Sachse, G. W., Fuelberg, H., Sessions, W. R., Harrigan, D. L., Huey,  
932 G., Liao, J., Case-Hanks, A., Jimenez, J. L., Cubison, M. J., Vay, S. A., Weinheimer, A. J., Knapp, D. J., Montzka,  
933 D. D., Flocke, F. M., Pollack, I. B., Wennberg, P. O., Kurten, A., Crounse, J., [St. Clair, J. M.](#), ~~St.~~, Wisthaler, A.,  
934 Mikoviny, T., Yantosca, R. M., Carouge, C. C., and Le Sager, P.: Nitrogen oxides and PAN in plumes from boreal  
935 fires during ARCTAS-B and their impact on ozone: an integrated analysis of aircraft and satellite observations,  
936 *Atmos. Chem. Phys.*, 10, 9739–9760, doi:10.5194/acp-10-9739-2010, 2010.

937 Alvarado, M. J., Yokelson, R. J., Akagi, S. A., Burling, I. R., Fischer, E., McMeeking, G. R., Travis, K., Craven, J.  
938 S., Seinfeld, J. H., Taylor, J. W., Coe, H., Urbanski, S. P., Wold, C. E., and Weise, D. R.: Lagrangian photochemical  
939 modeling of ozone formation and aerosol evolution in biomass burning plumes: toward a sub-grid scale  
940 parameterization, 12<sup>th</sup> Annual CMAS Conference, Chapel Hill, NC, 28-30 October, 2013.

941 Andreae, M. O. and Merlet, P.: Emission of trace gases and aerosols from biomass burning, *Global Biogeochem.*  
942 *Cy.*, 15(4), 955–966, doi:10.1029/2000GB001382, 2001.

943 Andreae, M. O., Artaxo, P., Fischer, H., Freitas, S. R., Grégoire, J. –M., Hansel, A., Hoor, P., Kormann, R., Krejci,  
944 R., Lange, L., Lelieveld, J., Lindinger, W., Longo, K., Peters, W., de Reus, M., Scheeren, B., Silvia Dias, M. A. F.,  
945 Ström, J., van Velthoven, P. F. J., and Williams, J.: Transport of biomass burning smoke to the upper troposphere by  
946 deep convection in the equatorial region, *Geophys. Res. Lett.*, 28, 951-954, doi: 10.1029/2000GL012391, 2001.

947 Atkinson, R., Aschmann, S. M., and Arey, J.: Reactions of OH and NO<sub>3</sub> radicals with phenol, cresols, and 2-  
948 nitrophenol at 296 ± 2K, *Environ. Sci. Technol.*, 26, 1397-1403, doi: 10.1021/es00031a018, 1992.

949 Azeez, A. M., Meier, D., and Odermatt, J.: Temperature dependence of fast pyrolysis volatile products from  
950 European and African biomasses, *J. Anal. Appl. Pyrolysis*, 90, 81-92, doi:10.1016/j.jaap.2010.11.005, 2011.

951 Barnes, I., Solignac, G., Mellouki, A., and Becker, K. H.: Aspects of the atmospheric chemistry of amides,  
952 *ChemPhysChem.*, 11, 3844-3857, doi: 10.1002/cphc.201000374, 2010.

953 Berndt, T., Böge, O., and Rolle, W.: Products of the gas-phase reactions of NO<sub>3</sub> radicals with furan and  
954 tetramethylfuran, *Environ. Sci. Technol.*, 31, 1157-1162, 1997.

955 Bierbach, A., Barnes, I., Becker, K. H., and Wiesen, E.: Atmospheric chemistry of unsaturated carbonyls:  
956 butenedial, 4-oxo-2-pentenal, 3-hexene-2,5-dione, maleic anhydride, 3H-furan-2-one, and 5-methyl-3H-furan-2-one,  
957 *Environ. Sci. Technol.*, 28, 715-729, doi: 10.1021/es00053a028, 1994.

958 Bierbach, A., Barnes, I., and Becker, K. H.: Product and kinetic study of the OH-initiated gas-phase oxidation of  
959 furan, 2-methylfuran, and furanaldehydes at 300K, *Atmos. Environ.*, 29, 2651-2660, doi: 10.1016/1352-  
960 2310(95)00096-H, 1995.

961 Bocchini, P., Galletti, G. C., Camarero, S., and Martinez, A. T.: Absolute quantitation of lignin pyrolysis products  
962 using an internal standard, *J. Chromatogr. A*, 773, 227-232, doi: 10.1016/S0021-9673(97)00114-3, 1997.

963 Bond, T. C., Streets, D. G., Yarber, K. F., Nelson, S. M., Woo, J.-H., and Klimont, Z.: A technology-based global  
964 inventory of black and organic carbon emissions from combustion, *J. Geophys. Res.*, 109, D14203,  
965 doi:10.1029/2003JD003697, 2004.

966 Bond, T. C., Doherty, S. J., Fahey, D.W., Forster, P. M., Berntsen, T., DeAngelo, B. J., Flanner, M. G., Ghan, S.,  
967 Kärcher, B., Koch, D., Kinne, S., Kondo, Y., Quinn, P. K., Sarofim, M. C., Schultz, M. G., Schulz, M.,

968 Venkataraman, C., Zhang, H., Zhang, S., Bellouin, N., Guttikunda, S. K., Hopke, P. K., Jacobson, M. Z., Kaiser, J.  
969 W. , Klimont, Z., Lohmann, U., Schwarz, J. P., Shindell, D., Storelvmo, T., Warren, S. G., and Zender, C. S.:  
970 Bounding the role of black carbon in the climate system: A scientific assessment, *J. Geophys. Res.*, 118, 5380-5552,  
971 doi:10.1002/jgrd.50171, 2013.

972 Burling, I. R., Yokelson, R. J., Griffith, D. W. T., Johnson, T. J., Veres, P., Roberts, J. M., Warneke, C., Urbanski,  
973 S. P., Reardon, J., Weise, D. R., Hao, W. M., and de Gouw, J.: Laboratory measurements of trace gas emissions  
974 from biomass burning of fuel types from the southeastern and southwestern United States, *Atmos. Chem. Phys.*, 10,  
975 11115–11130, doi:10.5194/acp-10-11115-2010, 2010.

976 Cabañas, B., Villanueva, F., Martin, P., Baeza, M. T., Salgado, S., and Jiménez, E.: Study of reaction processes of  
977 furan and some furan derivatives initiated by Cl atoms, *Atmos. Environ.*, 39, 1935-1944, doi:  
978 10.1016/j.atmosenv.2004.12.013, 2005.

979 Chan, M. N., Kautzman, K. E., Chhabra, P. S., Surratt, J. D., Chan, M. N., Crounse, J. D., Kurten, A., Wennberg, P.  
980 O., Flagan, R. C., and Seinfeld, J. H.: Secondary organic aerosol formation from photooxidation of naphthalene and  
981 alkylnaphthalenes: implications for oxidation of intermediate volatility organic compounds (IVOCs), *Atmos. Chem.*  
982 *Phys.*, 9, 3049-3060, doi:10.5194/acp-9-3049-2009, 2009.

983 Chhabra, P. S., Flagan, R. C., and Seinfeld, J. H.: Elemental analysis of chamber organic aerosol using an aerodyne  
984 high-resolution aerosol mass spectrometer, *Atmos. Chem. Phys.*, 10, 4111–4131, doi:10.5194/acp-10-4111-2010,  
985 2010.

986 Chhabra, P. S., Ng, N. L., Canagaratna, M. R., Corrigan, A. L., Russell, L. M., Worsnop, D. R., Flagan, R. C., and  
987 Seinfeld, J. H.: Elemental composition and oxidation of chamber organic aerosol, *Atmos. Chem. Phys.*, 11, 8827-  
988 8845, doi:10.5194/acp-11-8827-2011, 2011.

989 Christian, T., Kleiss, B., Yokelson, R. J., Holzinger, R., Crutzen, P. J., Hao, W. M., Saharjo, B. H., and Ward, D. E.:  
990 Comprehensive laboratory measurements of biomass-burning emissions: 1. Emissions from Indonesian, African,  
991 and other fuels, *J. Geophys. Res.*, 108, 4719, doi:10.1029/2003JD003704, 2003.

992 Christian, T. J., Kleiss, B., Yokelson, R. J., Holzinger, R., Crutzen, P. J., Hao, W. M., Shirai, T., and Blake, D. R.:  
993 Comprehensive laboratory measurements of biomass-burning emissions: 2. First intercomparison of open path  
994 FTIR, PTR-MS, GC-MS/FID/ECD, *J. Geophys. Res.*, 109, D02311, doi:10.1029/2003JD003874, 2004.

995 Coeur-Tourneur, C., Cassez, A., and Wenger, J. C.: Rate coefficients for the gas-phase reaction of hydroxyl radicals  
996 with 2-methoxyphenol (guaiacol) and related compounds, *J. Phys. Chem.*, 114, 11645-11650, doi:  
997 10.1021/jp1071023, 2010.

998 Crutzen, P. J. and Andreae, M. O.: Biomass burning in the tropics: Impact on atmospheric chemistry and  
999 biogeochemical cycles, *Science*, 250, 1669–1678, doi:10.1126/science.250.4988.1669, 1990.

1000 de Gouw, J. A., C. Warneke, D. D. Parrish, J. S. Holloway, M. Trainer, and F. C. Fehsenfeld, Emission sources and  
1001 ocean uptake of acetonitrile (CH<sub>3</sub>CN) in the atmosphere, *J. Geophys. Res.*, 108(D11), 4329,  
1002 doi:10.1029/2002JD002897, 2003.

1003 Desyaterik, Y., Sun, Y., Shen, X., Lee, T., Wang, X., Wang, T., and Collet Jr., J. L.: Speciation of “brown” carbon  
1004 in cloud water impacted by agricultural biomass burning in eastern China, *J. Geophys. Res. Atmos.*, 118, 7389-  
1005 7399, doi:10.1002/jgrd.50561, 2013.

1006 Dong, J., and DeBusk, S. M.: GC-MS analysis of hydrogen sulfide, carbonyl sulfide, methanethiol, carbon disulfide,  
1007 methyl thicyanate and methyl disulfide in mainstream vapor phase cigarette smoke, *Chromatographia*, 71, 259-265,  
1008 doi: 10.1365/s10337-009-1434-z, 2010.

1009 Fisseha, R., Dommen, J., Sax, M., Paulsen, D., Kalberer, M., Maurer, R., Hofler, F., Weingartner, E., and  
1010 Baltensperger, U.: Identification of organic acids in secondary organic aerosol and the corresponding gas phase from  
1011 chamber experiments, *Anal. Chem.*, 76, 6535–6540, doi:10.1021/Ac048975f, 2004.

1012 Friedli, H. R., E. Atlas, V. R. Stroud, L. Giovanni, T. Campos, and Radke, L. F.: Volatile organic trace gases  
1013 emitted from North American wildfires, *Global Biogeochem. Cy.*, 15(2), 435-452, doi: 10.1029/2000GB001328,  
1014 2001.

1015 Ge, X., Wexler, A. S., and Clegg, S. L.: Amospheric amines-Part I. A review, *Atmos. Environ.*, 45, 524-546,  
1016 doi:10.1016/j.atmosenv.2010.10.012, 2011.

1017 [Geron, C., and Hays, M.: Air emissions from organic soil burning on the coastal plain of North Carolina, \*Atmos.\*](#)  
1018 [Environ.](#), 64, 192-199, doi: 10.1016/j.atmosenv.2012.09.065, 2013.

1019 Gomez Alvarez, E. G., Borrás, E., Viidanoja, J., [and](#) Hjorth, J.: Unsaturated dicarbonyl products from the OH-  
1020 initiated photo-oxidation of furan, 2-methylfuran and 3-methylfuran, *Atmos. Environ.*, 43, 1603-1612,  
1021 doi:10.1016/j.atmosenv.2008.12.019, 2009.

1022 Goode, J. G., Yokelson, R. J., Susott, R. A., and Ward, D. E.: Trace gas emissions from laboratory biomass fires  
1023 measured by Fourier transform infrared spectroscopy: Fires in grass and surface fuels, *J. Geophys. Res.*, 104, 21237  
1024 – 21245, doi:10.1029/1999JD900360, 1999.

1025 Graus, M., Muller, M., and Hansel, A.: High Resolution PTR-TOF: Quantification and formula confirmation of  
1026 VOC in real time, *J. Am. Soc. Mass. Spectr.*, 21/6, 1037–1044, doi:10.1016/j.jasms.2010.02.006, 2010.

1027 Greenberg, J. P., Friedli, H., Guenther, A. B., Hanson, D., Harley, P., and Karl, T.: Volatile organic emissions from  
1028 the distillation and pyrolysis of vegetation, *Atmos. Chem. Phys.*, 6, 81–91, doi:10.5194/acp-6-81-2006, 2006.

1029 Grieshop, A. P., Logue, J. M., Donahue, N. M., and Robinson, A. L.: Laboratory investigation of photochemical  
1030 oxidation of organic aerosol from wood fires 1: measurement and simulation of organic aerosol evolution, *Atmos.*  
1031 *Chem. Phys.*, 9(4), 1263-1277, doi:10.5194/acp-9-1263-2009, 2009.

1032 Griffith, D. W. T.: Synthetic calibration and quantitative analysis of gas phase infrared spectra, *Appl. Spectrosc.*, 50,  
1033 59–70, 1996.

1034 Harrison, M. A. J.; Barra, S.; Borghesi, D.; Vione, D.; Arsene, C.; and Olariu, R. L.: Nitrated phenols in the  
1035 atmosphere: A review, *Atmos. Environ.*, 39, 231–248, doi: 10.1016/j.atmosenv.2004.09.044, 2005.

1036 Hawthorne, S. B., Krieger, M. S., Miller, D. J., and Mathiason, M. B.: Collection and quantitation of methoxylated  
1037 phenol tracers for atmospheric-pollution from residential wood stoves, *Environ. Sci. Technol.*, 23, 470-475, doi:  
1038 10.1021/es00181a013, 1989.

1039 Hawthorne, S. B., Miller, D. J., Langenfeld, J. J., and Krieger, M. S.: PM-10 High-volume collection and  
1040 quantitation of semivolatile and nonvolatile phenols, methoxylated phenols, alkanes, and polycyclic aromatic-  
1041 hydrocarbons from winter urban air and their relationship to wood smoke emissions, *Environ. Sci. Technol.*, 26,  
1042 2251–2262, doi:10.1021/es00035a026, 1992.

1043 Hatch, L. E., Luo, W., Pankow, J. F., Yokelson, R. J., Stockwell, C. E., and Barsanti, K. C.: Identification and  
1044 quantification of gaseous organic compounds emitted from biomass burning using two-dimensional gas  
1045 chromatography/time-of-flight mass spectrometry, *Atmos. Chem. Phys. Discuss.*, submitted, 2014.

1046 Heigenmoser, A., Liebner, F., Windeisen, E., and Richter, K.: Investigation of thermally treated beech (*Fagus*  
1047 *sylvatica*) and spruce (*Picea abies*) by means of multifunctional analytical pyrolysis-GC/MS, *J. Anal. Appl.*  
1048 *Pyrolysis*, 100, 117-126, doi: 10.1016/j.jaap.2012.12.005, 2013.

1049 Hennigan, C. J., Miracolo, M. A., Engelhart, G. J., May, A. A., Presto, A. A., Lee, T., Sullivan, A. P., McMeeking,  
1050 G. R., Coe, H., Wold, C.E., Hao, W. M., Gilman, J. B., Kuster, W. C., de Gouw, J., Schichtel, B. A., Collett Jr., J.  
1051 L., Kreidenweis, S. M., and Robinson, A. L.: Chemical and physical transformations of organic aerosol from the  
1052 photo-oxidation of open biomass burning emissions in an environmental chamber, *Atmos. Chem. Phys.*, 11, 7669-  
1053 7686, doi:10.5194/acp-11-7669-2011, 2011.

1054 Henze, D. K., Seinfeld, J. H., Ng, N. L., Kroll, J. H., Fu, T.-M., Jacob, D. J., and Heald, C. L.: Global modeling of  
1055 secondary organic aerosol formation from aromatic hydrocarbons: high- vs. low-yield pathways, *Atmos. Chem.*  
1056 *Phys.*, 8, 2405-2420, doi:10.5194/acp-8-2405-2008, 2008.

1057 Hildebrandt, L., Donahue, N. M., and Pandis, S. N.: High formation of secondary organic aerosol from the photo-  
1058 oxidation of toluene, *Atmos. Chem. Phys.*, 9, 2973–2986, doi:10.5194/acp-9-2973-2009, 2009.

1059 Hinkel, M., Reischl, A., Schramm, K.-W., Trautner, F., Reissinger, M., Hutzinger, O.: Concentration levels of  
1060 nitrated phenols in conifer needles, *Chemosphere*, 18, 2433–2439, 1989.



1061 Holzinger, R., Warneke, C., Hansel, A., Jordan, A., Lindinger, W., Scharffe, D. H., Schade, G., and Crutzen, P. J.:  
1062 Biomass burning as a source of formaldehyde, acetaldehyde, methanol, acetone, acetonitrile, and hydrogen cyanide,  
1063 *Geophys. Res. Lett.*, 26, 1161–1164, doi: 10.1029/1999GL900156, 1999.

1064 Iinuma, Y. Böge, O., Gräfe, R., and Herrmann, H.: Methyl-nitrocatechols: Atmospheric tracer compounds for  
1065 biomass burning secondary organic aerosols, *Environ. Sci. Technol.*, 44, 8453-8459, doi: 10.1021/es102938a, 2010.

1066 Im, Y., Jang, M., Beardsley, R. L.: Simulation of aromatic SOA formation using the lumping model integrated with  
1067 explicit gas-phase kinetic mechanisms and aerosol-phase reactions, *Atmos. Chem. Phys.*, 14,4013-4027,  
1068 doi:10.5194/acp-14-4013-2014, 2014.

1069 Ingemarsson, A., Nilsson, U., Nilsson, M., Pederson, J. R., and Olsson, J. O.: Slow pyrolysis of spruce and pine  
1070 samples studied with GC/MS and GC/FTIR/FID, *Chemosphere*, 36 (14), 2879-2889, doi: 10.1016/S0045-  
1071 6535(97)10245-4, 1998.

1072 Jetter, J., Zhao, Y., Smith, K. R., Khan, B., Yelverton, T., DeCarlo, P., and Hays, M. D.: Pollutant emissions and  
1073 energy efficiency under controlled conditions for household biomass cookstoves and implications for metrics useful  
1074 in setting international test standards, *Environ. Sci. Technol.*, 46, 10827-10834, doi:10.1021/es301693f, 2012.

1075 Jiang, G., Nowakowski, D. J., and Bridgwater, A. V.: Effect of the temperature on the composition of lignin  
1076 pyrolysis products, *Energy Fuels*, 24, 4470-4475, doi:10.1021/ef100363c, 2010.

1077 Jordan, T. B., and Seen, A. J.: Effect of airflow setting on the organic composition of woodheater emissions,  
1078 *Environ. Sci. Technol.*, 39, 3601-3610, doi: 10.1021/es0487628, 2005.

1079 Jordan, A., Haidacher, S., Hanel, G., Hartungen, E., Märk, L., Seehauser, H., Schotchkowsky, R., Sulzer, P., and  
1080 Märk, T. D.: A high resolution and high sensitivity proton-transfer-reaction time-of-flight mass spectrometer (PTR-  
1081 TOF-MS), *Int. J. Mass Spectrom.*, 286, 122–128, doi: 10.1016/j.ijms.2009.07.005, 2009.

1082 Karl, T. G., Christian, T. J., Yokelson, R. J., Artaxo, P., Hao, W. M., and Guenther, A.: The Tropical Forest and Fire  
1083 Emissions Experiment: method evaluation of volatile organic compound emissions measured by PTR-MS, FTIR,  
1084 and GC from tropical biomass burning, *Atmos. Chem. Phys.*, 7, 5883–5897, doi:10.5194/acp-7-5883-2007, 2007.

1085 Kerminen, V. M., Lihavainen, H., Komppula, M., Viisanen, Y., and Kulmala, M.: Direct observational evidence  
1086 linking atmospheric aerosol formation and cloud droplet activation, *Geophys. Res. Lett.*, 32, L14803,  
1087 doi:10.1029/2005gl023130, 2005.

1088 Kessel, S., Auld, J., Crowley, J., Horowitz, A., Sander, R., Tucceri, M., Veres P., and Williams, J.: Measurement of  
1089 carbon suboxide (C3O2) with PTR-TOF-MS – Atmospheric Sources and Sinks, 6th International Conference on  
1090 proton transfer reaction mass spectrometry and its applications, University of Innsbruck, February 3-8, 190-191,  
1091 2013.

- 1092 Kirkby, J., Curtius, J., Almeida, J., Dunne, E., Duplissy, J., Ehrhart, S., Franchin, A., Gagné, S., Ickes, L., Kürten,  
1093 A., Kupc, A., Metzger, A., Riccobono, F., Rondo, L., Schobesberger, S., Tsagkogeorgas, G., Wimmer, D., Amorim,  
1094 A., Bianchi, F., Breitenlechner, M., David, A., Dommen, J., Downard, A., Ehn, M., Flagan, R. C., Haider, S.,  
1095 Hansel, A., Hauser, D., Jud, W., Junninen, H., Kreissl, F., Kvashin, A., Laaksonen, A., Lehtipalo, K., Lima, J.,  
1096 Lovejoy, E. R., Makhmutov, V., Mathot, S., Mikkilä, J., Minginette, P., Mogo S., Nieminen, T., Onnela, A., Pereira,  
1097 P., Petäjä, T., Schnitzhofer, R., J. H. Seinfeld, Sipilä, M., Stozhkov, Y., Stratmann, F., Tomé, A., Vanhanen, J.,  
1098 Viisanen, Y., Vrtala, A., Wagner, P. E., Walther, H., Weingartner, E., Wex, H., Winkler, P. M., Carslaw, K. S.,  
1099 Worsnop, D. R., Baltensperger, U., and Kulmala, M.: Role of sulphuric acid, ammonia and galactic cosmic rays in  
1100 atmospheric aerosol nucleation, *Nature*, 476, 429–433, 2011.
- 1101 Kitanovski, Z., Grgić, I., Yasmeen, F., Claeys, M., and Čusak, A.: Development of a liquid chromatographic method  
1102 based on ultraviolet-visible and electrospray ionization mass spectrometric detection for the identification of  
1103 nitrocatechols and related tracers in biomass burning atmospheric organic aerosol, *Rapid Commun. Mass Sp.*, 26,  
1104 793–804, doi: 10.1002/rcm.6170, 2012.
- 1105 [Kudo, S., Tanimoto, H., Inomata, S., Saito, S., Pan, X., Kanaya, Y., Taketani, F., Wang, Z., Chen, H., Dong, H.,](#)  
1106 [Zhang, M., and Yamaji, K.: Emissions of nonmethane volatile organic compounds from open crop residue burning](#)  
1107 [in the Yangtze River Delta region, China, \*J. Geophys. Res. Atmos.\*, 119, 7684-7698, doi: 10.1002/2013JD021044,](#)  
1108 [2014.](#)
- 1109 Laaksonen, A., Hamed, A., Joutsensaari, J., Hiltunen, L., Cavalli F., Junkermann, W., Asmi, A., Fuzzi, S., and  
1110 Facchini, M. C.: Cloud condensation nucleus production from nucleation events at a highly polluted region,  
1111 *Geophys. Res. Lett.*, 32, L06812, doi:10.1029/2004gl022092, 2005.
- 1112 Lauraguais, A., Coeur-Tourneur, C., Cassez, A., Deboudt, K., Fourmentin, M., and Choël, M.: Atmospheric  
1113 reactivity of hydroxyl radicals with guaiacol (2-methoxyphenol), a biomass burning emitted compound: Secondary  
1114 organic aerosol formation and gas-phase oxidation products, *Atmos. Environ.*, 86, 155–163, doi:  
1115 10.1016/j.atmosenv.2013.11.074, 2014.
- 1116 Li, Q., Steele, P. H., Yu, F., Mitchell, B., and Hassan, E.-B., M.: Pyrolytic spray increases levoglucosan production  
1117 during fast pyrolysis, *J. Anal. Appl. Pyrolysis*, 100, 33-40, doi: 10.1016/j.jaap.2012.11.013, 2013.
- 1118 Liu, Y., Shi, Q., Zhang, Y., He, Y., Chung, K. H., Zhao, S., and Xu, C.: Characterization of red pine pyrolysis bio-  
1119 oil by gas chromatography–mass spectrometry and negative-ion electrospray ionization fourier transform ion  
1120 cyclotron resonance mass spectrometry, *Energy Fuels*, 26, 4532-4539, doi: 10.1021/ef300501t, 2012.
- 1121 Lobert, J. M., Scharffe, D. H., Hao, W. M., Kuhlbusch, T. A., Seuwen, R., Warneck, P., and Crutzen, P. J.:  
1122 Experimental evaluation of biomass burning emissions: Nitrogen and carbon containing compounds, in: *Global*  
1123 *Biomass Burning: Atmospheric, Climatic, and Biospheric Implications*, Levine, J. S., MIT Press, Cambridge, 289–  
1124 304, 1991.

1125 Ma, Y. and Hays, M. D.: Thermal extraction-two-dimensional gas chromatography-mass spectrometry with heart-  
1126 cutting for nitrogen heterocyclics in biomass burning aerosols, *J. Chromatogr. A*, 1200, 228-234, doi:  
1127 10.1016/j.chroma.2008.05.078, 2008.

1128 Mason, S. A., Trentmann, J., Winterrath, T., Yokelson, R. J., Christian, T. J., Carlson, L. J., Warner, T. R., Wolfe, L.  
1129 C., and Andreae, M. O.: Intercomparison of two box models of the chemical evolution in biomass-burning smoke  
1130 plumes, *J. Atmos. Chem.*, 55, 273-297, doi: 10.1007/s10874-006-9039-5, 2006.

1131 Meinardi, S., Simpson, I. J., Blake, N. J., Blake, D. R., and Rowland, F. S.: Dimethyl disulfide (DMDS) and  
1132 dimethyl sulfide (DMS) emissions from biomass burning in Australia, *Geophys. Res. Lett.*, 30(9), 1454,  
1133 doi:10.1029/2003GL016967, 2003.

1134 Mohr, C., Lopez-Hilfiker, F. D., Zotter, P., Prévôt, A. S. H., Xu, L., Ng, N. L., Herndon, S. C., Williams, L. R.,  
1135 Franklin, J. P., Zahniser, M. S., Worsnop, D. R., Knighton, W. B., Aiken, A. C., Gorkowski, K. J., Dubey, M. K.,  
1136 Allan, J. D., and Thornton, J. A.: Contribution of nitrated phenols to wood burning brown carbon light absorption in  
1137 Detling, United Kingdom during winter time, *Environ. Sci. Technol.*, 47, 6316–6324, doi:10.1021/es400683v, 2013.

1138 Müller, M., Graus, M., Ruuskanen, T. M., Schnitzhofer, R., Bamberger, I., Kaser, L., Titzmann, T., Hörtnagl, L.,  
1139 Wohlfahrt, G., and Hansel, A.: First eddy covariance flux measurements by PTR-TOF, *Atmos. Meas. Tech.*, 3, 387-  
1140 395, doi:10.5194/amt-3-387-2010, 2010.

1141 Müller, M., George, C., and D’Anna, B.: Enhanced spectral analysis of C-TOF aerosol mass spectrometer data:  
1142 iterative residual analysis and cumulative peak fitting, *Int. J. Mass Spectrom.*, 306, 1–8,  
1143 doi:10.1016/j.ijms.2011.04.007, 2011.

1144 Müller, M., Mikoviny, T., Jud, W., D’Anna, B., and Wisthaler, A.: A new software tool for the [S](#) analysis of high  
1145 resolution PTR-TOF mass spectra, *Chemometr. Intell. Lab.*, 127, 158–165, doi:10.1016/j.chemolab.2013.06.011,  
1146 2013.

1147 Na, K., Song, C., and Cocker III, D. R.: Formation of secondary organic aerosol from the reaction of styrene with  
1148 ozone in the presence and absence of ammonia and water, *Atmos. Environ.*, 40, 1889-1900, doi:  
1149 10.1016/j.atmosenv.2005.10.063, 2006.

1150 Natangelo, M., Mangiapan, S., Bagnati, R., Benfenati, E., [and](#) Fanelli, R.: Increased concentrations of nitrophenols  
1151 in leaves from a damaged forestal site, *Chemosphere*, 38, 1495–1503, doi: 10.1016/S0045-6535(98)00370-1, 1999.

1152 Ng, N. L., Kroll, J. H., Chan, A. W. H., Chhabra, P. S., Flagan, R. C., and Seinfeld, J. H.: Secondary organic aerosol  
1153 formation from m-xylene, toluene, and benzene, *Atmos. Chem. Phys.*, 7, 3909–3922, doi:10.5194/acp-7-3909-2007,  
1154 2007.

1155 Novakov, T. and Penner, J. E.: Large contribution of organic aerosols to cloud-condensation-nuclei concentrations,  
1156 *Nature*, 365, 823–826, 1993.

- 1157 Olariu, R. I., Klotz, B., Barnes, I., Becker, K. H., and Mocanu, R.: FT-IR study of the ring-retaining products from  
1158 the reaction of OH radicals with phenol, o-, m-, and p-cresol, *Atmos. Environ.*, 36, 3685–3697, doi: 10.1016/S1352-  
1159 2310(02)00202-9, 2002.
- 1160 Page, S. E., Siegert, F., Rieley, J. O., Boehm, H. D. V., Jaya, A., and Limin, S.: The amount of carbon released from  
1161 peat and forest fires in Indonesia during 1997, *Nature*, 420, 61–65, doi:10.1038/nature01131, 2002.
- 1162 Phouongphouang, P. T. and Arey, J.: Rate constants for the gas-phase reactions of a series of alkyl-naphthalenes  
1163 with the OH radical, *Environ. Sci. Technol.*, 36, 1947–1952, doi: 10.1021/es011434c, 2002.
- 1164 Pittman, C. U., Jr.: Mohan, D., Eseyin, A., Li, Q., Ingram, L., Hassan, E.-B., M., Mitchell, B., Guo, H., and Steele,  
1165 P. H.: Characterization of bio-oils produced from fast pyrolysis of corn stalks in an auger reactor, *Energy Fuels*, 26,  
1166 3816-3825, doi: 10.1021/ef3003922, 2012.
- 1167 Rehbein, P. J. G., Jeong, C.-H., J., McGuire, M. L., Yao, X., Corbin, J. C., and Evans, G. J.: Cloud and fog  
1168 processing enhanced gas-to-particle partitioning of trimethylamine, *Environ. Sci. Technol.*, 45, 4346-4352, doi:  
1169 10.1021/es1042113, 2011.
- 1170 Reid, J. S., Hobbs, P. V., Ferek, R. J., Martins, J. V., Blake, D. R., Dunlap, M. R., and Liousse, C.: Physical,  
1171 chemical, and radiative characteristics of the smoke dominated regional hazes over Brazil, *J. Geophys. Res.*, 103,  
1172 32059–32080, doi:10.1029/98JD00458, 1998.
- 1173 Rippen, G., Zietz, E., Frank, R., Knacker, T., Klöpffer, W.: Do airborne nitrophenols contribute to forest decline?  
1174 *Environ. Technol. Lett.*, 8, 475–482, doi: 10.1080/09593338709384508, 1987.
- 1175 Schade, G. W., and Crutzen, P. J.: Emission of aliphatic amines from animal husbandry and their reactions: Potential  
1176 source of N<sub>2</sub>O and HCN, *J. Atmos. Chem.*, 22, 319-346, doi: 10.1007/BF00696641, 1995.
- 1177 Shafizadeh, F.: Introduction to pyrolysis of biomass, *J. Anal. Appl. Pyrolysis*, 3, 283-305, doi: 10.1016/0165-  
1178 2370(82)80017-X, 1982.
- 1179 Shon, Z., and Kim, K.: Photochemical oxidation of reduced sulfur compounds in an urban location based on short  
1180 time monitoring data, *Chemosphere*, 63,1859-1869, doi: 10.1016/j.chemosphere.2005.10.021, 2006.
- 1181 Simmleit, N., and Schulten, H.-S.: Thermal degradation products of spruce needles, *Chemosphere*, 18, 1855-1869,  
1182 doi: 10.1016/0045-6535(89)90469-4, 1989.
- 1183 Simoneit, B. R. T., Rogge, W. F., Mazurek, M. A., Standley, L. J., Hildemann, L. M., Cass, G. R.: Lignin pyrolysis  
1184 products, lignans, and resin acids as specific tracers of plant classes in emissions from biomass combustion, *Environ.*  
1185 *Sci. Technol.*, 27, 2533–2541, doi: 10.1021/es00048a034, 1993.

1186 Simpson, I. J., Akagi, S. K., Barletta, B., Blake, N. J., Choi, Y., Diskin, G. S., Fried, A., Fuelberg, H. E., Meinardi,  
1187 S., Rowland, F. S., Vay, S. A., Weinheimer, A. J., Wennberg, P. O., Wiebring, P., Wisthaler, A., Yang, M.,  
1188 Yokelson, R. J., and Blake, D. R.: Boreal forest fire emissions in fresh Canadian smoke plumes: C1-C10 volatile  
1189 organic compounds (VOCs), CO<sub>2</sub>, CO, NO<sub>2</sub>, NO, HCN and CH<sub>3</sub>CN, *Atmos. Chem. Phys.*, 11, 6445-6463,  
1190 doi:10.5194/acp-11-6445-2011, 2011.

1191 Sjöström, E. *Wood chemistry: fundamentals and applications*, Second edition, Academic Press, San Diego, USA,  
1192 1993.

1193 Smith, J. N., Dunn, M. J., VanReken, T. M., Iida, K., Stolzenburg, M. R., McMurry, P. H., and Huey, L. G.:  
1194 Chemical composition of atmospheric nanoparticles formed from nucleation in Tecamac, Mexico: Evidence for an  
1195 important role for organic species in nanoparticle growth, *Geophys. Res. Lett.*, 35, L04808,  
1196 doi:10.1029/2007gl032523, 2008.

1197 Song, C., Na, K., Warren, B., Malloy, Q., and Cocker, D. R.: Impact of propene on secondary organic aerosol  
1198 formation from m-xylene, *Environ. Sci. Technol.*, 41, 6990–6995, doi: 10.1021/es062279a, 2007.

1199 Sotiropoulou, R. E. P., Tagaris, E., Pilinis, C., Anttila, T., and Kulmala, M.: Modeling new particle formation during  
1200 air pollution episodes: Impacts on aerosol and cloud condensation nuclei, *Aerosol Sci. Tech.*, 40, 557–572, doi:  
1201 10.1080/02786820600714346, 2006.

1202 St.-Clair, J. M., Spencer, K. M., Beaver, M. R., Crouse, J. D., Paulot, F., and Wennberg, P. O.: Quantification of  
1203 hydroxyacetone and glycolaldehyde using chemical ionization mass spectrometry, *Atmos. Chem. Phys.*, 14, 4251-  
1204 4262, doi:10.5194/acp-14-4251-2014, 2014.

1205 Stockwell, C. E., Yokelson, R. J., Kreidenweis, S. M., Robinson, A. L., DeMott, P. J., Sullivan, R. C., Reardon, J.,  
1206 Ryan, K. C., Griffith, D. W. T., and Stevens, L.: Trace gas emissions from combustion of peat, crop residue,  
1207 biofuels, grasses, and other fuels: configuration and FTIR component of the fourth Fire Lab at Missoula Experiment  
1208 (FLAME-4), *Atmos. Chem. Phys. Discuss.*, 14, 10061-10134, doi:10.5194/acpd-14-10061-2014, 2014.

1209 Strollo, C. M., and Ziemann, P. J.: Products and mechanism of secondary organic aerosol formation from the  
1210 reaction of 3-methylfuran with OH radicals in the presence of NO<sub>x</sub>, *Atmos. Environ.*, 77, 534-543, doi:  
1211 10.1016/j.atmosenv.2013.05.033, 2013.

1212 Tkacik, D., Robinson, E., Ahern, A., Saleh, R., Veres, P., Stockwell, C., Simpson, I., Meinardi, S., Blake, D., Presto,  
1213 A., Sullivan, R., Donahue, N., and Robinson, A.: A dual chamber enhancement method to quantify aerosol  
1214 formation: biomass burning secondary organic aerosol, in preparation, 2014.

1215 Toda, K., Obata, T., Obokin, V. A., Potemkin, V. L., Hirota, K., Takeuchi, M., Arita, S., Khodzher, T. V., and  
1216 Grachev, M. A.: Atmospheric methanethiol emitted from a pulp and paper plant on the shore of Lake Baikal, *Atmos.*  
1217 *Environ.*, 44, 2427-2433, doi: 10.1016/j.atmosenv.2010.03.037, 2010.

- 1218 Trentmann, J., Andreae, M. O., and Graf, H.-F: Chemical processes in a young biomass-burning plume, *J. Geophys.*  
1219 *Res.*, 108, 4705, doi: 10.1029/2003JD003732, 2003.
- 1220 Trentmann, J., Yokelson, R. J., Hobbs, P. V., Winterrath, T., Christian, T. J., Andreae, M. O., and Mason, S. A.: An  
1221 analysis of the chemical processes in the smoke plume from a savanna fire, *J. Geophys. Res.*, 110, D12301,  
1222 doi:10.1029/2004JD005628, 2005.
- 1223 Vakkari, V., Kerminen, V.-M., Beukes, J. P., Tiitta, P., van Zyl, P. G., Josipovic, M., Venter, A. D., Jaars, K.,  
1224 Worsnop, D. R., Kulmala, M., and Laakso, L.: Rapid changes in biomass burning aerosols by atmospheric oxidation,  
1225 *Geophys. Res. Lett.*, 41, 2644-2651, doi:10.1002/2014GL059396, 2014.
- 1226 Veres, P., Roberts, J. M., Burling, I. R., Warneke, C., de Gouw, J., and Yokelson, R. J.: Measurements of gas-phase  
1227 inorganic and organic acids from biomass fires by negative-ion proton-transfer chemical-ionization mass  
1228 spectrometry, *J. Geophys. Res.*, 115, D23302, doi:10.1029/2010JD014033, 2010.
- 1229 Villanueva, F., Barnes, I., Monedero, E., Salgado, S., Gómez, M.V., Martin, P.: Primary product distribution from  
1230 the Cl-atom initiated atmospheric degradation of furan: Environmental implications. *Atmos. Environ.*, 41, 8796–  
1231 8810, doi: 10.1016/j.atmosenv.2007.07.053, 2007.
- 1232 Wagner, V., Jenkin, M.E., Saunders, S.M., Stanton, J., Wirtz, K., Pilling, M.J.: Modelling of the photooxidation of  
1233 toluene: conceptual ideas for validating detailed mechanisms, *Atmos. Chem. Phys.*, 3, 89–106, doi:10.5194/acp-3-  
1234 89-2003, 2003.
- 1235 Ward, D. E. and Radke, L. F.: Emissions measurements from vegetation fires: A Comparative evaluation of methods  
1236 and results, in: *Fire in the Environment: The Ecological, Atmospheric and Climatic Importance of Vegetation Fires*,  
1237 edited by: Crutzen, P. J. and Goldammer, J. G., John Wiley, New York, 53–76, 1993.
- 1238 Warneke, C., Roberts, J. M., Veres, P., Gilman, J., Kuster, W. C., Burling, I., Yokelson, R. J., and de Gouw, J. A.:  
1239 VOC identification and inter-comparison from laboratory biomass burning using PTR-MS and PIT-MS, *Int. J. Mass*  
1240 *Spectrom.*, 303, 6–14, doi:10.1016/j.ijms.2010.12.002, 2011.
- 1241 Wiedinmyer, C., Akagi, S. K., Yokelson, R. J., Emmons, L. K., Al-Saadi, J.A., Orlando, J. J., and Soja, A.J.: The  
1242 Fire INventory from NCAR (FINN): a high resolution global model to estimate the emissions from open burning,  
1243 *Geosci. Model Dev.*, 4, 625-641, doi:10.5194/gmd-4-625-2011, 2011.
- 1244 Williams, C. J., and Yakvitt, J. B.: Botanical composition of peat and degree of peat decomposition in three  
1245 temperate peatlands, *Ecoscience*, 10, 85-95, 2003.
- 1246 Yee, L. D., Kautzman, K. E., Loza, C. L., Schilling, K. A., Coggen, M. M., Chhabra, P. S., Chan, M. N., Chan, A.  
1247 W. H., Hersey, S. P., Crouse, J. D., Wennberg, P. O., Flagan, R. C., and Seinfeld, J. H.: Secondary organic aerosol  
1248 formation from biomass burning intermediates: phenol and methoxyphenols, *Atmos. Chem. Phys.*, 13, 8019-8043,  
1249 doi:10.5194/acp-13-8019-2013, 2013.

1250 Yokelson, R. J., Griffith, D. W. T., and Ward, D. E.: Open path Fourier transform infrared studies of large-scale  
1251 laboratory biomass fires, *J. Geophys. Res.*, 101, 21067–21080, doi:10.1029/96JD01800, 1996.

1252 Yokelson, R. J., Goode, J. G., Ward, D. E., Susott, R. A., Babbitt, R. E., Wade, D. D., Bertschi, I., Griffith, D. W.  
1253 T., and Hao, W. M.: Emissions of formaldehyde, acetic acid, methanol, and other trace gases from biomass fires in  
1254 North Carolina measured by airborne Fourier transform infrared spectroscopy, *J. Geophys. Res.*, 104, 30109–30125,  
1255 doi:10.1029/1999jd900817, 1999.

1256 Yokelson, R. J., Karl, T., Artaxo, P., Blake, D. R., Christian, T. J., Griffith, D. W. T., Guenther, A., and Hao, W. M.:  
1257 The Tropical Forest and Fire Emissions Experiment: overview and airborne fire emission factor measurements,  
1258 *Atmos. Chem. Phys.*, 7, 5175–5196, doi:10.5194/acp-7-5175-2007, 2007.

1259 Yokelson, R. J., Crounse, J. D., DeCarlo, P. F., Karl, T., Urbanski, S., Atlas, E., Campos, T., Shinozuka, Y.,  
1260 Kapustin, V., Clarke, A. D., Weinheimer, A., Knapp, D. J., Montzka, D. D., Holloway, J., Weibring, P., Flocke, F.,  
1261 Zheng, W., Toohey, D., Wennberg, P. O., Wiedinmyer, C., Mauldin, L., Fried, A., Richter, D., Walega, J., Jimenez,  
1262 J. L., Adachi, K., Buseck, P. R., Hall, S. R., and Shetter, R.: Emissions from biomass burning in the Yucatan,  
1263 *Atmos. Chem. Phys.*, 9, 5785–5812, doi:10.5194/acp-9-5785-2009, 2009.

1264 Yokelson, R. J., Burling, I. R., Gilman, J. B., Warneke, C., Stockwell, C. E., de Gouw, J., Akagi, S. K., Urbanski, S.  
1265 P., Veres, P., Roberts, J. M., Kuster, W. C., Reardon, J., Griffith, D. W. T., Johnson, T. J., Hosseini, S., Miller, J. W.,  
1266 Cocker III, D. R., Jung, H., and Weise, D. R.: Coupling field and laboratory measurements to estimate the emission  
1267 factors of identified and unidentified trace gases for prescribed fires, *Atmos. Chem. Phys.*, 13, 89–116,  
1268 doi:10.5194/acp-13-89-2013, 2013.

1269 [Yu, F. and Luo, G.: Modeling of gaseous methylamines in the global atmosphere: impacts of oxidation and aerosol](#)  
1270 [uptake, \*Atmos. Chem. Phys.\*, 14, 12455–12464, doi:10.5194/acp-14-12455-2014, 2014.](#) ~~Yu, F., and Luo, G.:~~  
1271 ~~Modelling of gaseous dimethylamine in the global atmosphere: impacts of oxidation and aerosol uptake, *Atmos.*~~  
1272 ~~*Chem. Phys. Discuss.*, 14, 17727–17748, doi:10.5194/acpd-14-17727-2014, 2014.~~

1273 Zhang, X., Lin, Y. –H., Surratt, J. D., Zotter, P., and Weber, R. J.: Sources, composition and absorption Ångström  
1274 exponent of light-absorbing organic components in aerosol extracts from the Los Angeles Basin, *Environ. Sci.*  
1275 *Technol.*, 47, 3685–3693, doi:10.1021/ES305047B, 2013.

1276 Ziemann, P. J., and Atkinson, R.: Kinetics, products, and mechanisms of secondary organic aerosol formation,  
1277 *Chem. Soc. Rev.*, 41, 6582–6605, doi: 10.1039/c2cs35122f, 2012.

1278

1279 **Figure 1.** (a) The normalized response of calibration factors (“CF,” ncps/ppbv) versus mass (calibrated species  
1280 labeled by name) overlaid with the linearly fitted mass-dependent transmission curve (black markers and dotted  
1281 line). Separate linear approximations (b) oxygenated (blue) and (c) hydrocarbon (green) species used to calculate  
1282 approximate calibration factors for all observed masses where explicit calibrations were not available.

1283 **Figure 2.** A typical full mass scan of biomass burning smoke from the PTR-TOF-MS on a logarithmic (a) and a  
1284 smaller range linear (b) scale. The internal standard (1,3-diiodobenzene) accounts for the major peaks  $\sim m/z$  331 and  
1285 fragments at peaks near  $m/z$  204 and 205.

1286 **Figure 3.** ~~The emission factors ( $\text{g kg}^{-1}$ ) of total observed hydrocarbons and total observed species~~  
1287 ~~oxygenated to different degrees averaged for each fire type based on a synthesis of PTR-TOF-MS and OP-FTIR~~  
1288 ~~data. The patterned sections indicate the contribution to each of the above categories by selected functionalities~~  
1289 ~~discussed in the text (aromatic hydrocarbons, phenolics, furans). The parenthetical expressions indicate how many~~  
1290 ~~oxygen atoms are present. The distribution of oxygenated and hydrocarbon emission factors averaged for each fuel~~  
1291 ~~type where FTIR data were available. EFs are included for FTIR compounds and the 68 masses initially analyzed by~~  
1292 ~~PTR TOF MS. The patterned sections indicate the contributions from various “families” based on functionality and~~  
1293 ~~their oxygen content.~~

1294 **Figure 4.** (a) The EFs of the aromatics analyzed in all fires averaged and shown by fuel type. Individual  
1295 contributions from benzene and other aromatics are indicated by color. The EFs for p-Cymene ~~is~~ are only calculated  
1296 for select ~~burns fires~~ and should not be considered ~~an average for each particular fuel type~~ a true average. (b) The  
1297 correlation plots of selected aromatics with benzene during a black spruce fire (Fire 74). Similar behavior was  
1298 observed for all other fuel types.

1299 **Figure 5.** (a) The distribution in average fuel EF for several phenolic compounds, where compound specific  
1300 contributions are indicated by color. The EFs for ~~compounds~~ additionally analyzed ~~compounds a single time during~~  
1301 ~~for~~ select fires are included but ~~are not considered the fuel~~ are not a true average. (b) The linear correlation of select  
1302 phenolic compounds with phenol during an organic hay burn (Fire 119).

1303 **Figure 6.** (a) The distribution in average fuel EF for furan and substituted furans, where individual contributions are  
1304 indicated by color. ~~The EFs for substituted furans additionally analyzed a single time are not true averages~~ The EFs  
1305 ~~for additionally analyzed substituted furans are also include but should not be considered fuel averages~~ (b) The linear  
1306 correlation of furan with select ~~furan derivatives~~ substituted furans for an African grass fire (Fire 49).

1307 **Figure 7.** Expanded view of the PTR-TOF-MS spectrum at  $m/z$  69 demonstrating the advantage over unit mass  
1308 resolution instruments of distinguishing multiple peaks, in this instance separating carbon suboxide ( $\text{C}_3\text{O}_2$ ), furan  
1309 ( $\text{C}_4\text{H}_4\text{O}$ ), and mostly isoprene ( $\text{C}_5\text{H}_8$ ) in ponderosa pine smoke (fire 70).

1310 **Figure 8.** Expanded view of the PTR-TOF-MS spectrum of NC peat (fire 61) at  $m/z$  137 showing multiple peaks

1311 **Figure 9.** Emission factors ( $\text{g kg}^{-1}$ ) of aromatic hydrocarbons (a), phenolic compounds (b), and furans (c), for  
1312 traditional and advanced cookstoves. The EF for traditional stoves were adjusted from original lab data (Sect. 4.7)

1313



1314 Table 1. Quantities for various categories of compounds ( $\text{g kg}^{-1}$ ) and calculation of mass ratios and/or percentages for several fuel types.

1315

| Quantity or Ratio                        | Chaparral | Coniferous<br>Canopy | Peat | Grasses | Cooking<br>Fires | Crop<br>Residue | Trash |
|--|-----------|----------------------|------|---------|------------------|-----------------|-------|
| $\Sigma$ NMOCs                           | 13.1      | 23.9                 | 40.5 | 5.17    | 8.16             | 29.6            | 7.13  |
| $\Sigma$ I/SVOCs <sup>a</sup>            | 3.49      | 7.13                 | 14.6 | 1.38    | 1.33             | 7.21            | 1.83  |
| $\Sigma$ Tentatively assigned NMOCs      | 1.43      | 2.77                 | 7.01 | 0.72    | 0.72             | 4.38            | 0.51  |
| $\Sigma$ Unidentified NMOCs              | 1.23      | 1.79                 | 7.50 | 0.39    | 0.33             | 2.10            | 0.41  |
| $\Sigma$ (I/SVOCs) / $\Sigma$ NMOC       | 0.21      | 0.28                 | 0.37 | 0.26    | 0.15             | 0.24            | 0.26  |
| Percent NMOCs Tentatively assigned       | 8.35      | 9.74                 | 17.5 | 13.9    | 8.19             | 14.0            | 7.20  |
| Percent NMOCs Unidentified               | 7.24      | 6.75                 | 19.5 | 7.19    | 3.77             | 6.90            | 5.75  |
| Percent NMOCs Tentatively + Unidentified | 16        | 16                   | 37   | 21      | 12               | 21              | 13    |

<sup>a</sup> See section 3.2 for definition

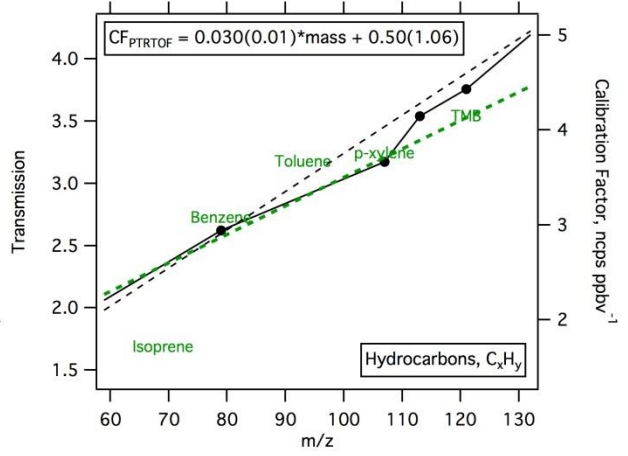
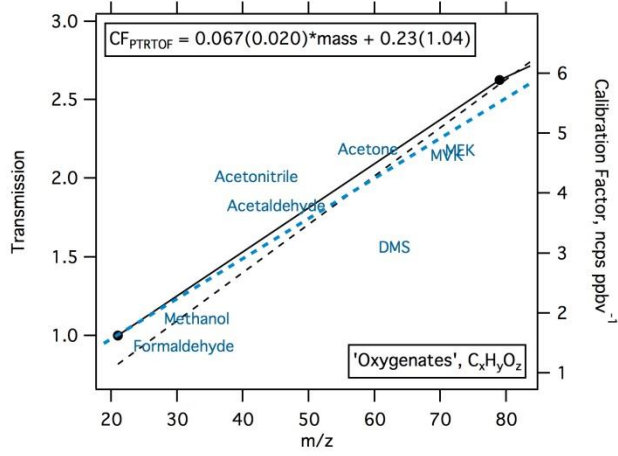
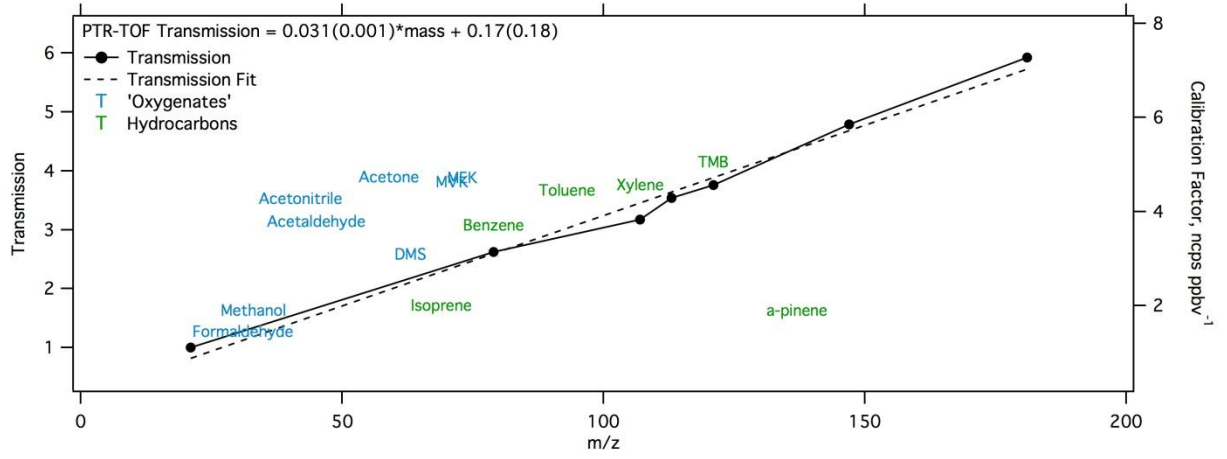
1316 | Table 2. Emission ratios to benzene, phenol, and furan for aromatic hydrocarbons, phenolic compounds, and substituted furans in lumped fuel-type categories.

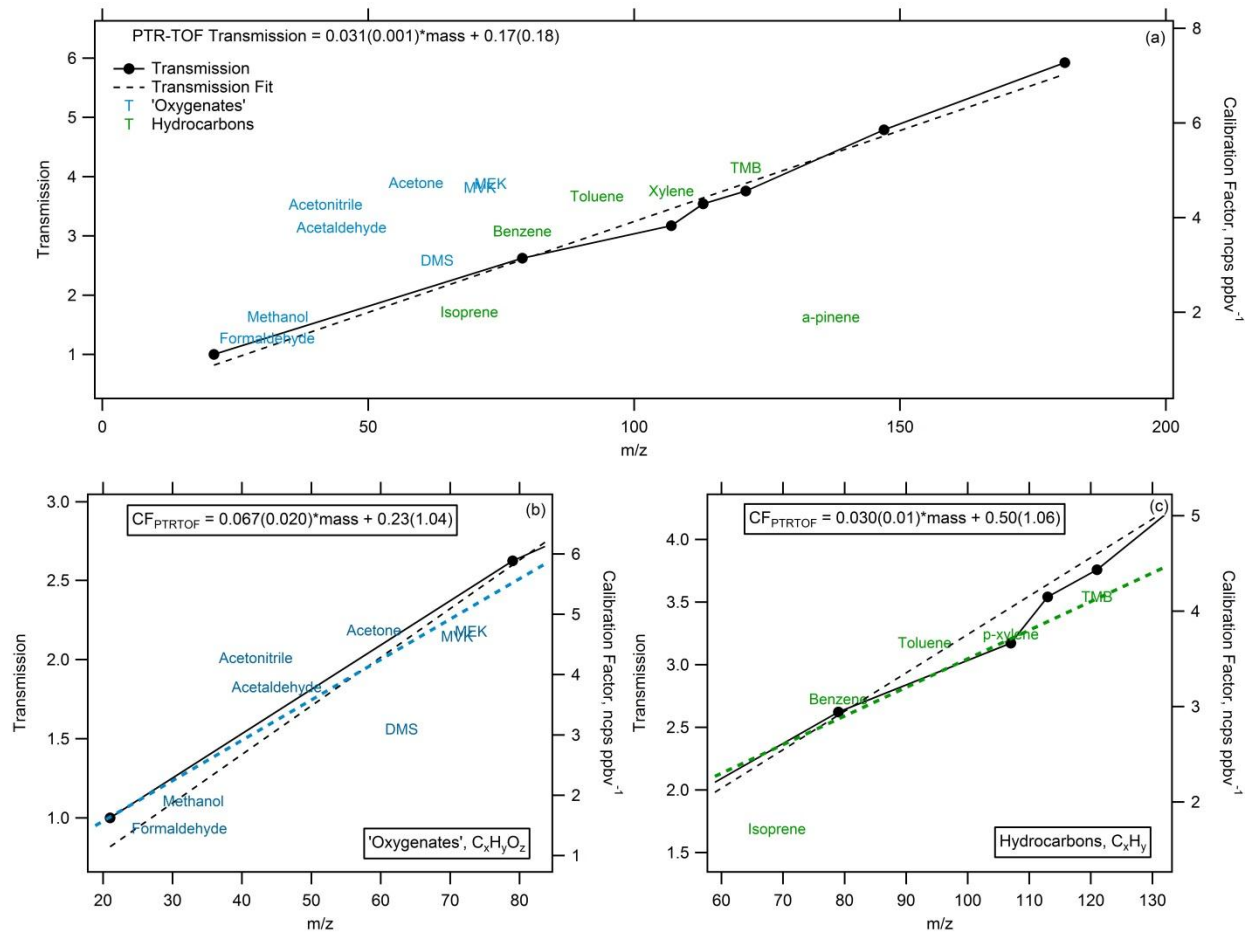
|   | Fuel Type (# burns)                           | Grasses (42) |              | Coniferous Canopy (14) |              | Chaparral (8) |              | Crop Residue (food, 19) |              | Crop Residue (feed, 9) |              | Open 3-Stone Cooking (3) |       | Rocket Cookstoves (5) |  | Gasifier Cookstove (1) |  | Trash (2) |  | Tires (1) |  | Plastic Bags (1) |  |  |
|---|---|--------------|--------------|------------------------|--------------|---------------|--------------|-------------------------|--------------|------------------------|--------------|--------------------------|-------|-----------------------|--|------------------------|--|-----------|--|-----------|--|------------------|--|--|
|   |   |              |              |                        |              |               |              |                         |              |                        |              |                          |       |                       |  |                        |  |           |  |           |  |                  |  |  |
| <b>ER/Benzene</b>                       | MCE   | 0.968(0.010) | 0.933(0.032) | 0.927(0.017)           | 0.767(0.074) | 0.946(0.022)  | 0.940(0.017) | 0.968(0.004)            | 0.972(0.015) | 0.984                  | 0.973(0.006) | 0.961                    | 0.994 |                       |  |                        |  |           |  |           |  |                  |  |  |
| Toluene                                 | C <sub>7</sub> H <sub>8</sub>                 | 0.44(0.26)   | 2.19(0.84)   | 0.49(0.17)             | 0.53(0.17)   | 0.70(0.22)    | 1.00(0.44)   | 0.095(0.029)            | 0.98(1.39)   | 0.24                   | 0.41(0.20)   | 0.056                    | 0.69  |                       |  |                        |  |           |  |           |  |                  |  |  |
| Phenylacetylene                         | C <sub>8</sub> H <sub>6</sub>                 | 0.094(0.022) | 0.13         | 0.067(0.039)           | -            | 0.65(0.45)    | 0.14(0.09)   | 0.10(0.05)              | -            | -                      | -            | 0.020                    | -     |                       |  |                        |  |           |  |           |  |                  |  |  |
| Styrene                                 | C <sub>8</sub> H <sub>8</sub>                 | 0.078(0.025) | 0.11(0.02)   | 0.074(0.020)           | 0.087(0.027) | 0.10(0.03)    | 0.14(0.05)   | 0.054(0.021)            | 0.076(0.023) | 0.042                  | 0.86(0.16)   | 0.064                    | 0.094 |                       |  |                        |  |           |  |           |  |                  |  |  |
| p-Xylene                                | C <sub>8</sub> H <sub>10</sub>                | 0.102(0.058) | 0.21(0.03)   | 0.12(0.03)             | 0.32(0.16)   | 0.20(0.08)    | 0.24(0.11)   | 0.052(0.034)            | 0.10(0.05)   | 0.048                  | 0.095(0.017) | 0.043                    | 0.029 |                       |  |                        |  |           |  |           |  |                  |  |  |
| Trimethylbenzene                        | C <sub>9</sub> H <sub>12</sub>                | 0.059(0.045) | 0.11(0.03)   | 0.043(0.023)           | 0.17(0.08)   | 0.11(0.05)    | 0.11(0.06)   | 0.014(0.007)            | 0.050(0.048) | 0.026                  | 0.033(0.016) | 0.011                    | 0.047 |                       |  |                        |  |           |  |           |  |                  |  |  |
| Naphthalene                             | C <sub>10</sub> H <sub>8</sub>                | 0.18(0.16)   | 0.13(0.05)   | 0.10(0.03)             | 0.15(0.09)   | 0.20(0.17)    | 0.18(0.11)   | 0.21(0.05)              | 0.30(0.17)   | 0.12                   | 0.10         | 0.19                     | 0.059 |                       |  |                        |  |           |  |           |  |                  |  |  |
| Dihydronaphthalene                      | C <sub>10</sub> H <sub>10</sub>               | 0.040(0.030) | 0.034(0.016) | 0.020(0.010)           | 0.050(0.019) | 0.059(0.028)  | 0.051(0.021) | 0.019(0.006)            | -            | -                      | -            | 9.81E-03                 | -     |                       |  |                        |  |           |  |           |  |                  |  |  |
| p-Cymene <sup>a</sup>                   | C <sub>10</sub> H <sub>14</sub>               | 0.018(0.013) | 0.11(0.01)   | 0.037                  | 0.15(0.12)   | 0.035(0.019)  | 0.11(0.03)   | 4.10E-03                | -            | nm                     | 0.018        | nm                       | nm    |                       |  |                        |  |           |  |           |  |                  |  |  |
| Methyl Naphthalenes                     | C <sub>11</sub> H <sub>10</sub>               | 0.032(0.009) | 0.053(0.005) | 0.033(0.007)           | -            | 0.19(0.09)    | 0.057(0.037) | -                       | -            | -                      | -            | 0.031                    | -     |                       |  |                        |  |           |  |           |  |                  |  |  |
| <b>ER/Phenol</b>                        |   |              |              |                        |              |               |              |                         |              |                        |              |                          |       |                       |  |                        |  |           |  |           |  |                  |  |  |
| Cresols (Methylphenols) <sup>a</sup>    | C <sub>7</sub> H <sub>8</sub> O               | 0.52(0.19)   | 0.55(0.07)   | 0.49                   | 0.29(0.18)   | 0.57(0.10)    | 0.61(0.14)   | -                       | 0.34(0.28)   | nm                     | nm           | nm                       | nm    |                       |  |                        |  |           |  |           |  |                  |  |  |
| Catechol (Benzenediols) <sup>b</sup>    | C <sub>6</sub> H <sub>6</sub> O <sub>2</sub>  | 0.73(0.41)   | 0.76(0.29)   | 1.72(1.28)             | 1.58(1.03)   | 0.93(0.45)    | 0.67(0.30)   | 0.74(0.65)              | 1.86(1.29)   | 0.49                   | 1.12(0.65)   | 0.082                    | 0.31  |                       |  |                        |  |           |  |           |  |                  |  |  |
| Vinylphenol                             | C <sub>8</sub> H <sub>8</sub> O               | 0.66(0.19)   | 0.33(0.09)   | 0.30(0.05)             | 0.18(0.05)   | 0.60(0.35)    | 0.29(0.06)   | 0.18(0.06)              | 0.25(0.18)   | 0.14                   | 0.34(0.02)   | 0.17                     | 0.33  |                       |  |                        |  |           |  |           |  |                  |  |  |
| Salicylaldehyde                         | C <sub>7</sub> H <sub>6</sub> O <sub>2</sub>  | 0.18(0.06)   | 0.17(0.04)   | 0.15(0.04)             | 0.20(0.13)   | 0.18(0.08)    | 0.11(0.04)   | 0.16(0.06)              | 0.27(0.15)   | 0.22                   | 0.28(0.09)   | 0.17                     | -     |                       |  |                        |  |           |  |           |  |                  |  |  |
| Xylenol (2,5-dimethyl phenol)           | C <sub>8</sub> H <sub>10</sub> O              | 0.25(0.09)   | 0.19(0.06)   | 0.11(0.06)             | 0.31(0.09)   | 0.34(0.07)    | 0.33(0.07)   | 0.18(0.09)              | 0.35(0.11)   | 0.11                   | 0.23(0.00)   | 0.026                    | -     |                       |  |                        |  |           |  |           |  |                  |  |  |
| Guaiacol (2-Methoxyphenol)              | C <sub>7</sub> H <sub>8</sub> O <sub>2</sub>  | 0.40(0.23)   | 0.42(0.12)   | 0.21(0.09)             | 0.71(0.36)   | 0.76(0.33)    | 0.47(0.16)   | 0.52(0.40)              | 1.30(0.73)   | 0.31                   | 0.54(0.32)   | 0.019                    | 2.02  |                       |  |                        |  |           |  |           |  |                  |  |  |
| Creosol (4-Methylguaiacol) <sup>a</sup> | C <sub>8</sub> H <sub>10</sub> O <sub>2</sub> | 0.21(0.16)   | 0.21(0.09)   | 0.067                  | 0.12(0.17)   | 0.19(0.10)    | 0.24(0.07)   | 0.46                    | 0.62(0.23)   | nm                     | 0.043        | nm                       | nm    |                       |  |                        |  |           |  |           |  |                  |  |  |
| 3-Methoxycatechol <sup>a</sup>          | C <sub>7</sub> H <sub>8</sub> O <sub>3</sub>  | 0.090(0.072) | 0.067(0.031) | 0.028                  | 0.19(0.04)   | 0.066(0.037)  | 0.063(0.035) | 0.28                    | 0.44         | nm                     | 0.14         | nm                       | nm    |                       |  |                        |  |           |  |           |  |                  |  |  |
| 4-Vinylguaiacol <sup>a</sup>            | C <sub>9</sub> H <sub>10</sub> O <sub>2</sub> | 0.29(0.19)   | 0.27(0.12)   | 0.052                  | 0.27(0.04)   | 0.37(0.19)    | 0.31(0.11)   | 0.34                    | 0.35(0.22)   | nm                     | 0.054        | nm                       | nm    |                       |  |                        |  |           |  |           |  |                  |  |  |
| Syringol <sup>a</sup>                   | C <sub>8</sub> H <sub>10</sub> O <sub>3</sub> | 0.13(0.07)   | 0.078(0.029) | 0.21(0.12)             | 0.22(0.07)   | 0.16(0.10)    | 0.12(0.02)   | 0.94                    | 0.92(0.53)   | nm                     | -            | nm                       | nm    |                       |  |                        |  |           |  |           |  |                  |  |  |
| <b>ER/Furan</b>                         |   |              |              |                        |              |               |              |                         |              |                        |              |                          |       |                       |  |                        |  |           |  |           |  |                  |  |  |
| 2-Methylfuran                           | C <sub>5</sub> H <sub>6</sub> O               | 0.53(0.27)   | 1.02(0.40)   | 0.77(0.30)             | 0.34(0.14)   | 1.50(0.66)    | 1.36(0.38)   | 0.95(0.33)              | 1.66(1.95)   | 0.55                   | 0.64(0.02)   | 2.10                     | 2.10  |                       |  |                        |  |           |  |           |  |                  |  |  |
| 2-Furanone                              | C <sub>4</sub> H <sub>4</sub> O <sub>2</sub>  | 0.93(0.50)   | 1.53(0.80)   | 0.96(0.49)             | 0.44(0.36)   | 2.05(1.09)    | 1.16(0.56)   | 0.73(0.21)              | 2.37(3.39)   | 1.28                   | 1.04(0.49)   | 3.02                     | -     |                       |  |                        |  |           |  |           |  |                  |  |  |
| 2-Furaldehyde (Furfural)                | C <sub>5</sub> H <sub>4</sub> O <sub>2</sub>  | 1.61(0.81)   | 1.82(0.85)   | 1.35(0.75)             | 1.34(0.85)   | 2.78(1.21)    | 1.69(0.96)   | 2.47(1.84)              | 5.69(8.46)   | 1.26                   | 1.03(0.29)   | 2.09                     | 0.39  |                       |  |                        |  |           |  |           |  |                  |  |  |
| 2,5-Dimethylfuran <sup>a</sup>          | C <sub>6</sub> H <sub>8</sub> O               | 0.27(0.09)   | 0.58(0.20)   | 0.615573               | 0.11(0.01)   | 0.62(0.77)    | 0.98(0.14)   | -                       | -            | nm                     | 0.2715416    | nm                       | nm    |                       |  |                        |  |           |  |           |  |                  |  |  |
| Furfuryl alcohol                        | C <sub>5</sub> H <sub>6</sub> O <sub>2</sub>  | 0.77(0.49)   | 1.23(0.57)   | 0.85(0.44)             | 0.25(0.21)   | 1.98(1.21)    | 1.21(0.55)   | 0.86(0.25)              | 1.35         | 0.00                   | 0.78(0.31)   | 1.06                     | 1.03  |                       |  |                        |  |           |  |           |  |                  |  |  |
| Methylfurfural <sup>b</sup>             | C <sub>6</sub> H <sub>6</sub> O <sub>2</sub>  | 0.42(0.24)   | 1.18(0.89)   | 1.95(1.49)             | 0.44(0.35)   | 0.98(0.52)    | 0.90(0.42)   | 0.59(0.20)              | 1.06(1.32)   | 0.37                   | 0.38(0.06)   | 1.33                     | 0.093 |                       |  |                        |  |           |  |           |  |                  |  |  |
| Benzenofuran                            | C <sub>8</sub> H <sub>6</sub> O               | 0.059(0.028) | 0.11(0.05)   | 0.10(0.05)             | 0.017(0.010) | 0.10(0.04)    | 0.11(0.05)   | 0.39(0.57)              | 0.041(0.030) | 0.069                  | 0.058(0.018) | 2.79                     | 0.056 |                       |  |                        |  |           |  |           |  |                  |  |  |
| Hydroxymethylfurfural                   | C <sub>6</sub> H <sub>6</sub> O <sub>3</sub>  | 0.21(0.16)   | 0.64(0.43)   | 0.28(0.19)             | 0.18(0.14)   | 0.49(0.35)    | 0.27(0.14)   | 0.20(0.06)              | 0.44(0.52)   | 0.30                   | 0.39(0.22)   | 0.28                     | -     |                       |  |                        |  |           |  |           |  |                  |  |  |
| Methylbenzenofuran isomers <sup>a</sup> | C <sub>9</sub> H <sub>8</sub> O               | 0.67(0.58)   | -            | -                      | -            | -             | -            | -                       | -            | nm                     | -            | nm                       | nm    |                       |  |                        |  |           |  |           |  |                  |  |  |

Note: "nm" indicates not measured; blank indicates species remained below the detection limits; values in parenthesis indicate one standard deviation

<sup>a</sup> Species were only selected for a few key fires and are not considered the average of each fuel type

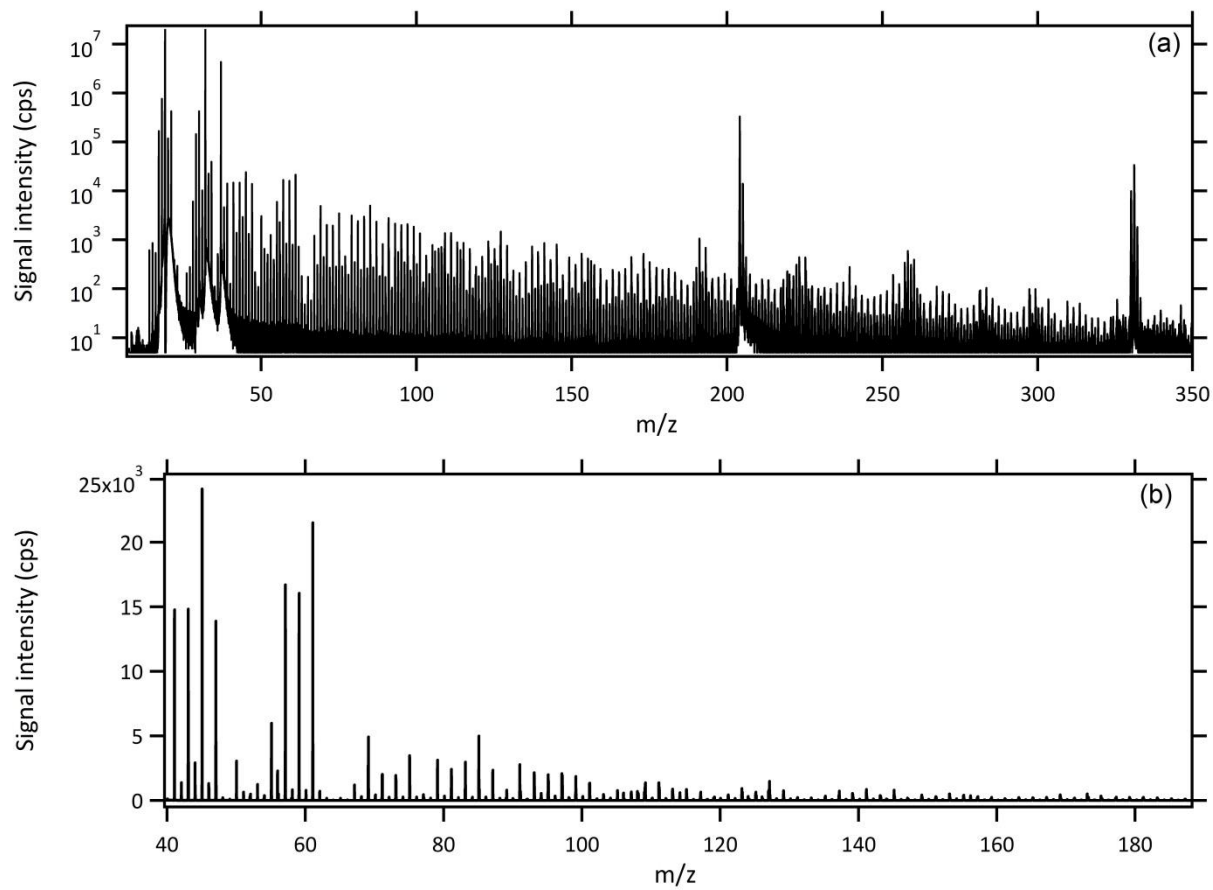
<sup>b</sup> Significant contributions from both methylfurfural and catechol reported in pyrolysis reference papers, thus there is no indication which species is the major contributor at this mass





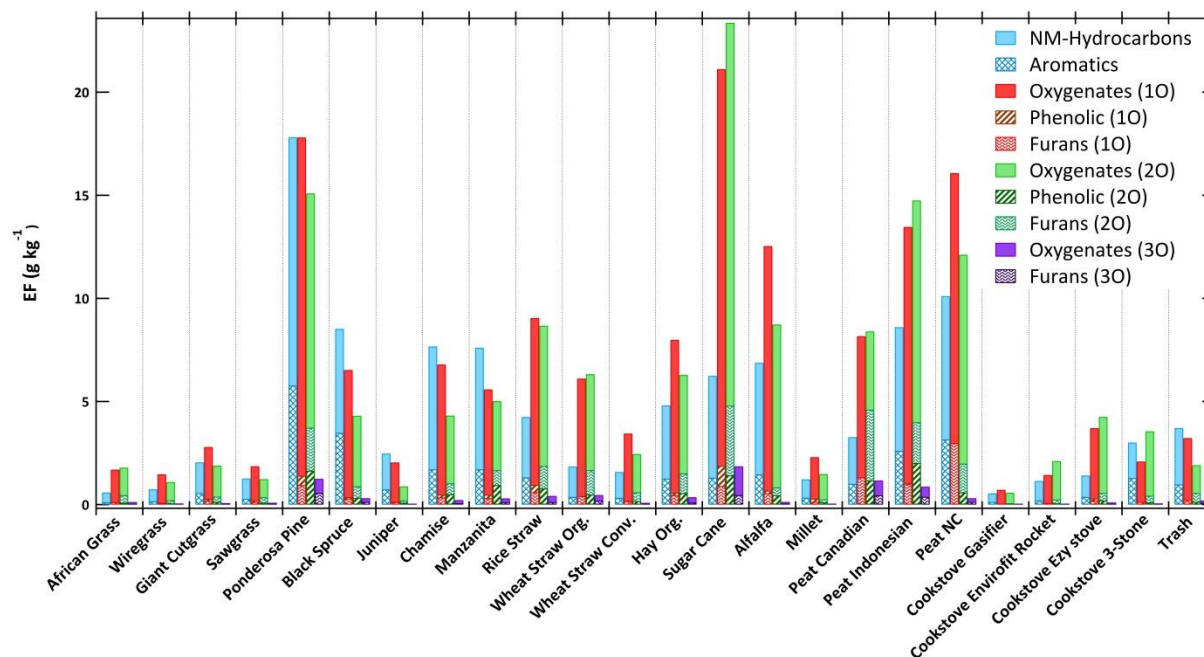
1318

1319 Figure 1. (a) The normalized response of calibration factors (“CF,” ncps/ppbv) versus mass (calibrated species  
 1320 labeled by name) overlaid with the linearly fitted mass-dependent transmission curve (black markers and dotted  
 1321 line). Separate linear approximations (b) oxygenated (blue) and (c) hydrocarbon (green) species used to calculate  
 1322 approximate calibration factors for all observed masses where explicit calibrations were not available.



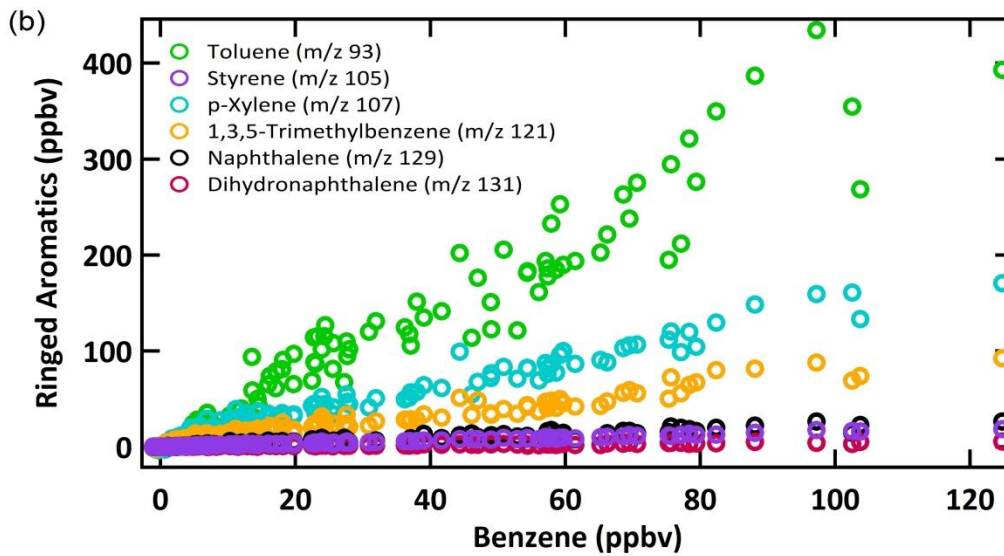
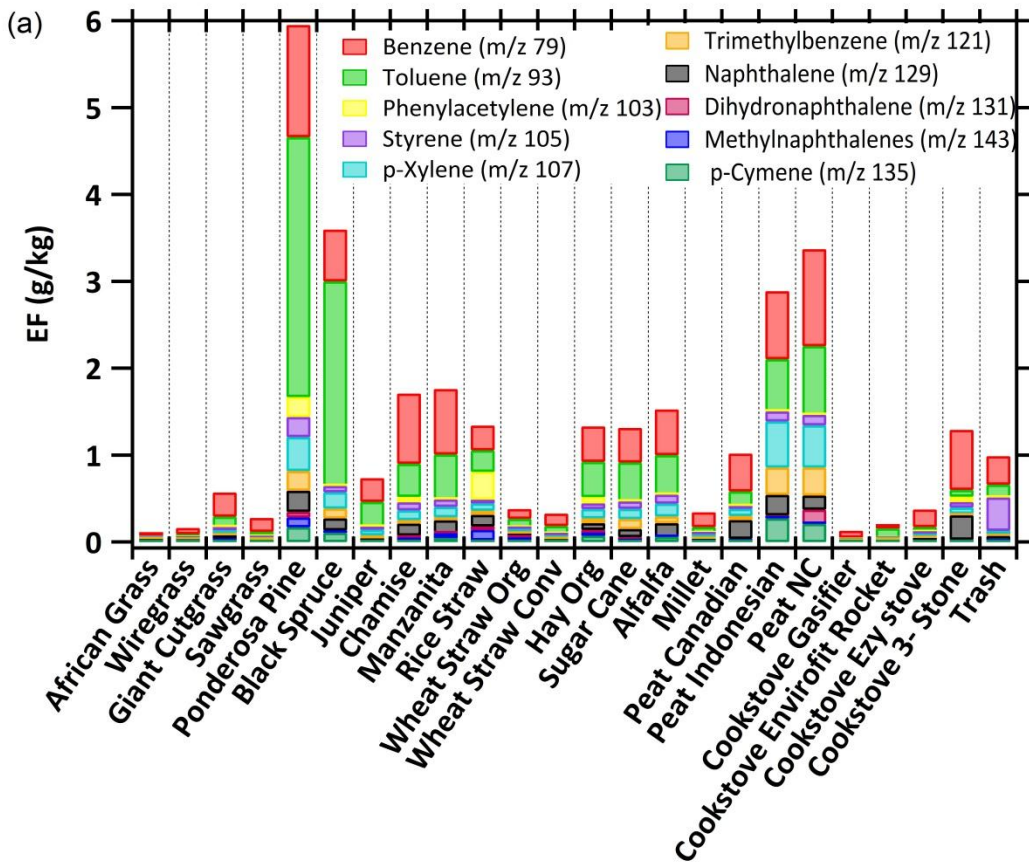
1323

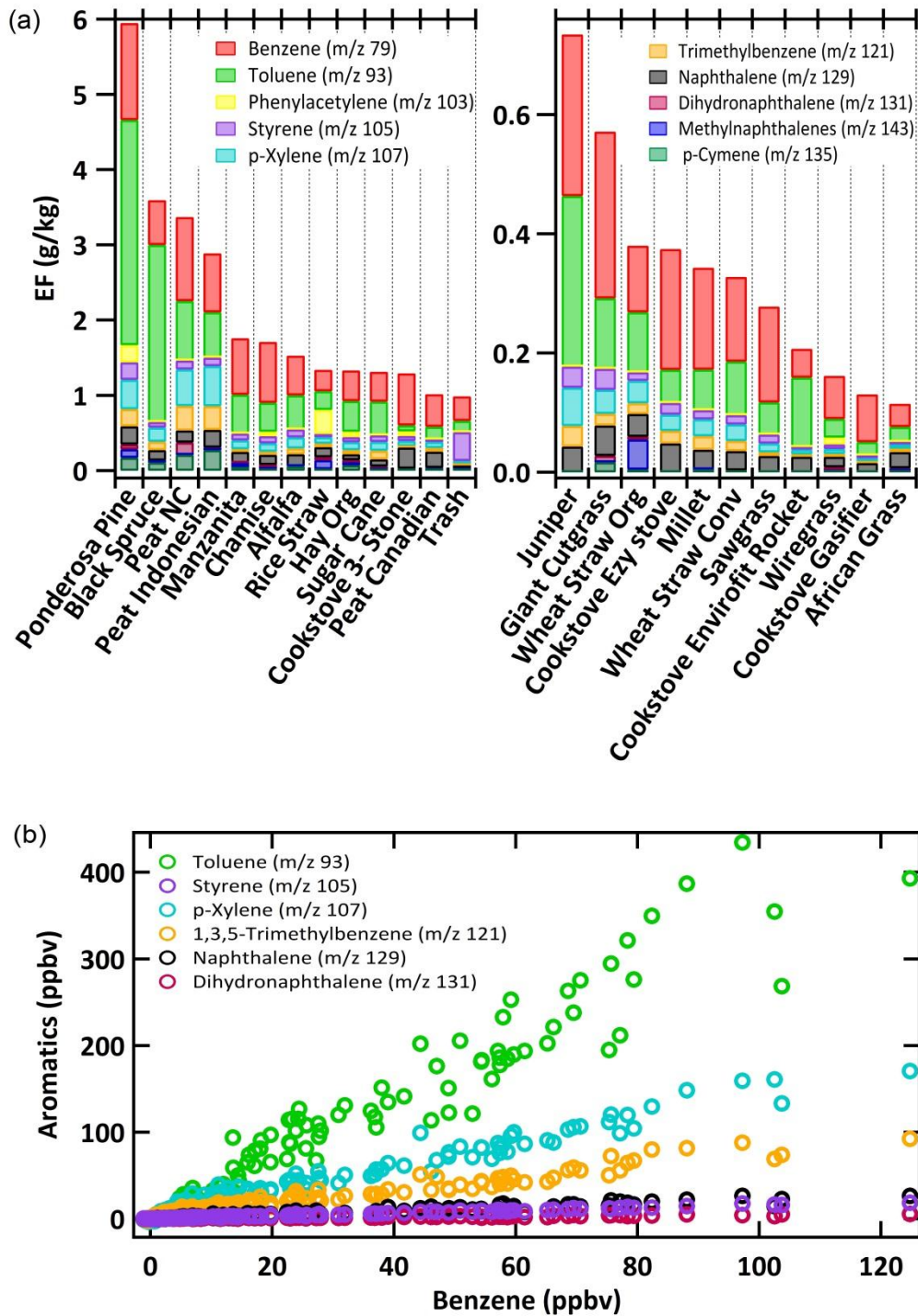
1324 Figure 2. A typical full mass scan of biomass burning smoke from the PTR-TOF-MS on a logarithmic (a) and a  
 1325 smaller range linear (b) scale. The internal standard (1,3-diiodobenzene) accounts for the major peaks  $\sim m/z$  331 and  
 1326 fragments at peaks near  $m/z$  204 and 205.



1327

1328 Figure 3. The emission factors ( $\text{g kg}^{-1}$ ) of total observed hydrocarbons and total observed species oxygenated to  
 1329 different degrees averaged for each fire type based on a synthesis of PTR-TOF-MS and OP-FTIR data. The  
 1330 patterned sections indicate the contribution to each of the above categories by selected functionalities discussed in  
 1331 the text (aromatic hydrocarbons, phenolics, furans). The parenthetical expressions indicate how many oxygen atoms  
 1332 are present. Figure 3. The distribution of oxygenated and hydrocarbon emission factors averaged for each fuel type  
 1333 where FTIR data were available. EFs are included for FTIR compounds and the 68 masses initially analyzed by  
 1334 PTR TOF MS. The patterned sections indicate the contributions from various “families” based on functionality and  
 1335 their oxygen content.

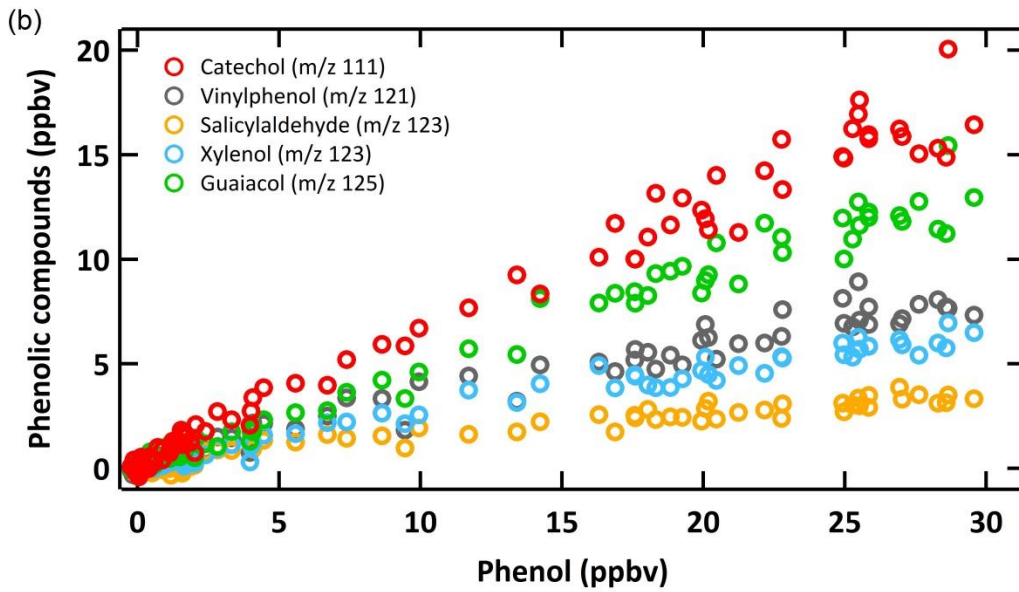
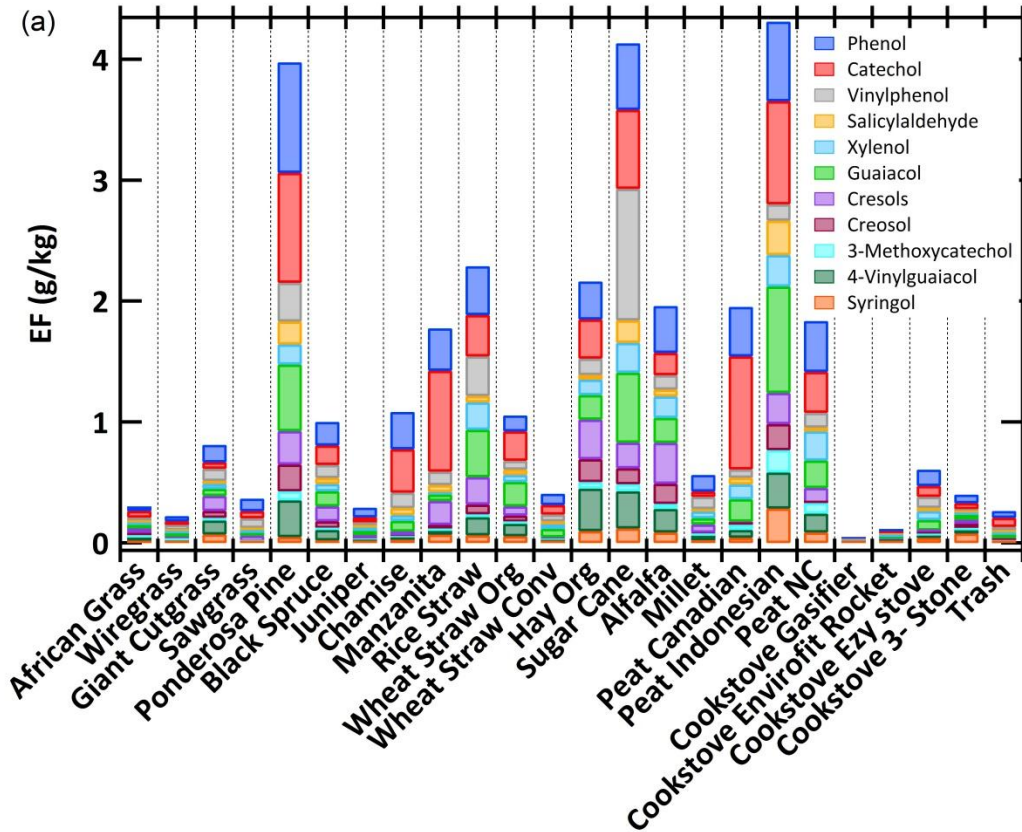


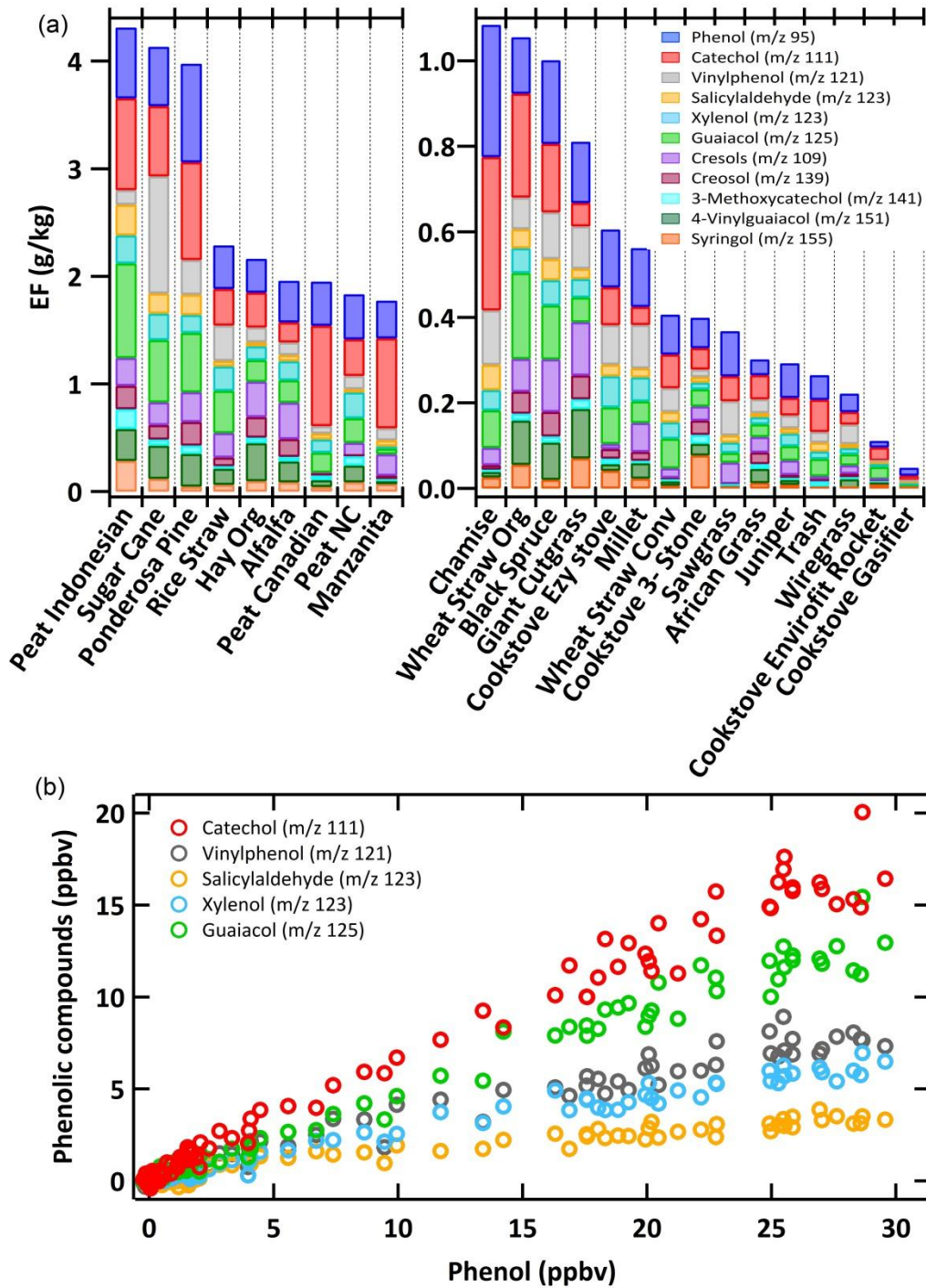


1337

1338 Figure 4. (a) The EFs of the aromatics analyzed in all fires averaged and shown by fuel type. Individual  
 1339 contributions from benzene and other aromatics are indicated by color. The EFs for for p-Cymene is-are only  
 1340 calculated for select burns-fires and should not be considered an average for each particular fuel type a true average.  
 1341 (b) The correlation plots of selected aromatics with benzene during a black spruce fire (Fire 74). Similar behavior  
 1342 was observed for all other fuel types.

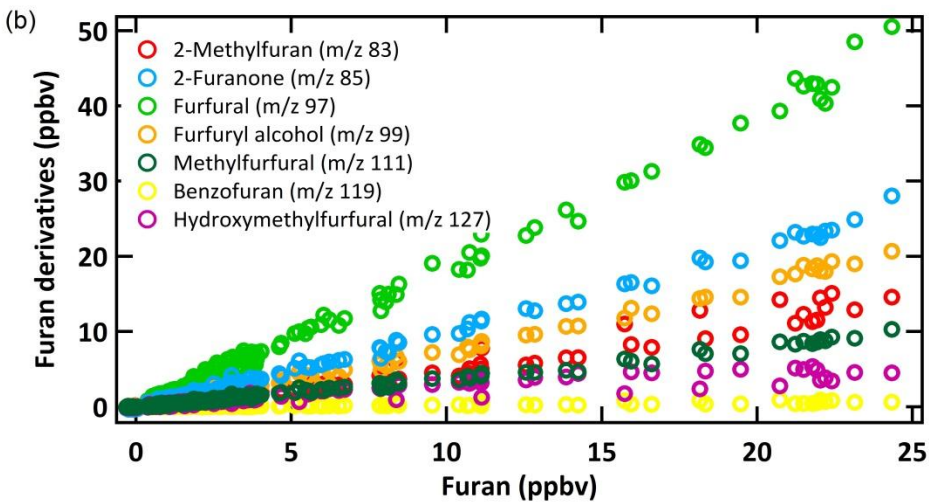
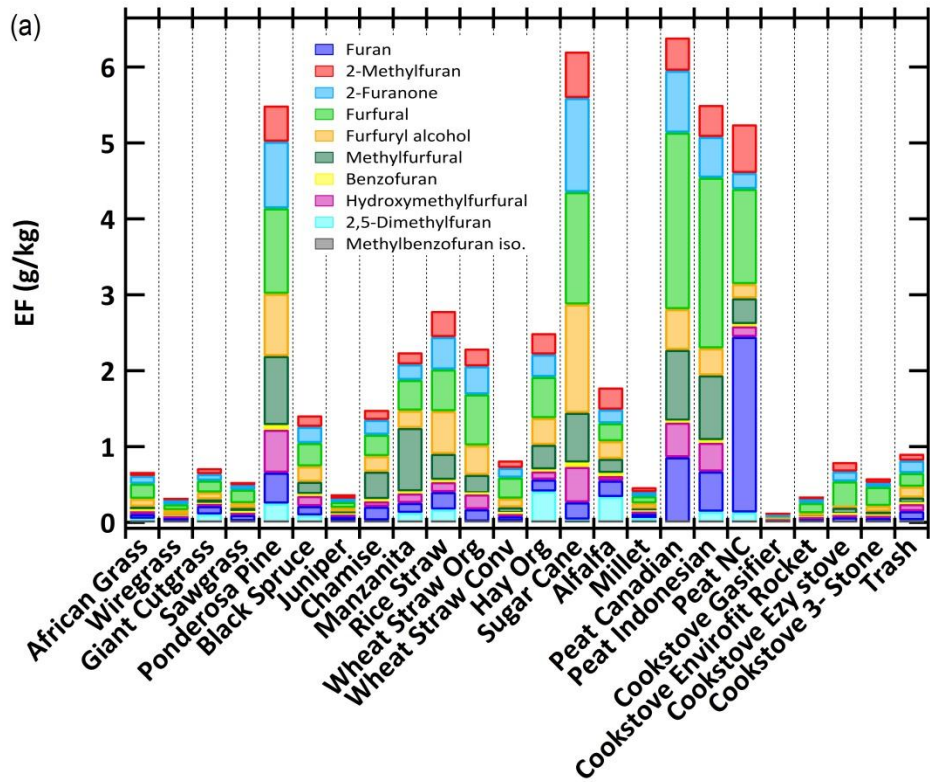


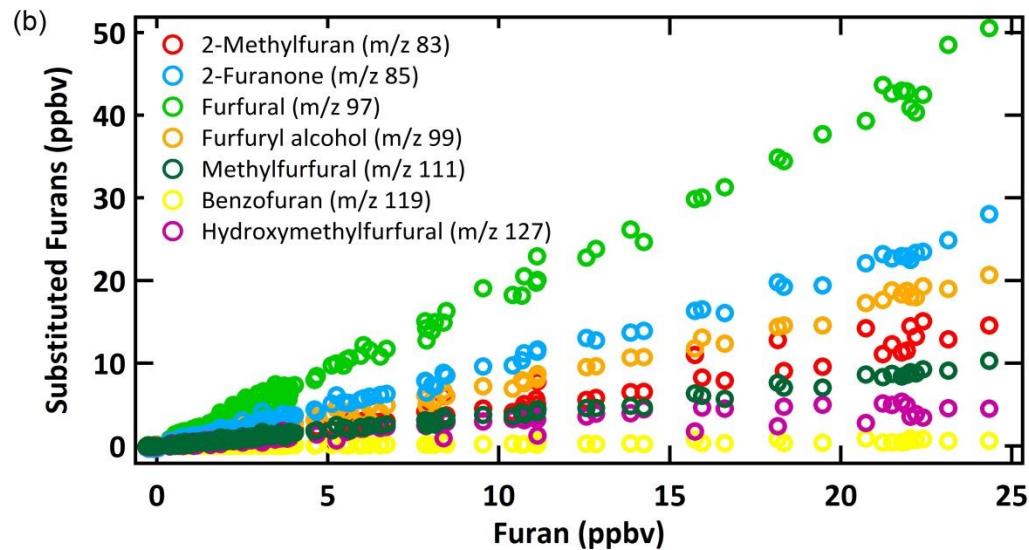
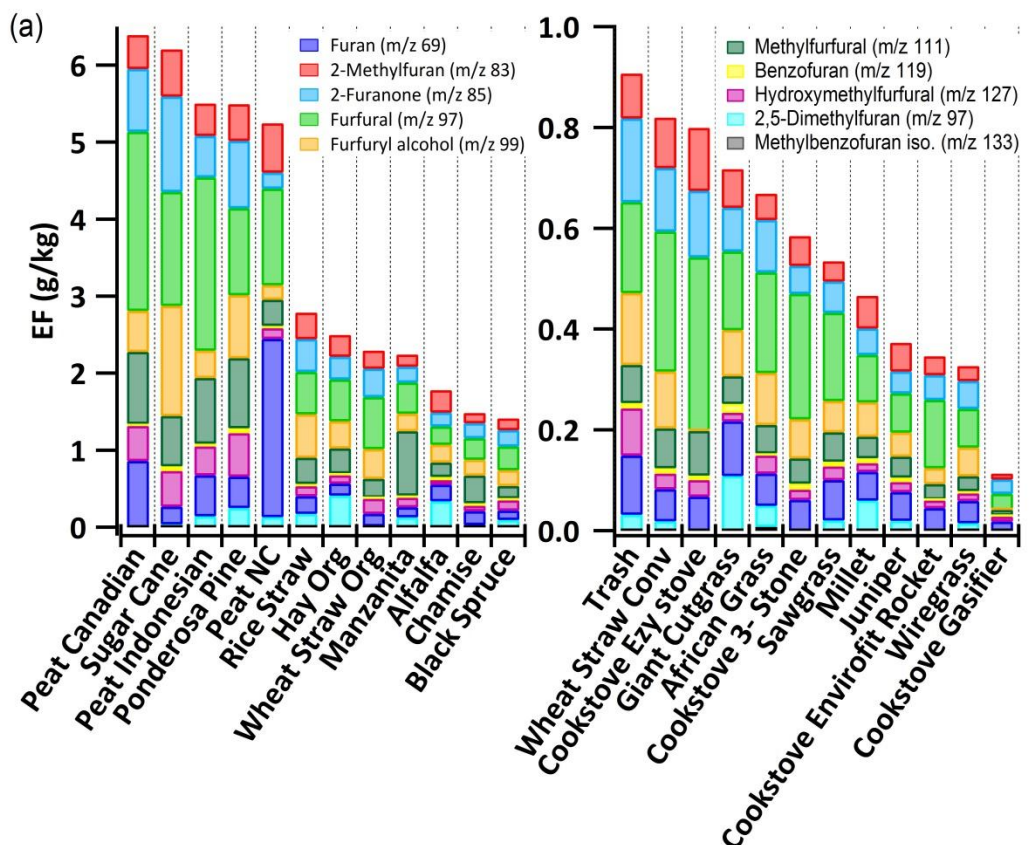




1344

1345 Figure 5. (a) The distribution in average fuel EF for several phenolic compounds, where compound specific  
 1346 contributions are indicated by color. The EFs for compounds additionally analyzed a single time fore  
 1347 during select fires are included but are not considered at the fuel average. (b) The linear correlation of select  
 1348 phenolic compounds with phenol during an organic hay burn (Fire 119).

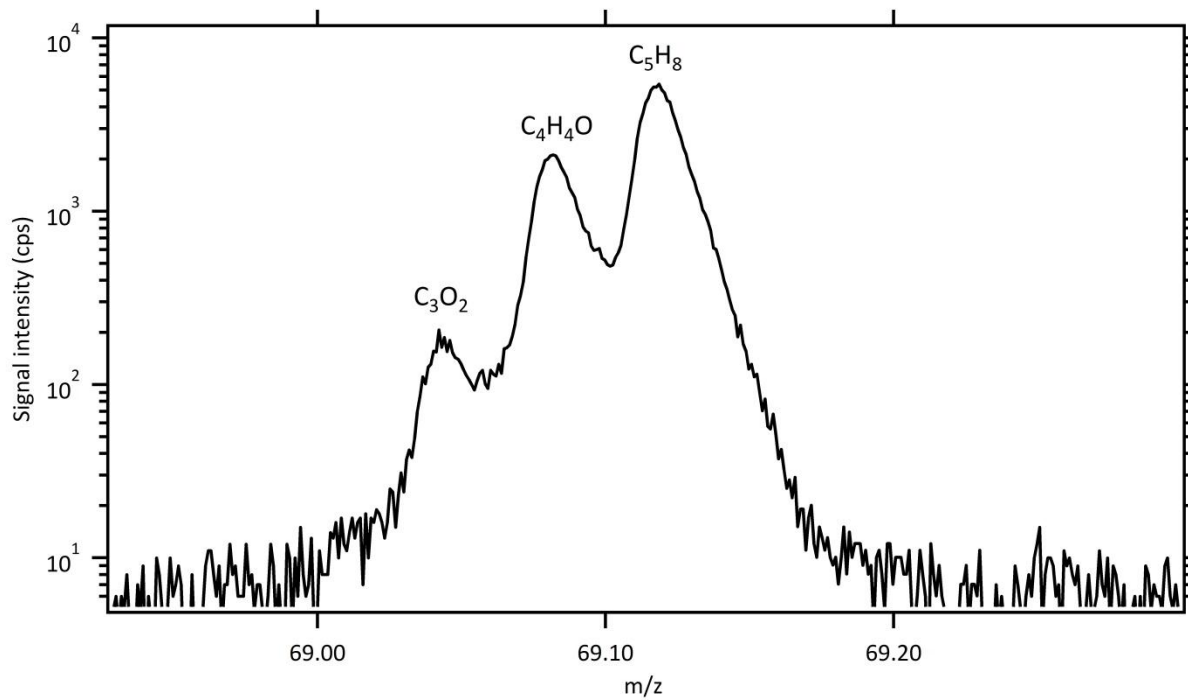




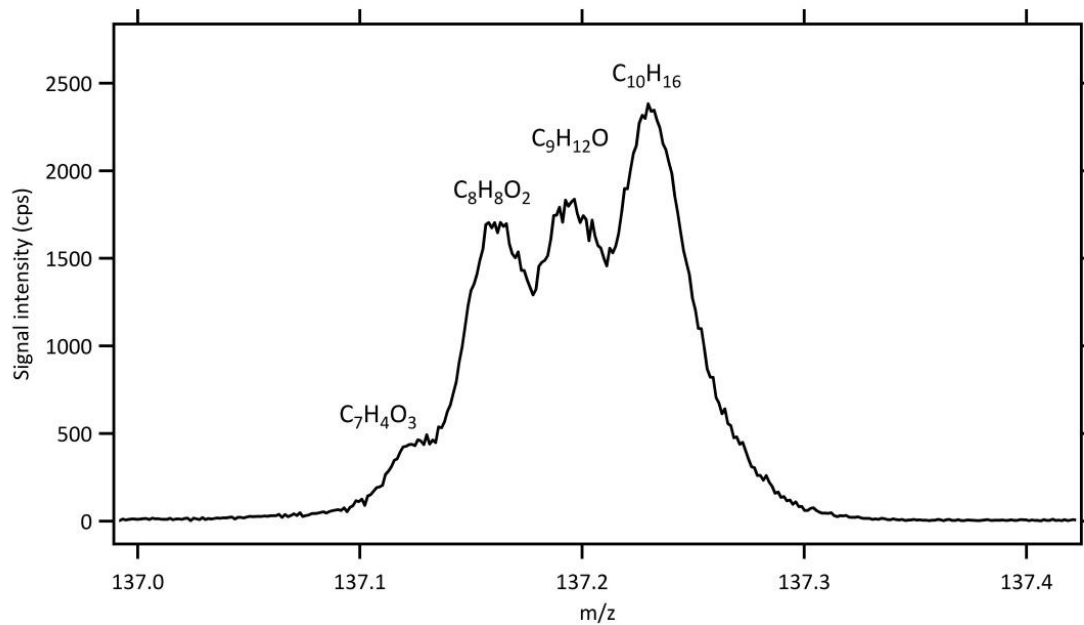
1350

1351 Figure 6. (a) The distribution in average fuel EF for furan and substituted furans, where individual contributions are  
 1352 indicated by color. The EFs for substituted furans additionally analyzed a single time are not true averages. (b) The  
 1353 linear correlation of furan with select substituted furans for an African grass fire (Fire 49). (a) The distribution in  
 1354 average fuel EF for furan and substituted furans, where individual contributions are indicated by color. The EFs for

1355 | ~~additionally analyzed substituted furans are also included but should not be considered fuel averages(b) The linear~~  
1356 | ~~correlation of furan with select furan derivatives for an African grass fire (Fire 49).~~

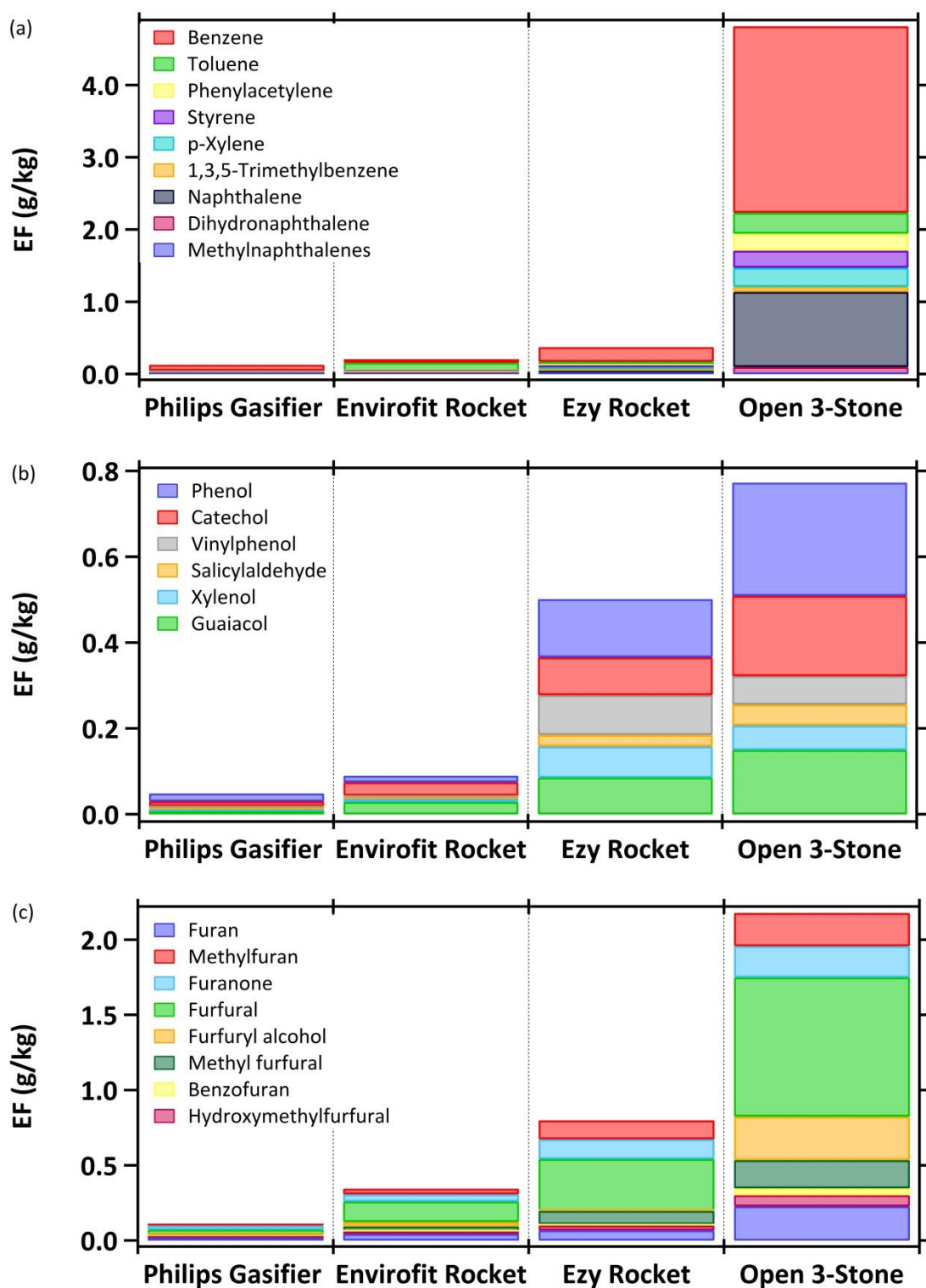


1357  
1358 Figure 7. Expanded view of the PTR-TOF-MS spectrum at  $m/z$  69 demonstrating the advantage over unit mass  
1359 resolution instruments of distinguishing multiple peaks, in this instance separating carbon suboxide (C<sub>3</sub>O<sub>2</sub>), furan  
1360 (C<sub>4</sub>H<sub>4</sub>O), and mostly isoprene (C<sub>5</sub>H<sub>8</sub>) in ponderosa pine smoke (fire 70).



1361  
1362

Figure 8. Expanded view of the PTR-TOF-MS spectrum of NC peat (fire 61) at  $m/z$  137 showing multiple peaks.



1363

1364 Figure 9. Emission factors ( $\text{g kg}^{-1}$ ) of aromatic hydrocarbons (a), phenolic compounds (b), and furans (c), for  
 1365 traditional and advanced cookstoves. The EF for traditional stoves were adjusted from original lab data (Sect. 4.7)